SYNTHESIS OF OCTENYL SUCCINATE PINEAPPLE STARCH AND EVALUATION FOR ITS APPLICATION AS NANOEMULSION STABILIZER

By
MISS Su Su LATT

A Thesis Submitted in Partial Fulfillment of the Requirements
for Doctor of Philosophy PHARMACEUTICAL ENGINEERING
(INTERNATIONAL PROGRAM)
Graduate School, Silpakorn University
Academic Year 2018

Synthesis of octenyl succinate pineapple starch and evaluation for its application as nanoemulsion stabilizer

โดย
MISSSu Su LATT

วิทยานิพนธ์นี้เป็นส่วนหนึ่งของการศึกษาตามหลักสูตรปรัชญาดุษฎีบัณฑิต
สาขาวิชาวิศวเภสัชกรรม ปริญญาปรัชญาดุษฎีบัณฑิต แบบ 1.1 (หลักสูตรนานาชาติ)
บัณฑิตวิทยาลัย มหาวิทยาลัยศิลปากร
ปีการศึกษา 2561

SYNTHESIS OF OCTENYL SUCCINATE PINEAPPLE STARCH AND EVALUATION FOR ITS APPLICATION AS NANOEMULSION STABILIZER

By

MISS Su Su LATT

A Thesis Submitted in Partial Fulfillment of the Requirements
for Doctor of Philosophy PHARMACEUTICAL ENGINEERING
(INTERNATIONAL PROGRAM)
Graduate School, Silpakorn University
Academic Year 2018

Title	Synthesis of octenyl succinate pineapple starch and evaluation for its application as nanoemulsion stabilizer
By	Su Su LATT
Field of Study	PHARMACEUTICAL ENGINEERING (INTERNATIONAL PROGRAM)
Advisor	Suchada Piriyaprasarth

Graduate School Silpakorn University in Partial Fulfillment of the Requirements for the Doctor of Philosophy

..... Dean of graduate school
(Associate Professor Jurairat Nunthanid, Ph.D.)

Approved by

..... Chair person
(Associate Professor Sontaya Limmatvapirat , Ph.D.)
..... Advisor
(Associate Professor Suchada Piriyaprasarth , Ph.D.)
..... Co Advisor
(Assistant Professor Vipaluk Patomchaiviwat , Ph.D.)
..... Examiner
(Professor Pornsak Sriamornsak , Ph.D.)
..... External Examiner
(Associate Professor Pienkit Dangprasert , Ph.D.)

57365803 : Major PHARMACEUTICAL ENGINEERING (INTERNATIONAL PROGRAM)
Keyword : Pineapple starch; Octenyl succinic anhydride; Functional properties; Multiple responses; Nanoemulsion; Itraconazole

MISS SU SU LATT : SYNTHESIS OF OCTENYL SUCCINATE PINEAPPLE STARCH AND EVALUATION FOR ITS APPLICATION AS NANOEMULSION STABILIZER THESIS ADVISOR : ASSOCIATE PROFESSOR SUCHADA PIRIYAPRASARTH, Ph.D.

The stem and rhizome waste of pineapple plant (*Ananas comosus* L. Merr.) is normally disposed of via a burning process, which can cause environmental pollution. In order to improve the limited properties of native pineapple starch (NPS) and to minimize waste, pineapple starch extracted from stem and rhizome was synthesized by octenyl succinic anhydride (OSA) using a fractional factorial central composite face centered (CCF) design. The Fourier transform infrared (FTIR) spectra results showed that new peak formation of ester carbonyl groups was found at 1716 cm^{-1} for octenyl succinate pineapple starch or OSA modified pineapple starch (OSAPS), indicating that the synthesis of pineapple starch by OSA was successful. Moreover, optimization of reaction conditions of OSAPS with multiple responses was successfully performed using response surface methodology (RSM). The OSA concentration was found to be the principal factor for the degree of substitution (DS), surface tension, and enthalpy model. The obtained OSAPS showed an increase in viscosity, clustering of granules and a decrease in surface tension, gelatinization temperature and enthalpy when compared with NPS. Moreover, the functional properties of OSAPS such as surface & interfacial tension, viscosity and emulsifying activity index were evaluated in order to apply as nanoemulsion stabilizer. An increase DS of OSAPS tended to statistically decrease the surface tension, interfacial tension, and increase the viscosity (p<0.05). The emulsifying activity index of OSAPS was higher than that of NPS. Then, itraconazole (ITZ)-loaded nanoemulsions containing OSAPS having high DS (DS=0.03) were prepared using fractional factorial CCF design by simple homogenization method. The prepared ITZ-loaded nanoemulsions exhibited nanosize <500 nm. The *in vitro* drug release demonstrated that the prepared ITZ-loaded nanoemulsions showed faster dissolution and significant higher drug release characteristics (p<0.05) in simulated gastric fluid when compared to intact ITZ. Moreover, drug kinetic model analysis showed that all prepared ITZ-loaded nanoemulsions followed Weibull model with best fit of high R^2. The prepared ITZ-loaded nanoemulsions containing OSAPS, NPS and control showed stable and no obvious change in phase separation or creaming after accelerated stability tests for three months and six cycles of temperature cycling test, suggesting as thermodynamically stable nanoemulsions. The preparation conditions of ITZ-loaded nanoemulsions with multiple responses could be optimized by RSM. The concentrations of OSAPS and polysorbate 80 were critical factors for the models of droplet size, polydispersity index, viscosity and *in vitro* drug release within 15 mins. Therefore, the effective functional property of OSAPS suggested that OSAPS could be applied as nanoemulsion stabilizer for pharmaceutical application.

ACKNOWLEDGEMENTS

First and foremost, I would like to special thank to my thesis advisor, Associate Professor Dr. Suchada Piriyaprasarth for her kind support, valuable suggestion, caring, patience and unique guidance throughout my study period. Her supervision is very great beyond description for my research performance.

I am also very greatful to express my gratitude to Assistant Professor Dr. Vipaluk Patomchaiviwat for her valuable advice and kind supports for my research work till the scholarship program finished. I also thank her very much for her kind care and patience. I would like to give my great thanks to Professor Dr. Pornsak Sriamornsak for good teaching, kind support and valuable good idea for research problem.

I would like to acknowledge to Associate Professor Dr. Jurairat Nunthanid, Associate Professor Dr. Sontaya Limmatvapirat, Associate Professor Dr. Thawatchai Phaechamud, Associate Professor Dr. Panida Asavapichayont, at the Department of Pharmaceutical Technology and Pharmaceutical Biopolymer group (PBig), Faculty of Pharmacy, Silpakorn University, for their supports and suggestions along four years of my study since start. In addition, I would like to give my special thanks to all research group members, all of my teachers and friends from both Thailand and Myanmar as well as most staffs from Faculty of Pharmacy, Silpakorn University to encourage me with their close friendship and to help without hesitate.

I would like to acknowledge the Silpakorn University Research and Development Institute, Thailand for research grant support to do my research work very well with a great concentration.

I wish to give my special sincere thank to my beloved mother, sisters, brothers and my relatives who always support, encourage, care and love me very much. Finally, I would like to thank everyone, especially Thai friends who give me kind support very well not only to finish my research work successfully but also to solve some personal affairs due to language barrier communication. May I request for some friends to whom I could not mention individually.

Su Su LATT

TABLE OF CONTENTS

Page

List of Tables

Page

List of Figures

Page

List of Abbreviations

NPS	Native pineapple starch
OSA	Octenyl succinic anhydride
OSAPS	Octenyl succinic anhydride modified pineapple starch
DS	Degree of substitution
RE	Reaction efficiency
Cl^-	Chloride
˚C	Degree centigrade
˚F	Degree fahrenheit
h	Hour
min	Minute
%w/w	Percent weight by weight
%w/v	Percent weight by volume
%v/v	Percent volume by volume
FTIR	Fourier Transform Infrared
SEM	Scanning Electron Microscopy
XRD	X-Ray Diffraction
RSM	Response surface methodology
k	Number of independent variables
N	Number of experimental runs
Y_{exp}	Experimental value
Y_{pred}	Predicted value
$\bar{Y}$	Mean response value
r^2	Correlation coefficient
RMSE	Root Mean Square Error
df	Degree of freedom
CI	Confidence interval
X(s)	Factors
Y(s)	Responses
K	Consistency index

n	Flow behavior index
C	Carbon
rpm	Revolution per minute
nm	nanometer
Δ	Delta
T_0	Onset temperature
T_p	Peak temperature
Te	End temperature
θ	Theta
kV	kilovolt
mV	millivolt
mPa.s	milli pascale
Pa.s	Pascale
SGF	Simulated gastric fluid
PDI	Polydispersity index

Chapter 1
Introduction

1.1 Statement and significance of the problems

Pineapple (*Ananas comosus* L. Merr.) is widely grown in Prachuap Khiri Khan Province, Thailand which is a top pineapple producing country. After harvesting, the pineapple stems and rhizome become agriculture waste which is destroyed by burning. The use of pineapple stems and rhizome can minimize waste and environmental pollution. This would add values to local agricultural waste products. However, there are a few reports on pineapple starch from stem. The native pineapple starch (NPS) was characterized (Nakthong, Wongsagonsup, & Amornsakchai, 2017) and investigated for utilization as co-emulsifier in itraconazole-loaded nanoemulsions (Latt et al., 2016).

Starch is a naturally biocompatible, biodegradable, inexpensive and abundantly available polysaccharide which is currently used as gelling, thickening, suspending agent, diluent, filler, binder and disintegrant (Aulton, 1988; Patomchaiviwat, Piriyaprasarth, Koorattanasiri, Kanoknirumdom, & Rattanasiha, 2011; Piriyaprasarth et al., 2010; Santana, Angela, & Meireles, 2014). The physicochemical, rheological and morphological properties of mango kernel starch (Bello-Pérez, Aparicio-Saguilán, Méndez-Montealvo, Solorza-Feria, & Flores-Huicochea, 2005), corn starch (Sandhu & Singh, 2007), *Tacca involucrata* starch (Nwokocha, Senan, & Williams, 2011), sweet potato starch (Moorthy, Sajeev, & Shanavas, 2012) and plantain starch (Hernández-Jaimes, Bello-Pérez, Vernon-Carter, & Alvarez-Ramirez, 2013) have been reported. However, starches have some limited properties in the native form. To develop desirable functional properties such as solubility, visicosity, amphiphilicity, or swelling characteristic, modification by physically, chemically, enzymatically or genetically is required (Kaur, Ariffin, Bhat, & Karim, 2012).

Chemical modification is widely used to improve native starch's functional property. Octenyl succinic anhydride (OSA) substitution is the esterification reaction at carbon 2, 3 and 6 of starch hydroxyls. There has been researched for OSA esterification of various starches including Indica rice starch (Song, Chen, Ruan, He, & Xu, 2006), potato starch (Hui, Qi-he, Ming-liang, Qiong, & Guo-qing, 2009), plantain starch (Bello-Flores, Nuñez-Santiago, Martín-Gonzalez, BeMiller, & Bello-

Pérez, 2014) and sago starch (Abiddin, Yusoff, & Ahmad, 2015). OSA synthesis condition is controlled by several factors. In order to determine the optimum condition for the system, optimization or response surface designs are used. Response surface methodology (RSM) is a gathering of statistical and mathematical method which is a sequential procedure and can be employed when a response or a set of responses of interest is influenced by several variables (Bezerra, Santelli, Oliveira, Villar, & Escaleira, 2008). The effects of the reaction conditions on the degree of substitution (DS) of OSA-modified starches using RSM have been reported for *Indica* rice starch (Song et al., 2006), corn starch (Wang et al., 2011) and starch from *Phaseolus lunatus* (Segura-Campos, Chel-Guerrero, & Betancur-Ancona, 2008). However, modification of pineapple starch by OSA has not been reported and no research on the optimization for OSA modification of pineapple starch with multiple responses has been conducted yet.

After OSA substitution into starch hydroxyl groups, an increase in hydrophobicity of starch produce extreme surface active property (Nilsson & Bergenståhl, 2007), good pasting property (Dokić, Krstonošić, & Nikolić, 2012), a decrease in interfacial tension (Zhao, Khalid, Shu, Neves, & Kobayashi, 2017) and emulsifying activity (Miao et al., 2014). The main important parameter for OSA substitution is DS. The permitted DS range (0.01-0.03) of OSA starch for food application is typically low and a wide use of OSA starch is due to its stability against high temperature, broad pH and ionic strength and tasteless (Sweedman, Tizzotti, Schafer, & Gilbert, 2013). It has been reported that OSA starch could be applied as emulsifiers (Pongsamart, Kleinebudde, & Puttipipatkhachorn, 2016), stabilizers for oil-in-water emulsions (Dokić et al., 2012; Miao et al., 2014; Sweedman, Schafer, & Gilbert, 2014; Zhao et al., 2017), an encapsulating agent for vitamin E nanocapsule (Hategekimana, Masamba, Ma, & Zhong, 2015) and nanoemulsion stabilizer for poorly water soluble curcumin using ultrasonics (Abbas, Bashari, Akhtar, Wei, & Zhang, 2014). However, the functional properties of octenyl succinate pineapple starch or OSA modified pineapple starch (OSAPS) have not been investigated as nanoemulsion stabilizer.

Nanoemulsion is a promisingly interesting thermodynamically stable colloidal system for oral administration because of its bioavailability improvement of poorly soluble drug (Jain, Kumar, Sood, & Gowthamarajan, 2013). It contains two

immiscible phases such as an oil phase with droplet size in the range of 20-500 nm (Debnath, Satayanarayana., & Kumar, 2011; Gupta, Eral, Hatton, & Doyle, 2016). and an aqueous phase as continuous phase together with emulsifier/surfactant (Gupta et al., 2016; Hanlor, Pande, Borawake, & Nagare, 2018; Silva, Cerqueira, & Vicente, 2011). Generally, nanoemulsions can be prepared by low and high energy method. Oil-in-water (O/W) nanoemulsions can be conducted using a simple homogenizer. Breaking of large oil droplets into small droplets and their stability depends on the type and concentration of emulsifiers and stabilizers. Emulsifiers can reduce the interfacial tension, thus, decreasing the energy is required for the droplet disruption. Additionally, the emulsifiers can adsorb to the freshly formed oil-water interface, thereby preventing the droplet re-coalescence and stabilize the emulsions (Abbas et al., 2014; Silva et al., 2011). However, the application of the OSAPS as stabilizer in nanoemulsion has not been researched.

Itraconazole (ITZ), a triazole antifungal agent, is poorly water soluble drug which is classified as Biopharmaceutic Classification System type II. Its activity shows a broad spectrum range against various pathogens (Glasmacher & Prentice, 2006). Poor solubility of drug in aqueous media is the major issue which negatively affects the bioavailability and efficacy of drug in the human body. The achieved success in case of ITZ with increased dissolution rate is limited (Patravale, Date, & Kulkarni, 2004). The previous studies on preparations containing ITZ for oral administration include pectin-based nanoemulsion (Burapapadh, Kumpugdee-Vollrath, Chantasart, & Sriamornsak, 2010), nanosuspension (Cerdeira, Mazzotti, & Gander, 2013), nanocrystals (De Smet et al., 2014), solid dispersion (Engers et al., 2010), dissolving tablet (Piao, Choe, Oh, Rhee, & Lee, 2014), cyclodextrin based solution (Berben, Mols, Brouwers, Tack, & Augustijns, 2017). However, Such drug molecule still have challenges to develop therapeutically effective products for clinical use since it has poor dissolution problem (Patravale et al., 2004). Therefore, ITZ is a good model drug for preparation of nanoemulsions due to its insolubility nature in gastrointestinal fluid.

In this study, the synthesis conditions of pineapple starch modified by OSA will be optimized using RSM and characterize the physicochemical properties of the OSAPS such as DS, reaction efficiency (RE), viscosity, surface tension, %crystallinity and enthalpy (ΔH_g). Moreover, the functional properties of the OSAPS

such as surface & interfacial tension, viscosity and emulsifying activity index (EAI) will be investigated. The ITZ-loaded nanoemulsions will be prepared by simple homogenization method using RSM and characterized for droplet size, polydispersity index (PDI), zeta potential, viscosity, %drug content, *in vitro* drug release and %creaming.

1.2 Objectives of research

The objectives of this study were

- To modify the pineapple starch by esterification with 2-octenyl succinic anhydride using optimization technique
- To characterize the physicochemical properties of the OSAPS; such as DS, RE, viscosity, surface tension, %crystallinity and enthalpy (ΔH_g)
- To evaluate the functional properties of OSAPS; such as interfacial tension, viscosity and EAI, in order to apply as nanoemulsion stabilizer
- To optimize ITZ-loaded nanoemulsions containing OSAPS using RSM and evaluate for droplet size, PDI, zeta potential, viscosity, %drug content, *in vitro* drug release and %creaming

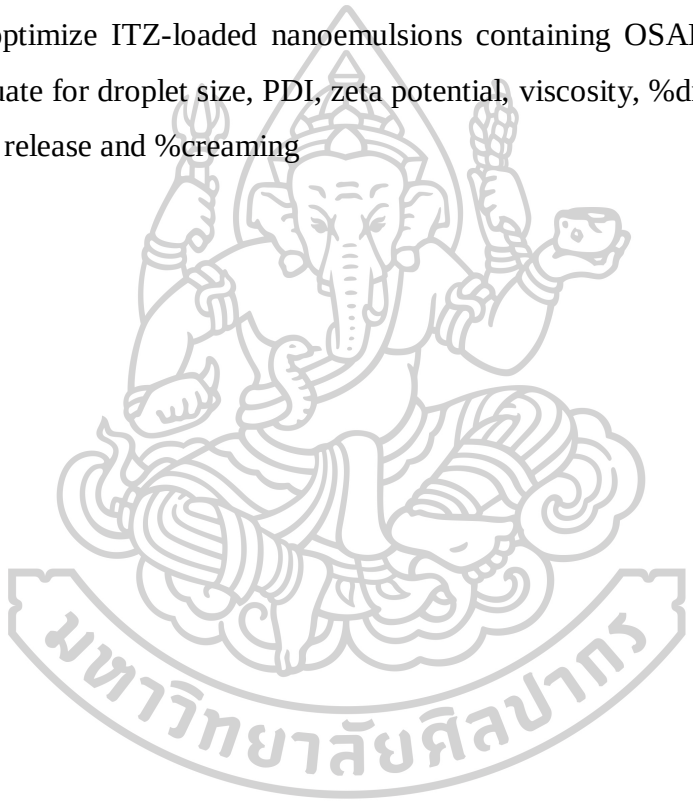

Chapter 2

Literature reviews

2.1 Starch

2.1.1 Chemical structure and composition

2.1.2 Starch granule appearance

2.1.3 Applications of starch

2.2 Chemical modifications

2.2.1 Etherification

2.2.2 Esterification

2.2.3 Acid modification

2.2.4 Oxidation

2.2.5 Cross-linking

2.3 Design of experiments

2.3.1 Full factorial design

2.3.2 Box-Behnken design

2.3.3 Central Composite design

2.4 Nanosized delivery vehicles for poorly water soluble drugs

2.4.1 Nanoemulsion

2.5 Itraconazole

2.1 Starch

Pharmaceutical excipients must be improved to have better functional properties rather than inert filler. Nowadays, natural excipients becomes more acute than synthetic polymers and animal-based products due to their safety and versatility (Gbenga, Olakunle, & Adedayo, 2014). They play a major role in pharmaceutical tabletting for drug delivery system. Starch is one of the most promising materials for future use as it contains no toxic residues and is widely available, naturally abundant inexpensive, and has broad-ranging biocompatibility (Rodrigues & Emeje, 2012). Several starches including mango kernel (Kaur, Singh, Sandhu, & Guraya, 2004), corn (Sandhu & Singh, 2007), *Tacca involucrate* (Nwokocha et al., 2011) and plantain (Hernández-Jaimes et al., 2013) have been structurally characterized and investigated for their physicochemical and rheological properties.

2.1.1 Chemical structure and composition

Starch is chemically composed of a number of anhydroglucouse units having empirical formula such as $(C_6H_{10}O_5)_n$, where n ranged from 300-1000 repeated glucose molecules. Starch has two parts being amorphous and crystalline part. 20-30% of the mass of starch granule is amorphous and 70-80% is crystalline part (Masina et al., 2017). The amorphous part consists mainly of amylose which is linear portion linked with alpha-D-(1,4) glucosidic bonds. The crystalline part has amylopectin which is anhydroglucose units linked together through alpha-D-(1,4) glucosidic bonds, periodic branches at the C-6 position by alpha-D-(1,6) glucosidic bonds (**Figure 1**) (Masina et al., 2017; Wurzburg, 1986).

The functional properties of starches such as thickening, gelling and stabilizing are strongly affected by amylose/amylopectin composition (Rolland-Sabaté et al., 2012). In addition, chemical modification such as esterification of starch primarily occurs in amorphous region related with amylose (Hui et al., 2009). Therefore, amylose composition becomes an interesting essential player to be researched for the properties and potential applications of starches in food and pharmaceuticals (Zhu, 2014).

The amylose level occurred in a variety of starches depend on botanical source. Most starches usually consist of amylose 15-25% (Chen & Liu, 1972). Corn,

wheat, potato, and tapioca starch contain about 18 to 28% amylose (Wurzburg, 1986). Sabate et al reported the level of amylose for cassava starch (~16%), potato starch (22.1%) and maize starch (28%) (Rolland-Sabaté et al., 2012). Moreover, the composition of amylose% has been researched for other unconventional starches such as pulse starch (11%) (Hoover, Hughes, Chung, & Liu, 2010), millet starch (6%) (Zhu, 2014), sweet potato starch (~25%) (Zhou et al., 2015). For pineapple stem starch, 36% of amylose content was observed by whereas amylose % of pineapple starch from stem and rhizome (*Ananas comosus* L. Merr.) grown in Prachuap Khiri Khan Province, Thailand was found to be 21.85% (Latt, Patomchaiviwat, Sriamornsak, & Piriyaprasarth, 2019). However, the amylose level of pineapple stem and rhizome starch is very close to potato starch.

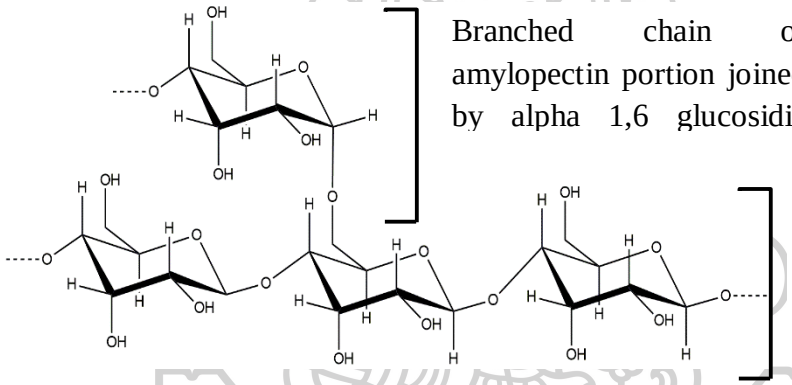

Figure 1 Starch chain along with amylose and amylopectin portions.

2.1.2 Starch granule appearance

Starch occurs as tiny granules. They are distributed in grain seeds, roots, tubers, stems and rhizomes of green leafy plants. There are various shape of starch granules being spherical, oval and polygonal etc. Their size ranges from < 1µm to 100µm µm (BeMiller & Whistler, 2009). Some commercial starches include corn (polygonal) found in cereal grains, potato (oval) from tubers and tapioca from roots etc. (BeMiller & Whistler, 2009; Chen & Liu, 1972). Small and large wheat starch granules have diameters of 2-3 µm and 22-36 µm, respectively. Potato granules (15-75 µm) are larger than maize granules (5-20 µm). The diameters of rice granules are 3-8 µm (BeMiller & Whistler, 2009). The starch granules' appearance, size, composition, physicochemical and functional properties are due to botanical source and culture

conditions. These properties can change depending on the treatment to which the granules are subjected (BeMiller & Whistler, 2009). Granules of pineapple starches are about 11-μm in diameter and have a central fissure of Y-shaped in its central area and high amount of pineapple starch is stored up in the stem of pineapple (Chen & Liu, 1972). Pineapple (*Ananas comosus* L. Merr.) is a native plant and a leading edible member of the Bromeliaceae family. Recently, pineapple starch was extracted from stem and rhizome waste, which is normally disposed of via a burning process, thereby polluting the environment (Nakthong et al., 2017). The application of pineapple starch in food and pharmaceuticals has been rarely reported (Latt et al., 2016).

2.1.3 Applications of starch

Starch is currently used in various applications as a gelling agent, thickener, suspending agent, diluent, filler, binder, and disintegrant (Aulton, 1988; Patomchaiviwat et al., 2011; Piriyaprasarth et al., 2010) although a wide range of applications have been reported on conventional starches. Moreover, the applications of some conventional and non-conventrional starches are summarized in **Table 1**. Starches found in legumes, rhizomes, herbs and seeds are considered as unconventional starches which may be used as ingredient materials in the same manner as starch from cereals and tuber because of their similar physicochemical properties and functional properties (Alcázar-Alay & Meireles, 2015). Modification treatment may be used to improve these properties, develop new process and consequently new products (Santana et al., 2014). However, there are limited studies on the use of unconventional starches (Daudt, Külkamp-Guerreiro, Cladera-Olivera, Thys, & Marczak, 2014; Rengsutthi & Charoenrein, 2011). Since, starches have some limited properties in the native form, modified starches have therefore played a significant role in the food and pharmaceutical industries over the past few decades. To improve their functional properties, including viscosity, hydrophilicity, and swelling characteristics, starches have been tailored by physically, chemically, enzymatically, and genetically (Kaur et al., 2012).

Table 1 Applications of some conventional and nonconventional starches.

No.	Starch source	Applications	References
1.	Starches from cereals, legumes and tubers	Mimetic agents of fats	(Alcázar-Alay & Meireles, 2015)
2.	Conventional starches such as wheat, corn, rice, potato and cassava	Modifier of texture, viscosity, adhesion, moisture rentention, gel formation and film	(Alcázar-Alay & Meireles, 2015)
3.	Maize starch	Foodstuffs, thickener, stabilizer, colloidal gelling agent, water retention agent and adhesive	(Zhu & Wang, 2013)
4.	Microgranules of starches	Sold matrix for encapsulation of food ingredients	(Santana et al., 2014)
5.	Conventional starches of potato, wheat, tapioca, corn and rice	Pore-forming agent in ceramic technology	(Gregorová, Pabst, & Bohačenko, 2006)
6.	Nonconventional starches of sweetsop and soursop starches	Thickener	(Nwokocha et al., 2011)
7.	Jack fruit seed starch	Stabilizer in high acid sauce	(Santana et al., 2014)
8.	Bean starches	Stabilizer in sausages	(Campechano-Carrera, Corona-Cruz, Chel-Guerrero, & Betancur-Ancona, 2007)
9.	Nonconventional starches of turmeric and annatto starches	Coloring agents in food, cosmetics and pharmaceutical products	(Santos et al., 2014)

2.2 Chemical modifications of starch

There are four kinds of methods to modify the starch. They are physical, chemical, enzymatic and genetic methods. The physical modifications including heat-moisture treatment (HMT) and annealing (ANN) method decrease leaching of amylose, swelling the granules, peak viscosity, and increase thermal stability and gelatinization temperatures of *African* yam bean starch (Adebowale, Henle, Schwarzenbolz, & Doert, 2009). Enzymatic modifications use hydrolyzing enzymes such as amylomaltases which break an α-1,4 linkage between two glucose molecules following a new α-1,4 bond forming. The resulted modified starch can be used in food staffs, cosmetic products, pharmaceutical products, detergents etc. Genetic modification use transgenic technique that oriented the enzymes to starch biosynthesis leading to produce amylose free starch and high amylose starch and altered amylopectin structure (Neelam, Vijay, & Lalit, 2012).

The chemical modification has advantageous over other methods which provides increasing molecular stability against mechanical shearing and hydrolysis due to acidic and high temperature; getting targeted viscosity; improving interaction with electronegative or electropositive ions and decreasing the retrogradation rate of native starch. The most commonly used chemical modifications are substitution reactions being etherification, esterification, acidification, oxidation and cross-linking (Hoover et al., 2010; Neelam et al., 2012).

There are two classes of chemical modifying reagents applied to modify the starch chemically, which include monofunctional or bifunctional reagents based on chemical nature. The mono-functional reagents consists of monochloroacetic acid or sodium chloroacetate, acetic anhydride or succinic anhydride etc. The chemical substitution reactions using monofunctional reagents include etherification, esterification, acidification, oxidation etc. which undergo changes in gelatinization and paste properties of native starches by producing a non-ionic, cationic, or hydrophobic or covalently bonded substituent group to starches. Such modification results in starch derivative having better stabilizing property than native starches (Masina et al., 2017; Sui & BeMiller, 2013). The cross-linking reaction using bi-functional reagents or multi-functional reagents such as sodium trimetaphosphate or phosphorous oxychloride, which produce cross-linked starch derivatives (Masina et al., 2017).

2.2.1 Etherification

Etherification reaction is one of the substituted reactions used to enhance physicochemical properties of starch (Lawal, Lechner, & Kulicke, 2008). The starch derivatives resulted in ether form received by replacement of starch hydroxyls with hydroxypropyl (hydroxypropylation) and/or hydroxyethyl (hydroxyethylation), carboxymethyl (carboxymethylation) etc. and leads to formation of ether functional group in starch derivative using sodium hydroxide as a catalyst (Masina et al., 2017). The most commonly used reaction techniques to etherify the native starch are hydroxypropylation and carboxymethylation as follows:

(i) Hydroxypropylation

Hydroxypropylation is introduction of hydroxypropyl groups into starch granules which renders hydrophilic nature and loose the internal structural bond strength which holds the starch granules together, consequently decrease the paste temperature (Neelam et al., 2012; Pal, Singhal, & Kulkarni, 2002; Wurzburg, 1986). and they are cold water swelling (Pal et al., 2002; Wurzburg, 1986). The higher the hydroxypropylation substitution level, the lower the pasting temperature (Wurzburg, 1986). The hydroxypropylated substitution reaction along the starch chains of repeated glucose units is dominant in amorphous regions (Pal et al., 2002). Hydroxypropylated starch derivatives can be prepared conventionally in an aqueous medium into which 5 to 10% of sodium sulfate is added with respect to starch solid weight to prevent starch swelling. In addition, 5% of sodium hydroxide is required to protect starch gelatinization and to adjust pH with vigorous shaking (Woggum, Sirivongpaisal, & Wittaya, 2015; Wurzburg, 1986). About 6-10% of propylene oxide as derivatization agent can be used and a temperature of approximately 110˚F or 40˚C is required (Masina et al., 2017; Wurzburg, 1986). This reaction takes time 24 h to end up reaction under the sealed condition (i.e. the condition kept at centrifuged bottles with successive shaking) (Woggum et al., 2015; Wurzburg, 1986). Moreover, non-aqueous reaction such as dry reaction or organic liquid slurry reaction can also be used as alternative method. Dry reaction with propylene oxide means that moisture level is limited. But starch moisture level < 5% is ineffective and 7-10% is necessary for ease and efficiency of reaction. This reaction needs heated pressure type mixer with good agitation, a temperature of 185˚F and pressure 45 psia. After the propylene

oxide reaction is completed, the container/mixer is purged with nitrogen and pH is adjusted with dry citric acid. For food application, the final product is necessary to be washed with water or water/alcohol mixture to discard undesired by-products (Wurzburg, 1986).

Furthermore, another organic liquid slurry medium can be selected for hydroxpropylated starch preparation using propylene oxide as reactant followed by adding desired organic solvent and catalyst. The use of this medium has advantageous over aqueous slurry and dry reaction method is that higher level of hydroxypropyl substitution can be obtained within shorter time at high temperatures. The main disadvantage is to recover and purify the organic liquid. The organic liquids can be high to low boiling state or gaseous state depending on types, sensitivity of product, reactants and reaction conditions. In addition, this system needs special requirements of gaseous systems such as freon or carbon dioxide (Wurzburg, 1986). However, the simple method of aqueous slurry medium is widely used due to its advantageous of maintaining the starch integrity and undesired by-products can be simply removed by filtration and washing the final product. The commercial hydroxypropylated starches for food industry has low DS value having “0.1”, i.e., one hydroxypropyl group per 10 anhydroglucose units (Wurzburg, 1986).

For hydroxypropylated starches, molar substitution (MS) is used and it is main parameter to determine hydroxypropyl group (%) and subsequently analyze the MS because hydroxypropyl group can further react with reagent to form polymeric units of substituents. Pal et al prepared hydroxypropylated corn and amaranth starches using conventional method and found that hydroxypropylated starch of amaranth having MS 0.1 and 0.13 are excellent thickeners for frozen foods (Pal et al., 2002). Moreover, the physicochemical properties of native rice starch after hydroxypropylation were improved by decreasing gelatinization, pasting temperature and crystallinity with respect to high concentration of propylene oxide and viscosity was higher than native rice starch. The hydroxypropylated rice starch having MS 0.02-0.03 were achieved (Woggum et al., 2015). Furthermore, Lee and Yoo modified sweet potato starch by hydroxypropylation which produce MS 0.042-0.153 which affected on physicochemical and rheological properties with related to increasing of MS (Lee & Yoo, 2011). Li et al studied on dual modification of acidification and

hydroxypropylation of potato starch and the combination reaction technique affected structural and pasting properties. The potential applications of dual modified potato starch as coating, encapsulation and formation of hydrogen have been reported (Li et al., 2018). The physicochemical properties of hydroxypropylated starches are similar to those by carboxymethylation modification method (Masina et al., 2017) except the ability of the bulky group of hydroxypropyls to break the inter and intra hydrogen bonds of starch molecules (Masina et al., 2017; Neelam et al., 2012). Another most common etherification of starch is carboxymethylation.

(ii) Carboxymethylation

There are three steps for preparation of carboxymethylated starches in the presence of monochloroacetic acid or sodium chloroacetate. The following steps can be expressed by equations (Lawal et al., 2008; Lefnaoui & Moulai-Mostefa, 2015).

(1) Initiation of the starch for reaction using sodium hydroxide (alkalinization),

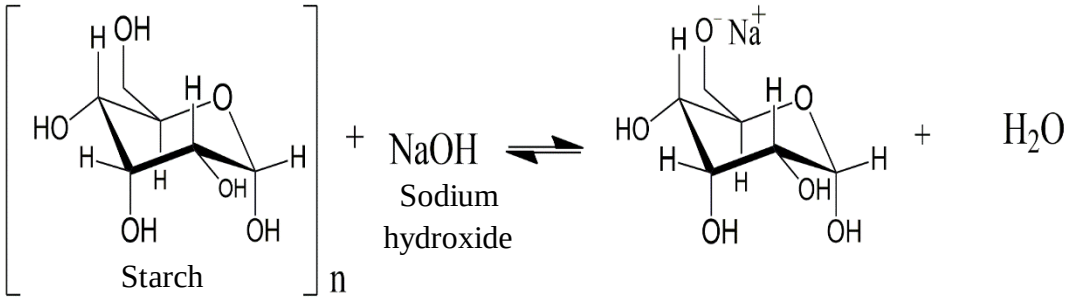

(2) Introduction of the carboxymethyl substituent into starch granules in the presence of sodium chloroacetate or monochloroacetic acid,

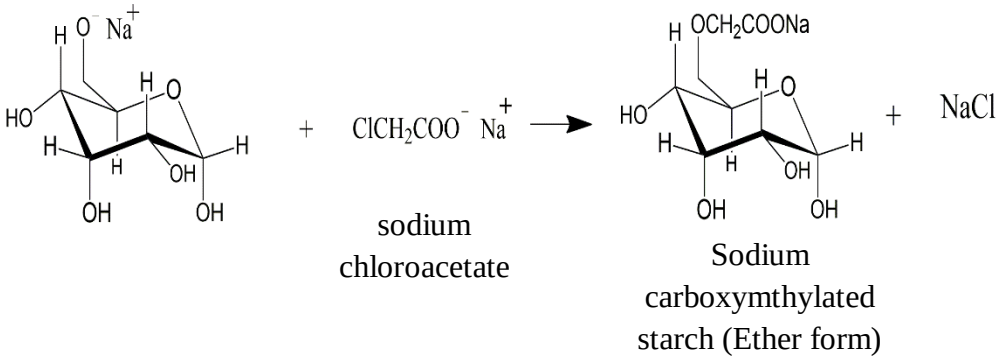

(3) Formation of unwanted side reactions,

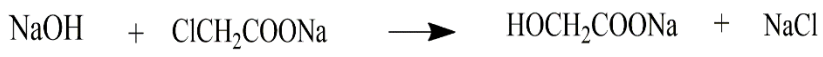

sodium chloroacetate — Sodium glycolate

Lawal et al synthesized carboxymethylated water yum starch using single step and multi-steps (nine times of single step in repeatition) which influenced DS and RE. Optimal DS and RE were 0.98 and 70.5% for single step and DS 2.24 for complete 9 steps as well as RE 82.1% after 7^{th} times which decreased again with increasing of synthesis steps. After carboxymethylation, the thermal stability of native yum starch was improved and crystallinity was decreased significantly (Lawal et al., 2008). Moreover, carboxymethylation enhanced the physicochemical properties of native mungbean starch (Kittipongpatana, Sirithunyalug, & Laenger, 2006) and pregelatinized corn starch (Lefnaoui & Moulai-Mostefa, 2015). For carboxymethylation, the reaction medium is aqueous alcoholic mixture. The yield% was greatly influenced by the organic solvents/water ratio, sodium hydroxide/monochloroacetic acid ratio, reaction temperature (Gotlieb & Capelle, 2005). Kittipongpatana et al prepared carboxymethylated mungbean starch in a variety of organic solvents such as methanol, ethanol and propranolol and ethanol solvent (92.7%) was found to be the best solvent for preparation but methanol was the suitable solvent providing high viscous pasting property of modified starches having DS 0.06-0.66 (Kittipongpatana et al., 2006). Lefnaoui and Moulai-Mostefa reported pregelatinized carboxymethylated modified corn starch as pharmaceutical excipient. The preglatinized starch was prepared first and then carboxymethylation using sodium chloroacetate in alcoholic medium was conducted. The modified starch having different DS 0.12-0.55 affecting drug release was found to be tablet excipient suitable for sustained drug release delivery (Lefnaoui & Moulai-Mostefa, 2015). Similarly, it has been reported that increasing DS of carboxymethylated Indian Palo starch decreased the paracetamol drug release and had potential application for extended release tablets (Das, Jha, & Kumar, 2015). Overall, carboxymethylation improve the properties of native starch which is insoluble in cold water (Lefnaoui & Moulai-

Mostefa, 2015; Neelam et al., 2012). The resulted carboxymethylated starches produce an increase in solubility, pasting property (Kittipongpatana et al., 2006), water absorption power (Massicotte, Baille, & Mateescu, 2008), and applied as tablet disintegrating agent (Gotlieb & Capelle, 2005; Neelam et al., 2012), as pharmaceutical excipient for sustained drug delivery system (Das et al., 2015; Lefnaoui & Moulai-Mostefa, 2015) and also used as a sizing and printed material for textile factory (Neelam et al., 2012).

2.2.2 Esterification

Esterification is a chemical substituted reaction which are prepared by substitution of starch hydroxyl groups by alkoxy (-O-alkyl) group and lead to esterfied starches having ester functional group (RCOOR). Standard esterification reaction in which three kinds of starch ester forms are established:

i. Starch succinates, being derived from reaction of succinic anhydride

ii. Alkenyl succinates, resulting from the reaction of substituted succinic anhydride i.e. alkyl or alkenyl succinic anhydrides (eg., octenyl succinic anhydride)

iii. Sulfosuccinate, which result from the saturation of the double bond in starch maleate esters with sodium bisulfate or from the reaction of starch with sulfosuccinic anhydride or its alkyl or alkenyl substituted form (Caldwell, Hills, Wurzburg, & Babylon, 1953).

Among three types of esterification, OSA esterified starches have becoming widely used in the food product and pharmaceutical field as they have some unique properties including its solubility in water, improvement of pasting profiles, lowering gelatinization temperature, decreasing retrogradation and wide range of stability in pH, etc. which are suitable for development of new products (Santana et al., 2014; Sweedman, Tizzotti, et al., 2013).

DS is the important parameter for chemical substitution reactions of starch. The DS means the average number of sites per anhydroglucose units of the starch molecule on which there are substituent groups at carbon 2, 3 and 6 positions. Thus, if one hydroxyl is esterified with acetyl groups, the DS is 1. If all three hydroxyl groups are esterified, the DS is 3. Most of the commercially available modified starch has

low DS value being 0.1. DS of food grade OSA starch are typically low in the range of 0.01-0.03 (Sweedman, Tizzotti, et al., 2013).

The modification of starch with OSA provide the OSA starches. Chemical reaction during OSA modification is shown in **Figure 2** and chemical structure of OSA modified starch is exhibited in **Figure 3**. They are amphiphilic character due to attaching of hydrophobic octenyl group of OSA to the repeat glucose units of starch and improve the functional properties of native starch. They function as emulsion stabilizers and encapsulating agent and are widely used in the pharmaceutical, food and biodegradable plastics industries (Shi & He, 2012; Sweedman, Tizzotti, et al., 2013). Some commercial OSA starches include waxy maize (N-CreamerTM, purity GumTM, CAPSULTM, Hi-CAPTM and Mira-CapTM) or normal maize (DRYFLOTM) manufactured by National starch and Tapioca (ClearamTM) produced by Roqutte. There are narrow lists for the commercial products of OSA starches (Sweedman, Tizzotti, et al., 2013).

OSA substitution into starch hydroxyl groups results in an increase in hydrophobicity of starch which provide extreme surface active property (Nilsson & Bergenståhl, 2007), good pasting property (Dokić et al., 2012), a decrease in interfacial tension (Zhao et al., 2017), and emulsifying activity (Miao et al., 2014). OSA synthesis reaction is controlled by multiple factors such as OSA concentration, reaction pH, reaction temperature, reaction time, starch concentration, OSA: ethanol dilution ratio (Shi & He, 2012), and OSA addition method (Sui, Huber, & Bemiller, 2013). The OSA syntheis of starches using a one-factor-at-a-time is shown in **Table 2**. The previous studies of OSA esterification have been conducted on different starches such as Tapioca and rice starch (Thirathumthavorn & Charoenrein, 2006), waxy corn and amaranth starch (Bhosale & Singhal, 2006), potato starch (Hui et al., 2009), waxy maize starch (Bai, Kaufman, Wilson, & Shi, 2014; Bai & Shi, 2011; Bai, Shi, Herrera, & Prakash, 2011), waxy maize and sorghum starch (Sweedman, Hasjim, Tizzotti, Schafer, & Gilbert, 2013), corn starch (Zhu, Li, Chen, & Li, 2013), normal maize starch (Sui & BeMiller, 2013), mixture of granular waxy maize starch and soluble maltodextrin (Bai & Shi, 2013), normal cornstarch (Chang, He, Fu, Huang, & Qiu, 2014), Indica rice starch (Song, Pei, Zhu, Fu, & Ren, 2014), plantain starch (Bello-Flores et al., 2014), and sugary maize soluble starch and waxy maize starch

(Ye et al., 2017). The esterification reaction with OSA has been improved to speed up the reaction with the aid of enzymes such as lipase or protease and protect undesired side reaction for corn starch (Xu et al., 2012). However, there has been no extensive research for synthesis of the OSA modified pineapple starch (OSAPS).

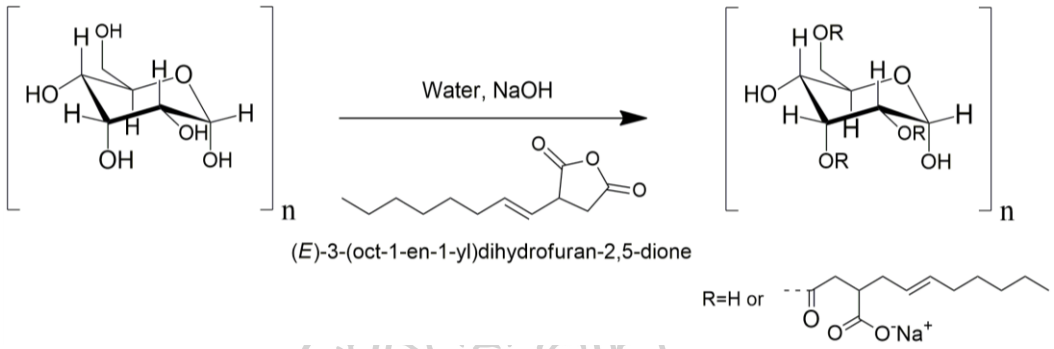

Figure 2 Schematic diagram showing OSA modification of starch.

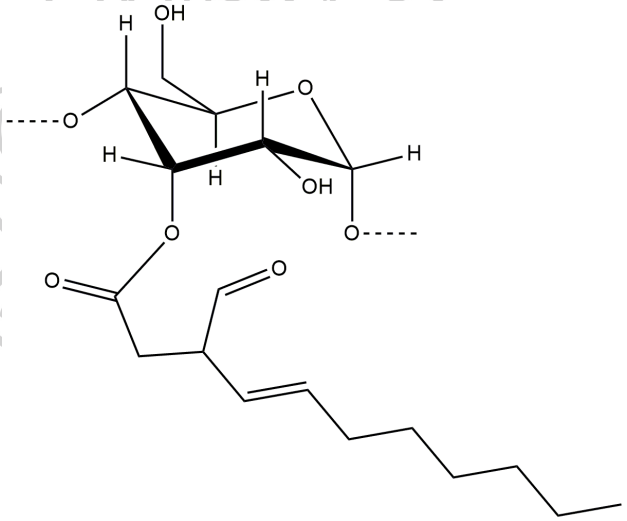

Figure 3 Chemical structure of OSA modified starch.

Table 2 OSA synthesis conditions of various starches using a one-factor-at a-time.

No.	Factors	Starch	Findings	References
1.	OSA concentration (1-3) Reaction pH (7-11) Reaction time (6-30 h) Reaction temperature (20-60˚C)	Amaranth and corn	OSA amaranth starch-OSA concentration (3%), pH 8, reaction time 6h and Temperature 30˚C,OSA corn starch-influenced factors are the same except reaction time of 24 h. (DS is 0.02 for both starhes)	Bhosale & Singhal, 2006
2.	OSA concentration (1-10%) Starch concentration (20-40%) Reaction pH (7-9.5) Reaction time (2-6h) Reaction temperature (25-45˚C) OSA dilution times (1:3, 1:5, 1:7 & 1:9)	Potato	OSA potato starch-OSA concentration (3%), starch concentration 35%, pH 8, reaction time 3h, Temperature 35˚C and OSA : ethanol=(1:5), (DS 0.117, RE 72%) OSA modification did not change on crystalline pattern High viscosity	Hui et al. 2009
3.	OSA concentration (3-50%) Starch concentration (30-60%) Reaction pH (7.5-9.5) Reaction time (0.5-2h) OSA addition method (poured, slow addition and slow addition plus predissolved in ethanol)	Soluble maltodex-trin and granular maize	OSA maltodextrin is DS 0.27 and OSA granular maize is DS 0.12, pH 7.5 & Time 1.5h for both, OSA addition was done for granular maize and slow addition/plus predissolve in ethanol was the same and better than pour condition. %RE increased with increasing OSA concentration, according to NMR, both differ in structural, OSA substitution at C2 and C3 in granular starch, all three positions of C-2, 3 & 6 for maltodextrin.	Bai & Shi, 2011

No.	Factors	Starch	Findings	References
4.	OSA concentration (1-5) Starch brand* Reaction pH (7-10) Reaction time (1-3h) Reaction temperature (30-50) OSA:ethanol dilution (1:3-1:7)	Cassava	OSA cassava starch-OSA concentration (3%), pH 8.2, reaction time 2.5 h, Temperature 38˚C and OSA : ethanol 1:5 (DS 0.0165 and RE 71%), *Starch brand affected OSA modification.	Shi & He, 2012
5.	OSA concentration (1-15%) Reaction time (0.5-2h)	Soluble maltodex-trin and granular maize	After 0.5h, OSA soluble maltodextrin had DS 0.02, 0.03, 0.08 and 0.1 for OSA concentration 1.5, 3, 9 and 15 %, respectively, After 0.5h, OSA granular maize stach DS produced DS 0.002, 0.005, 0.014 and 0.016 for the same four level of OSA%, OSA reacted more with soluble maltodextrin than semi-crystalline granular starch.	Bai & Shi, 2013
6.	OSA concentration	Maize	Emulsifying activity and zeta potential increased with respect to high DS, DS 0.0192 functioned as particle stabilizer for oil in water (o/w) emulsion.	Miao et al. 2014

OSA:octenyl succinic anhydride; DS: degree of substitution; RE: reaction efficiency; C 2, 3 & 6: carbon 2.3 and 6.

2.2.3 Acid modification

Acid modification is the use of mineral acids such as hydrochloric acid, sulphuric acid, nitric acid or phosphoric acid etc. to hydrolyze the native starch called acid hydrolysis of starch or named acid treatment (acidification) to starch or termed acid conversions (Singh & Ali, 2008; Wurzburg, 1986). Among several acids, hydrochloric acid is mostly used to be intended in paper, textile and foods (Singh & Ali, 2008) and pharmaceutical applications (Odeku & Akinwande, 2012; Okunlola & Akingbala, 2013). The characteristics and properties of native starches such as fluidity of hot paste, hot paste viscosity, intrinsic viscosity, molecular weight, iodine binding affinity, alkali number-reducing value, solubility, granule appearance and film strength are altered depending upon degree of acid modification. Several attempts have been made upon acid hydrolysis to modify and improve the functional properties of native starch for industrial applications (Wurzburg, 1986). Generally, molecular cleavage during acidification happens in amorphous part related to alpha 1,4 glucopyranose links in spite of some cleavage at alpha 1,6 glucosidic linkages (Wurzburg, 1986; Zhu, 2014).

The preparation of acid modified starches are very simple and use concentrated starch suspension of 36-40% solids and heated to a temperature of 40-60˚C which must be lower than gelatinization temperature of starch. Then mineral acid is added and stirred for specific period from an hour to several hours till the targeted degree of acidification and viscosity is achieved. After that, the neutralization of acid is done, the final product is filtered or centrifuged, washed and dried (Wurzburg, 1986). The acid modification reaction of starch is influenced by several factors such as type of mineral acid, the concentration of acid, the concentration of starch, reaction temperature and reaction time which depend on the manufacturer and targeted properties and applications (Okunlola & Akingbala, 2013; Wurzburg, 1986).

Singh and Ali studied the effect of different acids such as HCl, HNO_3, H_2SO_4 and H_3PO_4 on characteristics and properties of various starches such as wheat, millet, tapioca, green gram, chick pea and potato after acidification. Acid modification increased the alkali fluidity number (AFN) of native starches but highest in cereal and millet starches and AFN in the descending order of mineral acids: $HCl > HNO_3 > H_2SO_4 > H_3PO_4$ was obtained (Singh & Ali, 2008). Similarly, it has been

reported that alkali number of corn starch was increased after acidification (Wurzburg, 1986). The degree of hydrolysis was propotional to molecular weight of native starch in HCl and HNO_3 except other acids. In addition, intrinsic viscosity of modified starches by HCl and HNO_3 showed negative correlation to molecular weight against native starches (Singh & Ali, 2008). However, the intrinsic viscosity of corn starch was decreased as there might be effect of acidification on molecular weight (Wurzburg, 1986). During acid modification, starch solubility increased (Singh & Ali, 2008; Wurzburg, 1986). However, type of mineral acid affected starch solubility which showed highest in HCl and lowest for H_3PO_4 (Singh & Ali, 2008). Another characteristics of iodine affinity which can vary after acid modification depending on type of starch (Wurzburg, 1986). Singh and Ali also found that iodine binding capacity of various starch sources had no particular pattern after acidification (Singh & Ali, 2008).

Okunlola and Akingbala studied the effect of different factors such as nature (X_1), concentration of starch (X_2) and packing fraction (X_3) on crushing strength/friability ratio (CSFR), disintegration time and dissolution time of acid modified Chinese yam starch as a binder using 2^3 full factorial design and compared with native yam starch. The binding properties of acid modified yam starch was superior to native starch and showed increase in CSFR and disintegration time (Okunlola & Akingbala, 2013). Moreover, Odeku and Akinwande reported on efficiency of disintegration of acid modified yam starches of two species such as water and white yam which showed faster disintegration than acidified corn starch of paracetamol tablet (Odeku & Akinwande, 2012). Acid modified starches can be used as tablet disintegrant in pharmaceuticals (Odeku & Akinwande, 2012; Okunlola & Akingbala, 2013).

2.2.4 Oxidation

Oxidized starch derivatives are formed when the starch is treated with several oxidizing agents such as sodium hypochlorite, hydrogen peroxide, peracetic acid, permanganate, persulfate, halogens such as chlorine, bromine, hypobromite (Wurzburg, 1986), ozone and sodium periodate (Vanier, El Halal, Dias, & da Rosa Zavareze, 2017). Oxidation of native starch in the presence of sodium hypochlorite, hydroxyl groups in starch chain polymers are oxidized to carboxyl groups (Vanier et

al., 2017). Specifically, the aldehydic reducing end groups on amylose and amylopectin are easily oxidized to carboxyls rather than hydroxyls (Wurzburg, 1986). It has been reported that the physicochemical properties were improved by oxidation on a variety of starches which include potato starch with sodium hypochlorite (Fonseca et al., 2015), corn, pea and sweet potato with combination of copper sulphate ($CuSO_4$) as catalyst and oxidant hydrogen peroxide (H_2O_2) (Zhang, Wang, Zhao, & Wang, 2012). Peruvian carrot starch of two species with H_2O_2 (Matsugume et al., 2009) and maize starch using H_2O_2 combination with cross-linking (Liu et al., 2014).

Fonseca et al studied the effects of oxidation on physicochemical properties of potato starch using hypochlorite as oxidant by varying concentration of starch and active chlorine to make biodegradable films. Oxidized starch films having highest active chlorine levels showed lower tensile strength, water solubility and water vapor permeability when compared with native starch (Fonseca et al., 2015). The oxidized starches have been reported to be applied as films, adhesive agents in formulations and promoter for sustained release active agents in drug delivery system (Masina et al., 2017). Moreover, Zhang et al studied the effect of different factors such as starch type, the concentration of oxidizing agents, catalyst concentration, reaction temperature and reaction time on degree of oxidation (DO) and viscosity using $CuSO_4$ and H_2O_2. They found that DO differs with respect botanical origin of starch. DO increased with increasing oxidizing concentration, catalyst concentration, temperature and time. Combination with catalyst reduced the reaction time. However, oxidation leads to decrease in viscosity and thermal stability of oxidized potato starch (Zhang et al., 2012) as well as increase in paste clarity of two varieties of Peruvian carrot starch (Matsugume et al., 2009). Furthermore, the physicochemical properties of cross-linked oxidized maize starch was improved after dual modification, thereby leading to increase in solubility, light transmittance, the rate of retrogradation and showed the best stability after freeze-thaw (Liu et al., 2014).

2.2.5 Cross-linking

The most commonly used cross-linkers are sodium trimetaphosphate and phosphorous oxychloride. During cross-linking, they can react with starch hydroxyl groups of more than one and can form stabilized starch (Masina et al., 2017; Neelam et al., 2012; Singh & Ali, 2008), resulting in more hydrophilic, an increase in solubility and crystallinity of phosphate starches (Gutiérrez, Morales, Pérez, Tapia, & Famá, 2015). Jane et al has also reported that cross-linking primarily took place in amylopectin rather than amylose molecules leading to increase in viscosity of cross-linked corn starch (Gutiérrez et al., 2015). Therefore, highly crossed-linked starches namely distarch phosphates can dramatically alter the pasting and gelling properties of starches even though monostarch phosphate can have a high DS value. The DS for cross-linking is very low for food application (Singh & Ali, 2008). 3% of sodium trimetaphosphate for cross-linking of starch is limited to be intended for use in food industry and low DS was found to be 0.008 and 0.017 at 3% level of cross-linker sodium trimetaphosphate for modified cross-linked cassava and cush-cush yam, respectively (Gutiérrez et al., 2015).

Cross-linked taro, corn and potato starches can be used as food thickener due to high viscosity (Karmakar, Ban, & Ghosh, 2014). However, Sui and Bemiller found that the cross-linked maize and corn starches showed higher enthalpy value and lower viscosity when compared with OSA starches (Sui & BeMiller, 2013). Singh et al reported that highly cross-linked starches can produce incomplete gelatinization and decreased swelling due to high resistant heating temperature and time, thereby extreme resistant to swelling characteristics which concerns with decreased paste clarity (Singh, Kaur, & McCarthy, 2007). However, the reagent type, botanical source of starch, starch granules' appearance impact on rate and efficiency of chemical modification reaction (Sandhu & Singh, 2007).

Overall, the synthesis of hydroxypropylated starches are formed when the starch is treated with propylene oxide using strong alkalinization agent as a catalyst at 40˚C temperature in the aqueous slurry form of reaction condition (Masina et al., 2017; Neelam et al., 2012). The oxidized starches are derived from the reaction of starch with sodium hypochlorite. The reaction medium must be acidic medium to improve the rate of reaction. The oxidized starches are used in mayonnaise, salad

cream with desired low viscosity (Hoover et al., 2010). The acidified starches can be prepared by suspending the starch in the water to be concentrated and the concentrated starch suspension is reacted with HCl, HNO_3, H_2SO_4 and H_3PO_4 below gelatinization temperature. Generally, the substituted starches have been synthesized in an alkaline medium using alkyl or alkenyl succinic anhydride, monochloroacetic acid, propylene oxide. Similarly, cross-linked starches are also synthesized in the alkaline medium in the presence of phosphorus oxychloride, sodium trimetaphosphate and mixtures of adipic acid and acetic anhydride. The reaction time must be fixed and depends on targeted viscosity or degree of the process to be converted (Kaur et al., 2012; Neelam et al., 2012).

2.3 Design of experiments

Design of experiment (DoE) is a structured, organized method that is used to determine the relationship between the different factors (Xs) influencing the process and the response (Y). Nowadays, the DoE has becoming used in many fields of research and development to conduct as few experiments as possible because DoE requires only a small set of experiments and helps to reduce cost and time. The flow chart of DoE selection is shown in **Figure 4.**

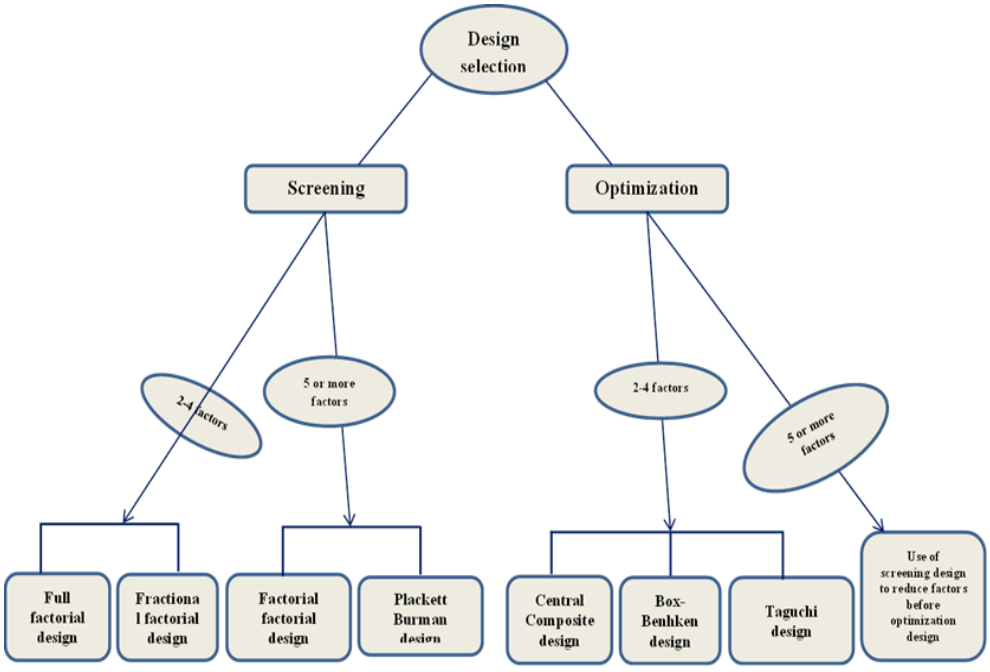

Figure 4 Flow chart of design selection, adapted from Sharif et al., 2014.

The screening or optimization designs can be selected for the experiments depending on the purpose to be studied. Screening designs include two level full factorial (2^k) where k is independent variables or factors, fractional factorial (2^{k-f}) where f is fraction of full factorial: f=1 (half-fraction) and Plackett-Burman (k=N-1) where N is number of the experimental runs. All of them require two levels for each factor (Candioti, Zan, Camara, & Goicoechea, 2014; Sharif et al., 2014). The advantages and disadvantages of these three designs are summarized in **Table 3.**

Table 3 Advantages and disadvantages of screening designs from Sharif et al., 2014.

Design	Advantages	Disadvantages
Two level full factorial	The main effect and the interaction of factors can be identified	The design is not feasible for screening more than sixteen factors
Two level fractional factorial	Less number of experimental runs as compared to full factorial design for the equal number of factors	The interactions fator effect is limited and may be misguided as there is no measurement of error in this design
Plackett-Burman	Large number of variables can be examined with a very few experimental runs	The design is only useful to identify significant main effect and do not consider any two factors interaction effect

The optimization or response surface designs are used to determine the optimum operating conditions for the system. RSM is an approach to optimization. RSM is a gathering of mathematical and statistical methods. It is useful for modeling and analysis in applications where a response or a set of responses are influenced by several variables. RSM is a sequential procedure. Factorial or fractional factorial experiment can be planned to find the relationship between the response and independent variables. If a response is well modeled by a linear function of independent variables, the function is the first-order model and the data fits to a linear model. If curvature is present in the system, then a model such as the second-order

model may be used and fits a quadratic. The most widely used optimization designs include full factorial design at three levels (3-FFD), Box–Behnken design (BBD), central composite design (CCD), Doehlert matrix design (DMD) etc. as shown in **Table 4**.

Table 4 Most commonly used optimization designs adapted from Candioti et al., 2014.

Design	Type of factors	Factor levels	Experimental number	Rotatability	Orthogonability
CCD	Numerical Categorical	5	2^k+2k+C_p	Yes-No[a]	Yes-No[b]
BBD	Numerical Categorical	3	$2k(k-1)+C_p$	Yes	Yes
3-FFD	Numerical Categorical	3	3^k	No	Complete orthogonal
DMD	Numerical Categorical	Different for each factor	k^2+k+C_p	No	No

[a]Rotatable if $\alpha=(f)^{1/4}$, where α is star point distance and f is the number of factorial point.
[b]Orthogonal if $C_p \approx \alpha\sqrt{f+4-f}$, where C_p is the number of center points.

2.3.1 Full factorial design

Three level full factorial design is a design matrix that can be used for optimization but its application in RSM is limited in case of higher factor number more than two is required due to high experimental runs which can be calculated from $N=3^k$. For example, in case of 3^3 design, a number of design experiments is large (27 runs) to obtain a complete three level full factorial design for three factors, thereby its efficiency may be lost in analysis of quadratic modeling, which becomes its disadvantages over other designs of small experiments such as BBD, CCD and so on (Bezerra et al., 2008). 3^k designs can be used in area of analytical chemistry especially chromatography.

2.3.2 Box-Behnken design (BBD)

The BBD contains three levels factorial design points and can be rotatable. This design has no experimental points at extreme condition because BBD does not include combinations of highest and lowest level for every factor. BBD must have at least three factors and the experiments can be calculated using $N=2k(k-1)+C_p$, where k is the number of factors and C_p is the replicate number of the central points in the design. In this way, BBD can reduce the experiments number as compared to 3^k design for large number of factors. Therefore, the efficiency of BBD is better than 3^k design and satisfactory results can be obtained due to absence of design points at extreme condition (Bezerra et al., 2008). In addition, the significant effects can be examined by analysis of variance (ANOVA) and optimal response can be analysed using mathematical regression equation from model (Sharif et al., 2014).

2.3.3 Central composite design (CCD)

The CCD includes two-level factorial design points such as low and high expressed as (–1 and +1), "star" points with low and high alpha level (± α) and center points with all factors assigned to 0. The α value determines the location of the star points in the design. The rotatable CCD require an experimental runs according to $N= 2^k +2k+C_p$. The alpha values base on the number of factorial points (n_f) and can be achieved using $\alpha=(n_f)^{1/4}$.

There are three types of CCDs which include (i) Circumscribed, (ii) Inscribed and (iii) Face centered depending on the location of the star points. Central Composite Circumscribed (CCC) type is the original of CCD and the star points for the low and high settings for all factors. Central Composite Inscribed (CCI) design is derived from CCC design in which each factor is divided by α value producing the CCI design. Both CCC and CCI require five levels for each factor. Central Composite Face centered (CCF) design in which the star points are located at the center of each face of the cube (http://www.itl.nist.gov). This design has only three levels for each factor, so $\alpha = \pm 1$. It is the advantage of CCF but this design cannot be rotatable (Bezerra et al., 2008). Song et al. and Abiddin et al. used CCD for optimization of reaction conditions of OSA esterification on *Indica* rice starch and sago starch from *Metroxylon sagu*, respectively whereas Wang et al. employed CCF to optimize the OSA esterification

reaction condition of corn starch. Segura-campos et al. reported modification of *Phaseolus lunatus* starch using 2^3 factorial design. The summary of OSA synthesis of starches using experimental design is shown in **Table 5**. However, the modification condition of OSAPS using experimental design has not been researched yet.

Table 5 Summary of OSA synthesis conditions of starches using experimental design.

No	Starch type	Parameters	Response	Design used	Model	Findings (ANOVA output)	Reference
1.	*Indica* rice starch	Reaction Temperature (26-43 ºC) (X_1) Reaction pH (6-10) (X_2) Starch concentration (26 -43%) (X_3)	DS, RE	Rotatable CCD	Quadratic	X_1^2, X_2^2, X_3^2 Significant influence on OSA modification at 95% level	(Song et al., 2006)
2.	*Phaseolus Lunatus*	OSA concentration (1-3%) (A) Reaction pH (7-9) (B) Reaction time (30-60 mins) (C)	Succinyl group (%)	2^3 factorial	First order polynomial model	A, C, AB, BC, ABC	(Segura-Campos et al., 2008)
3.	Corn starch	OSA/ Starch ratio(3:1-5:1) (X_1) Reaction Temperature (90-100ºC) (X_2) Reaction time (2-3 h) (X_3)	DS	CCF	Quadratic	X_1, X_2, X_3, X_2X_3, X_1^2, X_2^2, X_3^2	(Wang et al., 2011)
4.	Sago starch	OSA concentration (1-6%) (X_1) Reaction pH (5-10) (X_2) Reaction time (6-24 h) (X_3)	DS	Rotatable CCD	Quadratic	X_1, X_2, X_3, X_2^2,X_3^2, X_1X_3	(Abiddin et al., 2015)

ANOVA: analysis of variance ; CCD: central composite design; CCF: central composite face centered design.

2.4 Nanosized delivery vehicles for poorly water soluble drugs

Nowadays, formulation strategies still have challenges for pharmaceutical product development to solve the low aqueous solubility problem of biopharmaceutical classification system (BCS) class II drugs in order to raise dissolution and improve oral bioavailability of poorly water soluble drugs for clinical use. Nanosized delivery vehicles have evolved as new nanoplatforms through nanonization techniques for poorly water soluble drugs. These nanoplatforms include nanocrystals, polymeric micelles and nanoemulsion (Chen, Khemtong, Yang, Chang, & Gao, 2011). Nanocrystal is a common technique and popular in pharmaceutical area as it is very suitable for most drugs having poor solubility issues. Fu et al., proposed various formulation techniques such as solid dispersion, micronization and nanocrystals loaded with lacidipine and reported comparative *in vitro* and *in vivo* assessment of the three formulations. Micronized and nanocrystals lacidipine made by different milling of jet and bead produce 112,00 nm and 623 nm, respectively and they differ greatly in particle size. Among three formulations, commercial lacidipine solid dispersion (lacipril®) showed higher dissolution whereas nanocrystals provided more enhancement of oral bioavailability of lacidipine (Fu et al., 2015). Therefore, unspecial form of nanocrystals are not available for anti-cancer drugs as their dissolution rate is very fast and lack of controlled release kinetics. Moreover, nanocrystals needs high energy consumption for particle size reduction to nano range which is not cost-effective. Furthermore, nanocrystals formation has special requirements for stability (Lu & Park, 2013).

After nanocrystals, further two nanotechniques include polymeric micelle and nanoemulsion which are capable of solubilizing the poorly water soluble drugs in the hydrophobic core. The preparation methods involve dialysis and emulsification process for polymeric micelle and high and low energy methods for nanoemulsion.

2.4.1 Nanoemulsion

Nanoemulsion is thermodynamically stable colloidal system containing two immiscible phases such as an oil phase with droplet size in the range of 20-500 nm (Debnath et al., 2011; Gupta et al., 2016) and an aqueous phase as continuous phase together with emulsifier (Gupta et al., 2016; Hanlor et al., 2018). The nanoemulsions need external mechanical shear to rupture larger droplets into smaller

ones. This process is said to be “emulsification”. They do not form spontaneously. Alternative terms for nanomeulsions include miniemulsions, submicron emulsions and ultrafine emulsions. Based on the composition of oil/water portion, the nanoemulsions are of three types such as oil-in-water, water-in-oil and bicontinuous nanoemulsions (Hanlor et al., 2018; Mason, Wilking, Meleson, Chang, & Graves, 2006). The advantages and disadvantages of nanoemulsions are as follows:

Advantages of nanoemulsions

- High drug loading can be achieved with nanoemulsion.
- It can be used for various routes of administration.
- It can enhance oral bioavailablity by increasing gastrointestinal tract (GI) and mucous permeability which can be beneficial to BCS class IV drugs.
- It is cost effective.
- It is non-toxic and non-irritant.
- It can have higher absorption after oral administration due to small nano droplet size having high surface area.
- It is also one of the taste masking techniques. (Chen et al., 2011; Hanlor et al., 2018; Lu & Park, 2013)

Disadvantages of nanoemulsions

- It can cause flocculation and coalescence.
- Large amount of surfactant or emulsifier are required to provide stablility of nanodroplet.
- It has poor stability in systemic circulation.
- The choice of non-toxic surfactant is also necessary for pharmaceutical applications. (Chen et al., 2011; Hanlor et al., 2018)

It has been reported on comparison of the therapeutic efficacy, toxicity and drug resistance of polymeric micelles and nanoemulsions as drug carriers for anti-cancer paclitaxel. Micelles with elastic cores was superior to solid cores as drug carriers. Both polymeric micelles and nanoemulsions showed high therapeutic

efficacy but nanoemulsions showed lower systemic haematotoxicity than micelles (Gupta, Shea, Scafe, Shurlygina, & Rapoport, 2015).

The nanoemulsions composed of oil phase such as organic solvents or vegetable oils and water phase plus surfactants/emulsifiers. The organic solvents used in nanoemulsion preparation include chloroform, tetradecane, dichloromethane, n-hexane etc. (Silva et al., 2011). It has been reported that Burapapadh et al fabricated ITZ-loaded nanoemulsions containing pectin as polymeric emulsifier using chloroform as oil phase (Burapapadh et al., 2010). Rao & McClements studied a model oil/water/surfactant system in which tetradecane as oil phase and surfactant displacement approach were used for phase inversion temperature nanoemulsion and improved its stability (Rao & McClements, 2010). Moreover, Li et al also developed a novel double nanoemulsion of *Hohenbuehelia serotina* polysaccharide containing dichloromethane as oil phase by using high speed homogenization method and optimized the preparation condition of nanoemulsion (Li, Wang, & Wang, 2017). However, the toxic potential of organic solvents and ease of their removal from formulation should be considered when formulating nanoemulsions.

Nowadays, use of organic solvents have been replaced by vegetable oils. The oils used in preparation of nanoemulsions are captex 355, captex 8000, capryol 90, castor oil, cinnamon oil, olive oil, oleic acid, isopropyl myristate, myritol 318, medium chain triglyceride (MCT), sefsol 218, triacetin and witepsol. Selection of suitable oil is an important criterion in oral nanoemulsion development as the ability of nanoemulsion to maintain the drug in the soluble form is strongly governed by drug solubility in oil phase. Water-in-oil (w/o) nanoemulsions are designed for hydrophilic drugs whereas oil-in-water (o/w) nanoemulsions are best choice for hydrophobic drugs (Gupta et al., 2016; Hanlor et al., 2018).

The unique property of oil phase not only solubilize the lipophilic drug molecule but also penetrate the cell wall, thereby improving the absorption through lipid layer present in the body (Hanlor et al., 2018). Liang et al constructed oil-in-water β-carotene nanoemulsion containing OSA modified waxy maize starch as stabilizer and MCT as oil phase and improved bioaccessibility of β-carotene (Liang, Shoemaker, Yang, Zhong, & Huang, 2013). Moreover, Ali & Hussein prepared oral nanoemulsion of candexartan cilexitil by varying cinnamon oil ratio, polysorbate 80

with different poloxamer type and enhanced its solubility, dissolution and then modified drug release characteristics (Ali & Hussein, 2017).

After oil, surfactant is also one of the components of nanoemulsion formulation. There are three classes of surfactants such as non-ionic, cationic and anionic surfactants. O/W nanoemulsions can be divided into three classes namely neutral o/w nanoemulsion, cationic o/w nanoemulsion and anionic o/w nanoemulsion based on the type of surfactant used. Polysorbate 20, polysorbate 60, polysorbate 80, cremophor, polyethylene glycol (PEG) MW>4000, different types of Imwitor® and poloxamar are commonly used surfactant. Choice of surfactant in nanoemulsion system should be taken into account carefully as they have toxicity concerns. Use of significant excess amount of surfactant can irritate the gastrointestinal tract and skin for oral and topical administration, respectively (Hanlor et al., 2018). However, non-ionic surfactants are suitable for oral use due to their low toxicity. In addition, they are stable to the effects of heat, pH change and high concentration of electrolytes (Aulton, 1988).

Cosurfactants are also added to nanoemulsion formulation to reduce the surfactant concentration (Talegaonkar, Mustafa, Akhter, & Iqbal, 2010). It has been reported that combination of surfactant polysorbate 20 (19%w/w) and cosurfactant carbitol (19%w/w) produced thermodynamically stable nanoemulsion which increased solubility and enhanced the oral bioavailability of atorvastatin (Talegaonkar et al., 2010). Kumar and Pathak prepared o/w nanoemulsion using polysorbate 80 as surfactant and combination of cosurfactants such as PEG and Transcutol and improved drug release characteristics (Kumar, Pathak, & Misra, 2009). An *in vitro* and *in vivo* assessment of silymarin could be enhanced by nanoemulsion formation containing polysorbate 80 and ethanol as co-surfactant which was reported by (Parveen et al., 2011). Similarly, Chhabra et al fabricated amlodipine loaded nanoemulsions using combination of polysorbate 80 and ethanol and increased bioavailability of amlodipine (Chhabra, Chuttani, Mishra, & Pathak, 2011). Moreover, Jain K et al found that an increase in absorption of atorvastatin from nanoemulsion using combination of surfactants polysorbate 80 plus Brij 35 and together with cosurfactant ethanol improved oral bioavailability of atorvastatin (Jain et al., 2013). Harika et al observed that amphotericin B nanoemulsion containing

polysorbate 20 and ethanol as cosurfactant showed higher drug release than suspension form (Harika, Debnath, & Babu, 2015). However, Abbas et al and Sharif et al prepared curcumin loaded nanoemulsion and nanoemulsion containing eugenol using OSA starch as emulsifier with free of surfactant but the success in nanosized emulsion preparation was achieved by using ultrasonic and microfluidizer, respectively (Abbas et al., 2014; Sharif et al., 2017). Therefore, method of preparation is also essential to form nanoemulsion system.

Generally, nanoemulsions are prepared by low and high energy method. A variety of researches have been performed on preparation of nanoemulsion using low energy method (i.e. spontaneous emulsification) especially together with combination of surfactant and co-surfactant (Bhattacharjee, Verma, Verma, Singh, & Chakraborty, 2017; Chhabra et al., 2011; Harika et al., 2015; Kotta, Khan, Ansari, Sharma, & Ali, 2015; Kumar et al., 2009; Parmar, Patel, & Sheth, 2015; Parveen et al., 2011; Talegaonkar et al., 2010). High energy techniques involving high pressure homogenization and microfludization can provide extremely fine droplets of emulsion with great efficiency and can be used in both laboratory and industrial scale. The only disadvantage is use of high energy, intense turbulent flow, hydraulic shear force and producing high heat during processing of emulsion (Debnath et al., 2011). Extreme shear is one of the factors controlling to rupture microscale droplets into nanodroplets.

High speed rotor/stator devices such as Ultra-Turrax can not provide good dispersion in terms of droplet size when compared with other high energy approaches (Silva et al., 2011). Nevertheless, Burapapadh et al proved that nanoemulsion could be successfully prepared by simple homogenization method to avoid high pressure condition (Burapapadh et al., 2010). Li et al also developed a novel double nanoemulsion of *Hohenbuehelia serotina* polysaccharide by using Ultra-Turrax homogenizer (Li et al., 2017). However, to prevent shear-induced coalescence, the continuous phase requires a significant excess of surfactant. They can easily and quickly adsorb onto the surfaces of newly fresh created droplets (Mason et al., 2006). Mixture of emulsifier and surfactant can also be used to rupture the droplets effectively. The preparation of oral nanoemulsion loaded with candexartan cilexitil containing cinnamon oil, combination of surfactant polysorbate 80 and emulsifier poloxamar has been reported by (Ali & Hussein, 2017).

Although lower concentrations of protein-based emulsifiers are required, they are prone to denaturation and precipitation due to their sensitivity to higher processing temperatures and the pH fluctuations of medium, respectively (Mason et al., 2006). OSA starches are extensively used due to their advantages such as stability against high temperature, broad pH and ionic strength and tasteless (Sweedman, Tizzotti, et al., 2013). It has been reported that OSA starch could be applied as emulsifiers (Pongsamart et al., 2016), stabilizers for oil-in-water emulsions (Dokić et al., 2012; Miao et al., 2014; Sweedman et al., 2014; Zhao et al., 2017), an encapsulating agent for vitamin E nanocapsule (Hategekimana et al., 2015) and nanoemulsion stabilizer for poorly water soluble curcumin (Abbas et al., 2014). However, the functional properties of octenyl succinate pineapple starch or OSAPS have not been investigated as nanoemulsion stabilizer and the application of the OSAPS as stabilizer in nanoemulsion has not been researched.

Nowadays, nanoemulsions have been focused to be applied in different fields of biology, food and pharmaceuticals because nanoemulsions have attracted in research as a drug delivery carrier for poorly water soluble drugs to improve their bioavailability (Gupta et al., 2016). Poor solubility of drugs in aqueous media becomes the major problem which not only affects the bioavailability but also efficacy of the drug in the human body. Such drug molecules still have challenges for product development to use clinically since they have poor dissolution or poor permeability which leads to poor bioavailability issues (Patravale et al., 2004).

2.5 Itraconazole

Itraconazole (ITZ) is one of the poorly water soluble drugs belonging to BCS class II with low aqueous solubility and high permeability (Amidon, Lennernas, Shah, & Crison, 1995). It is a synthetic triazole derivative having 3 nitrogens in ring (triazole ring), an azole antifungal agent. The drug's characteristics is white to slightly yellowish color, powder in nature, water insolubility and very sparingly soluble in alcohol. Typically, ITZ is insoluble in water with a solubility of ~1ng/mL at neutral pH whereas its maximum solubility in gastric acid of 4µg/mL at pH 1.0. It has high molecular weight (705.641 g/mol) and molecular formula $C_{35}H_{38}Cl_2N_8O_4$. ITZ chemical structure is shown in **Figure 5.** It is a weak basic drug with a pKa of 3.7 and

highly liphophilic with a log *P* of 7.13 (Peeters, Neeskens, Tollenaere, Van Remoortere, & Brewster, 2002). ITZ blocks the synthesis of ergosterol in fungal cell membrane resulting in death of fungi and used in oropharyngeal, a variety of fungal diseases and opportunistic infections of immuno-compromised patients due to its activity against various pathogens, including *Aspergillus* species (Glasmacher & Prentice, 2006). Commercially available ITZ preparations are oral capsules 100 mg (Sporanox, Ortho-McNeil-Jansssen) and oral solution 10 mg/mL (Sporanox, Centocor Ortho Biotech). ITZ also has been administered by IV infusion; however, as IV preparation of the drug is no longer commercially available in the US (McEovy et al., 2016).

Recently, attempts have been made on research of ITZ challenges for oral dosage forms using different formulation strategies like pectin-based nanoemulsion (Burapapadh et al., 2010), nanosuspension (Cerdeira et al., 2013), nanocrystals (De Smet et al., 2014), solid dispersion (Engers et al., 2010; Zhang et al., 2013), dissolving tablet (Piao et al., 2014), cyclodextrin based solution (Berben et al., 2017). However, the success in case of ITZ with increased dissolution rate is limited Nevertheless, nanoemulsions could overcome this limitation by increasing dissolution rate and enhancement of oral bioavailability for amlodipine (Chhabra et al., 2011), Mebudipine (Khani, Keyhanfar, & Amani, 2016), and atenolol (Bhattacharjee et al., 2017) as compared to the conventional preparations and/or pure drug have been reported. Therefore, ITZ is a good model drug for preparation of nanoemulsions due to its insolubility nature in gastrointestinal fluid.

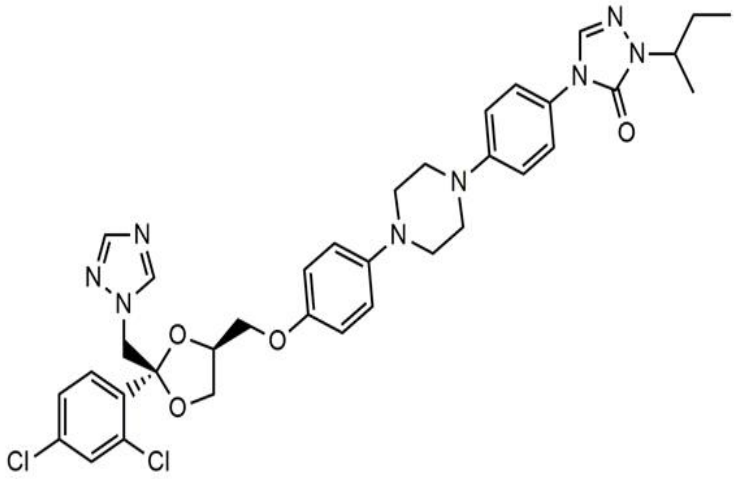

Figure 5 Chemical structure of ITZ.

Chapter 3
Materials and methods

3.1 Materials

3.1.1 Pineapple starch extracted from stem and rhizome of *Ananas comosus* (L.) Merr (Bromeliaceae) (Lot No. 0010)

3.1.2 Sodium hydroxide (Lot No. B0503198 028, Merck, Germany)

3.1.3 2-Octenyl succinic anhydride (Lot No. WW2JMBM, Tokyo Chemical Industry (TCI) Co., Ltd., Japan)

3.1.4 Silver nitrate AR (Lot No. 08G100014, VWR Prolabo, Belgium)

3.1.5 Phenolphthalein AR (Lot No. 318763/2 892, Fluka Chemika, Germany)

3.1.6 Hydrochloric acid 37% (Lot No. 09070158, RCI Labscan Ltd., Thailand)

3.1.7 99.99% ethanol AR (Lot No. K40541983-948, Merck, Germany)

3.1.8 2-propanol (Isopropyl alcohol) AR (Lot No. 165341-1220, QReC, New Zealand)

3.1.9 Potassium bromide (Lot No. B0517507-025, Merck, Germany)

3.1.10 Itraconazole Pharmaceutical grade (Megafine Pharma (P) Ltd, India)

3.1.11 Methanol HPLC grade (Lot No.1692260, Fisher Scientific, UK)

3.1.12 Acetonitrile HPLC grade (Lot No. 10913991 740, Merck, Germany)

3.1.13 99.5% Diethylamine (Lot No. 0000111700, Panreac Quimica SA, E.U)

3.1.14 Orthophosphoric acid (Lot No. AA311005, Ajax Finechem, Australia)

3.1.15 Almond oil (Lot No. 5113808, P.C. Drug Center, Thailand)

3.1.16 Castor oil (Lot No. 1707140, P.C. Drug Center, Thailand)

3.1.17 Oleic acid (Lot No. 0001021940, AppliChem Panreac ITW Co., Ltd., Germany)

3.1.18 Peanut oil (Lot No. 2007021308, P.C. Drug Center, Thailand)

3.1.19 Sesame oil (Lot No. 61030011-1/0105, P.C. Drug Center, Thailand)

3.1.20 Sunflower oil (Lot No. 5718102, P.C. Drug Center, Thailand)

3.1.21 Sodium lauryl sulphate (Lot No. 0016122486, P.C. Drug Center, Thailand)

3.1.22 Polysorbate 80 (Tween 80®) (Lot No. 0000703038, AppliChem Panreac ITW Co., Ltd., Germany)

3.1.23 Sodium chloride (Lot No. 1105238, Ajax Finechem Pty Ltd., New Zealand)

3.2 Equipments

3.2.1 Analytical balance (Sartorius, CP 224s, Germany)

3.2.2 100-mesh nylon sieve (0.15 mm opening)

3.2.3 0.22-µm nylon membrane filter (WHATMAN)

3.2.4 0.45-µm nylon membrane filter (WHATMAN)

3.2.5 pH meter (Sartorius, PP15-P11, Germany)

3.2.6 Hot air oven (D63450, Heraeus, Germany)

3.2.7 Centrifuge (320r, Hettich, Germany)

3.2.8 Water-bath (SPC Group Analog Heat, Model No. AH-30-110, Scientific Promotion Co., Ltd., Thailand)

3.2.9 Moisture analyzer (Sartorius, L420s, Germany)

3.2.10 Magnetic stirrer (Aris, Model M-IX, Thailand)

3.2.11 Rheometer (Kinexus, Malvern Instruments Ltd., UK)

3.2.12 Drop shape instrument (FTA 1000, First Ten Angstorms, USA)

3.2.13 Desktop X-ray diffractometer (Miniflex II, Rigaku Corp. Tokyo, Japan)

3.2.14 Differential Scanning Calorimeter (Pyris Sapphire DSC, Standard 115V, Perkin Elmer instruments, Japan)

3.2.15 Scanning Electron microscope (SEM) (LEO 1450 VP, Zeiss, USA)

3.2.16 Fourier transform infrared spectrometer (FTIR) (NICOLET 4700; Thermo Electronic Corporation, USA)

3.2.17 Incubator shaker (WY-200, COMECTA, S.A, Spain)

3.2.18 Vortex mixer (VX-100, Gibthai, Thailand)

3.2.19 Ultrasonic cleaner (230D, CREST Ultrasonics, Malaysia)

3.2.20 High Performance Liquid Chromatography (Agilent Technologies 1100 series, USA)

3.2.21 Homogenizer (IKA®, T25 Digital Ultra Turrax®, Germany)

3.2.22 Spectrophotometer (T60 UV/Vis spectrophotometer, PG Instruments Ltd, UK)

3.2.23 Particle size analyzer (Zetasizer Nano-ZS, Malvern Instrument, Worcestershire, UK)

3.2.24 Laminar air flow cabinet (Hera Safe, Heraeus, Germany)

3.2.25 Dissolution testor (DT70, Erweka, Germany)

3.3 Methods

3.3.1 Part I: Optimization of reaction conditions of octenyl succinic anhydride (OSA) modified pineapple starch (OSAPS) using fractional factorial central composite face-centered (CCF) design

3.3.1.1. Synthesis of pineapple starch with OSA

OSAPS was prepared according to the procedure described by (Hui et al., 2009). The schematic diagram for synthesis of OSAPS is shown in **Figure 6**. Briefly, aqueous suspension (30% w/w) of pineapple starch was prepared using a magnetic stirrer. The 3% w/v NaOH solution was added to starch suspension at the pH of 7-9 in order to initiate the reaction for starch in an alkaline medium. OSA [1-30%, in proportion to the starch weight; dry basis] was diluted five times with 99.99% ethanol (v/v) and was added dropwise to the previous mixture for 2 h. The reaction was continued for the time of 2-5 h at the temperature of 25-50 °C. After the reaction completed, the pH value was adjusted to 6.5 with 3% w/v HCl solution. Subsequently, the mixture was centrifuged at 8000 rpm for 5 min and washed twice with distilled water. The mixture was washed twice with 70% ethanol (v/v). Finally, the solids were dried at 50 °C for 24 h and passed through a 100-mesh sieve.

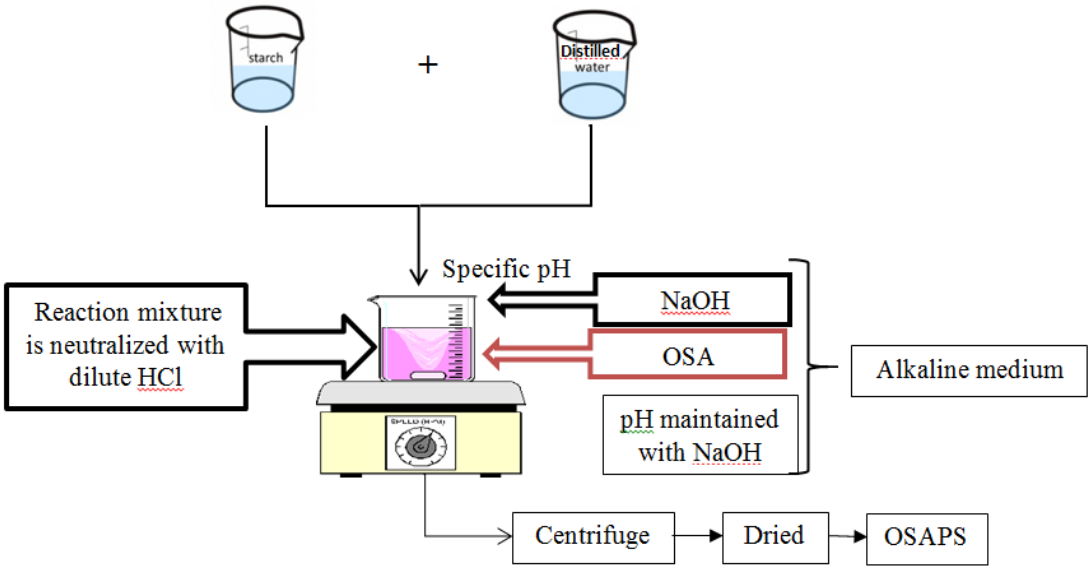

Figure 6 Schematic diagram for synthesis of OSAPS.

3.3.1.2 Optimization of the OSA synthesis conditions of pineapple starch

A fractional factorial CCF design was generated using the Design-Expert® software package (version 8.0.7.1; Stat-Ease, Inc., USA) and used for optimizing the OSA synthesis conditions of pineapple starch. The four independent variables were OSA concentration (X_1), pH of the reaction system (X_2), reaction temperature (X_3), and reaction time (X_4). RSM was used to estimate the effects of independent variables on the response variables. Randomization of experiments is required to minimize the effects of unexplained variability in the observed responses due to the presence of extraneous factors (Samavati, 2013). A set of 21 experiments was performed by half-fractionating the full factorial (i.e. f=1 for half-fraction), with each variable varied at three coded levels: −1, 0, and +1. The independent variables and the corresponding levels used in the CCF design are listed in **Table 6**. The applied formula for fractional factorial CCF design was $N=2^{k-f}+2k+C_p$, where N is number of the experimental runs, k is number of independent variables, f is fraction of full factorial and C_p is the replicate number of central points. Therefore, the design comprises eight factorial points, eight axial points, and five repetitions at the central points and the experiments were conducted randomly according to CCF design with coded and experimental values shown in **Table 7**. The results were analyzed by analysis of variance (ANOVA). The quadratic equation for the four independent variables can be expressed as follows (Bezerra et al., 2008):

$$Y = \beta_0 + \sum_{i=1}^{k} \beta_i X_i + \sum_{i=1}^{k} \beta_{ii} X_i^2 + \sum_{1 \le i \le j}^{k} \beta_{ij} X_{ij} \quad (1)$$

where Y represents the predicted response variables; β_0 is the intercept; β_i, β_{ii}, and β_{ij} are the regression coefficients of the model; and X_i and X_j (i = 1, 2, 3, 4; j = 1, 2, 3, 4) represent OSA concentration, pH, reaction temperature, and reaction time, respectively. The correlation coefficient (r^2) and the root-mean-square error (RMSE) were used for evaluating the polynomial model. The applied equations for r^2, RMSE , predicted r^2 (*Pred* r^2) and standard error for prediction are as follows (Casella & Berger, 2002; Montgomery, 1998):

$$r2 = \frac{SSR}{SST} = 1 - (SSE/SST) = 1 - \frac{\sum_{i=1}^{n}(Y_{expi} - Y_{predi})2}{\sum_{i=1}^{n}(Y_{expi} - \bar{Y})2} \quad (2)$$

where SSR is regression sum of squares, SSE is sum of squares error or residual, SST is sums of square of total, Y_{expi} is experimental value, Y_{Predi} is predicted value and $\bar{Y}$ is mean response value.

$$Pred\ r2 = [1 - (PRESS/SST)] * 100 \quad (3)$$

where PRESS is predictive residual error sum of squares.

$$RMSE = \frac{\sqrt{\sum_{i=1}^{n}(Y_{expi} - Y_{predi})2}}{T} \quad (4)$$

where T is total number.

$$Standard\ error\ for\ prediction = \frac{\sqrt{\sum_{i=1}^{n}(Y_{expi} - Y_{predi})2}}{t} \quad (5)$$

where t is total test number.

The desirability function approach was used for the optimization of multiple response processes (Myers, Montgomery, & Anderso-Cook, 2009). It is based on the idea that the quality of a product or process that has multiple quality characteristics, with one of them outside of some desired limits, is completely unacceptable. The method finds operating conditions x that provide the most desirable response values.

Table 6 Fractional factorial CCF design used for OSA synthesis of pineapple starch.

Independent variables	Symbols	Levels		
		−1	0	+1
OSA concentration (%)	X_1	1	15.5	30
pH	X_2	7	8	9
Temperature (°C)	X_3	25	37.5	50
Time (h)	X_4	2	3.5	5
Response variables				
Degree of substitution	Y_1			
Surface tension	Y_2			
Enthalpy	Y_3			

Table 7 Fractional factorial CCF Design of coded and experimental values of four independent variables for OSA synthesis of pineapple starch.

Std	Run	Coded values				Experimental values			
		X_1	X_2	X_3	X_4	OSA (%w/w)	pH	Temperature (°C)	Time (h)
1	9	1	1	1	-1	30	9	50	2
2	21	1	1	-1	-1	30	9	25	2
3	1	1	-1	1	1	30	7	50	5
4	6	-1	1	-1	1	1	9	25	5
5	7	1	-1	-1	1	30	7	25	5
6	10	-1	-1	1	-1	1	7	50	2
7	2	-1	1	1	1	1	9	50	5
8	16	-1	-1	-1	-1	1	7	25	2
9	11	-1	0	0	0	1	8	35.5	3.5
10	17	1	0	0	0	30	8	35.5	3.5
11	3	0	-1	0	0	15.5	7	35.5	3.5
12	5	0	1	0	0	15.5	9	35.5	3.5
13	13	0	0	-1	0	15.5	8	25	3.5

14	4	0	0	1	0	15.5	8	50	3.5
15	14	0	0	0	-1	15.5	8	35.5	2
16	18	0	0	0	1	15.5	8	35.5	5
17	12	0	0	0	0	15.5	8	35.5	3.5
18	20	0	0	0	0	15.5	8	35.5	3.5
19	19	0	0	0	0	15.5	8	35.5	3.5
20	15	0	0	0	0	15.5	8	35.5	3.5
21	8	0	0	0	0	15.5	8	35.5	3.5

3.3.1.3 DS and RE determination

DS is the average number of sites per anhydroglucose unit bearing substituent groups. The DS of OSAPS was analyzed by the titrimetric method reported by (Hui et al., 2009). The schematic diagram of DS determination is shown in **Figure 7**. An OSAPS sample (5 g, dry weight) was accurately weighed and dispersed by stirring for 10 min in 100 mL of 90% v/v aqueous isopropyl alcohol solution. Then, 25 mL of 2.5 M HCl-isopropyl alcohol solution was added to the suspension. The suspension was stirred for additional 30 min and filtered. The residue was washed with 90%v/v (aqueous) isopropyl alcohol solution until no more Cl^- could be detected using a 0.1 M $AgNO_3$ solution. Starch was redispersed in 300 mL of distilled water, and the dispersion was then heated in a boiling water bath for 20 min. The starch solution was titrated with 0.1 M standard NaOH solution using phenolphthalein as an indicator. NPS served as a blank and was simultaneously titrated. DS was calculated using the following equation:

$$\mathrm{DS} = \frac{0.162\times(A\times M)}{1-[0.210\times(A\times M)/W]} \quad (6)$$

where A is the titration volume of NaOH solution (mL),

M is the molarity of NaOH solution, and

W is the dry weight (g) of the OSAPS

The RE will be calculated as follows:

$$RE = \frac{Actual\ DS}{Theoretical\ DS} \text{ x } 100\% \quad (7)$$

The theoretical DS will be assumed that all of the added anhydride reacted with starch to obtain the ester form.

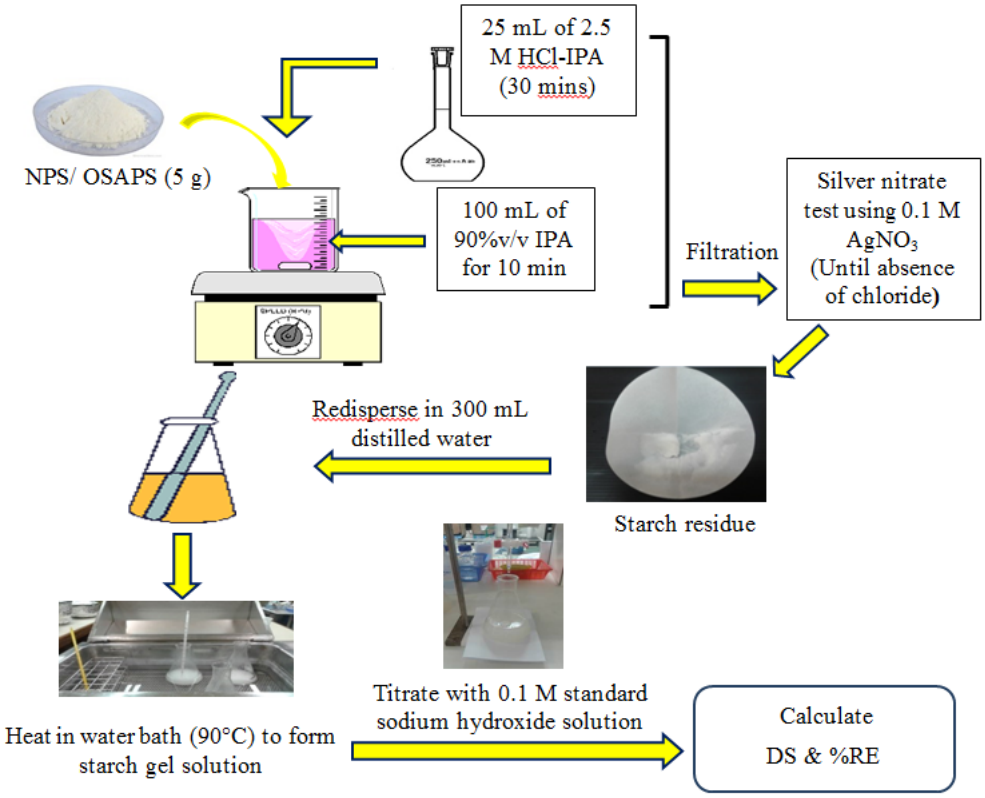

Figure 7 Schematic diagram for determination of DS.

3.3.1.4 Surface tension measurements

Surface tension was measured using drop shape analysis instrument (FTA 1000°, USA) at room temperature. Aqueous solution (3% w/w) of NPS and OSAPS were prepared to form gel solution using a boiling water bath. Each determination was performed in triplicate.

3.3.1.5 Differential scanning calorimetry

Starch gelatinization was determined by differential scanning calorimetry (Pyris Sapphire DSC, Standard 115V, Perkin Elmer instruments, Japan) using the technique described by (Segura-Campos et al., 2008). The data were analyzed using the Pyris software package (Perkin Elmer, Japan). To study the starch

gelatinization property, 2 mg (dry basis) of starch was placed in an aluminium pan and 8 mg of deionized water was added. The pan was sealed and left to equilibrate for 2 h at room temperature. Then, it was placed in the calorimeter and heated from 30 °C to 120 °C at a heating rate of 10 °C/min under 30 mL/min nitrogen flow using an empty pan as a reference. The gelatinization temperature was determined by automatically computing the onset temperature (T_o), peak temperature (T_p), end temperature (T_e), and enthalpy (ΔH_g) from the resulting thermograms.

3.3.1.6 Pasting properties

The pasting properties were evaluated according to the procedure described by (Bello-Flores et al., 2014). NPS and OSAPS were heated in a stress rheometer (Kinexus; Malvern). In brief, 4% w/w (dry basis) starch suspension was heated from 30 °C to 90 °C at a rate of 2.5 °C/min, held at this temperature for 40 min, and cooled to 30 °C at the same rate. Additionally, the peak viscosity was analyzed.

3.3.1.7 Powder X-ray diffraction analysis

The powder X-ray diffraction (XRD) patterns of NPS and OSAPS were analyzed by using an X-ray diffractometer (Miniflex II, Rigaku Corp. Tokyo, Japan) operated at 40 mA and 40 kV. The scanning region of the diffraction angle (2ɵ) was from 5º to 40º using Cu Kα radiation wavelength of 1.5406 Aº. The starch samples were equilibrated at 50ºC for 24 h prior to the analysis. The crystallinity was calculated using the following equation (Frost, Kaminski, Kirwan, Lascaris, & Shanks, 2009),

$$Crystallinity = \frac{area\ of\ crystalline\ peak}{(crystalline+amorphous)area} \quad (8)$$

3.3.1.8 Scanning electron microscopy

The NPS and OSAPS samples were attached to the sample holders with conducting glue and sputtered with a layer of gold. These samples were then examined via scanning electron microscopy (SEM; LEO 1450 VP; Zeiss, USA) using beam voltage 10.00 kV and working distance (WD) of 9 mm. A magnification of 2000× was used.

3.3.1.9 Fourier transform infrared (FTIR) spectroscopy

The changes in the chemical structure of OSAPS were qualitatively analyzed using FTIR spectroscopy (NICOLET 4700; Thermo Electronic Corporation, USA). The NPS and OSAPS samples preparation were carried out using KBr disc method. Each sample was grinded together with KBr powder and compressed to form a pellet at a pressure of 5 tons before placing in the sample holder. The spectra were recorded over a wavenumber range of 400–4000 cm^{-1} with 32 scans at a resolution of 4 cm^{-1}.

3.3.2 Part II: Evaluation of OSAPS as nanoemulsion stabilizer and optimization of ITZ-loaded nanoemulsion containing OSAPS

3.3.2.1 Solubility studies of ITZ in oils

ITZ is a triazole antifungal agent and weak base. It is classified BCS class II type because of its low solubility and high permeability (Amidon et al., 1995). The solubility of ITZ was studied in various oil sources such as almond, castor, oleic acid, sesame, sunflower and peanut oils or combination of oils which were selected due to high molecular weight. Briefly, 2 mL of oils were placed in glass test tubes. An excess amount of ITZ was added and mixed thoroughly using a vortex mixer. The test tubes were then kept at 25±1.0°C in incubator with shaking for 72 h. After equilibrium, the tubes were centrifuged at 8000 rpm for 15 min. The clear supernatant was diluted with isopropanol, mixed and sonicated for 10 min. Then, it was filtered through a Whatman (0.22µm) nylon membrane filter. The amount of ITZ in oils was determined using HPLC method (Sriamornsak & Burapapadh, 2015). Firstly, the standard curve of ITZ was performed. HPLC (Agilent Technologies 1100 series, USA) consists of a quarternary pump, a diode array detector (DAD), a degasser, a reverse-phase column (ACE 5 µm C18, 250 x 4.6 mm) and chemstation software (Rev. A. 10. 02.). The mobile phase consists of a mixture of acetonitrile, distilled water and diethylamine in the ratio of 63:37:0.05 (%v/v) and it was adjusted to pH 2.45 with orthophosphoric acid. The flow rate of the mobile phase was 1 ml/min and the volume of sample to be injected was 20 µL. The UV detection at wavelength 263 nm was used.

3.3.2.2 Evaluation of functional properties of OSAPS

3.3.2.2.1 Surface and interfacial tension measurement

Different concentrations (0.5 %, 1%, 3%, 5% and 10%) of NPS and OSAPS having different DS were prepared in aqueous phase to form gel solution using (boiling) water bath. Then, surface and interfacial tension of starch solution were determined by drop shape analysis instrument (FTA 1000°, USA) at room temperature. Each measurement was carried out in triplicate.

3.3.2.2.2 Rheological measurement

The rheological property of NPS and OSAPS gel solutions in various concentrations (0.5-5%) was measured by Rheometer (Kinexus, Malvern instruments Ltd., UK) with cone and plate (CP) geometry (CP diameter = 40 mm and gap=0.1410). The measurements were carried out at constant temperature 25°C. 1 mL of sample was loaded under cone and plate and each measurement was conducted in triplicate. The viscosity was measured by a steady state flow program with a shear rate ranging from $0.1s^{-1}$ to 100 s^{-1}. Experimental flow curves were fitted to a power law model:

$$\eta=K\gamma n^{-1} \quad (9)$$

where η is viscosity (Pa.s), K is the consistency index ($Pa.s^n$), γ is the shear rate (s^{-1}) and n is the flow behavior index which has three characteristics based on values: $n<1$ shows a shear thinning behavior; $n=1$ stands for a Newtonain behavior and $n>1$ is a shear thickening behavior.

3.3.2.2.3 Emulsifying activity index (EAI) measurement

Aqueous suspension (3%w/w) of NPS and OSAPS were prepared and heated to form gel. The gel was mixed with the selected oil from section *3.3.2.1* and homogenized at 20,000 rpm for 20 mins using homogenizer (T25 Digital ultra turrax, IKA, Germany). The EAI of both starch was determined and calculated with the method described by Pearce and Kinsella (Pearce & Kinsella, 1978). Briefly, 10 µL of freshly prepared emulsion was pipetted into 5 mL of sodium dodecyl sulfate (0.1%w/v) and the sample was measured the absorbance using spectrophotometer (T60 UV/Vis spectrophotometer, PG Instruments Ltd, UK) at 500 nm. Each measurement was conducted in triplicate.

3.3.2.3 Preliminary screenings for ITZ-loaded nanoemulsions

Preliminary screening was first conducted to investigate the effects of different parameters such as homogenization speed (15000-20000 rpm), homogenization time (15-25min), OSAPS concentration (1-3%w/w) and polysorbate 80 concentration (15-20%w/w) on droplet size of ITZ-loaded nanoemulsions using a one-factor-at-a-time method. Based on the single factor test, the preparation of ITZ-loaded nanoemulsions was continued using fractional factorial CCF design as the next study.

3.3.2.4 Preparation of ITZ-loaded nanoemulsions

The composition of nanoemulsion formulations are shown in **Table 8**. The schematic diagram of ITZ-laoded nanoemulsion preparation is shown in **Figure 8**. An aqueous phase contained polysorbate 80, OSAPS and distilled water. The selected oil from section *3.3.2.1* was fixed at the concentration of 30%w/w. The aqueous phase was prepared by heating OSAPS slurry (1-3%w/w) to form gel solution using a boiling water bath at 90°C for 20 min, mixed with polysorbate 80 (15-20) %w/w and heated at 75°C. ITZ was added into the oil phase and heated at 73°C. The oil phase was poured to the aqueous phase and then mixed using homogenizer (T25 Digital ultra turrax, IKA, Germany) at 20,000 rpm for (20-30 min). The prepared-ITZ loaded nanoemulsions were stored at approximately 4°C for further study. The flow chart is shown in **Figure 8**.

Table 8 Composition of nanoemulsion formulations.

Composition	Concentraion (%w/w)		
	Control	NPS	OSAPS
Oil	30	30	30
ITZ	0.0369	0.0369	0.0369
Polysorbate 80	17.5	17.5	15-20
NPS	-	2	-
OSAPS	-	-	1-3
Distilled water to	100	100	100

NPS: Native pineapple starch; OSAPS: OSA modified pineapple starch; Homogenization time: 20-30 mins.

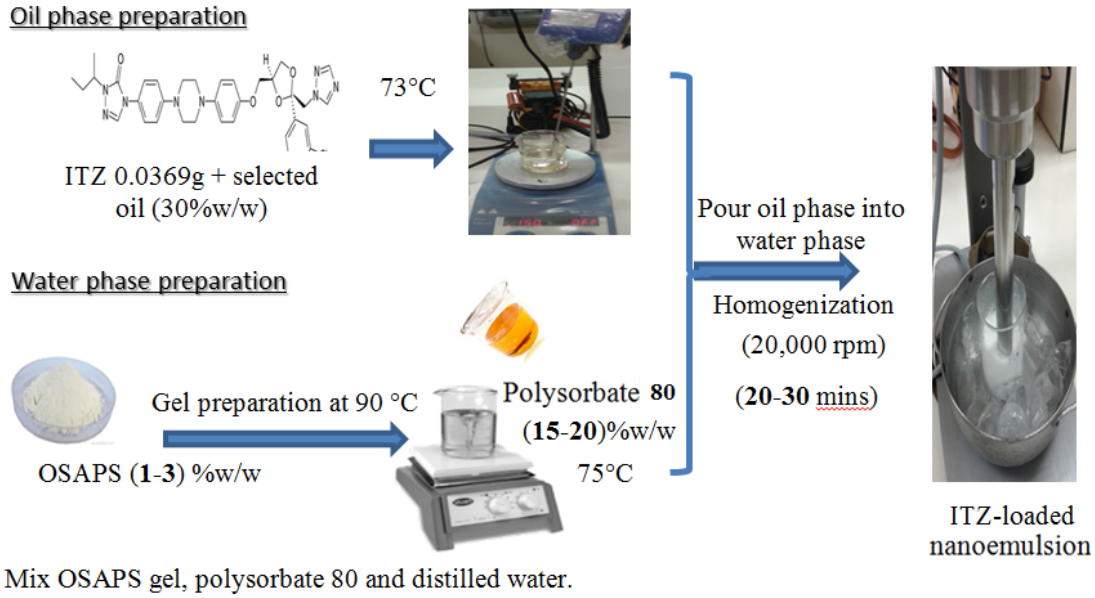

Figure 8 Schematic diagram for preparation of ITZ-loaded nanoemulsions using OSAPS

3.3.2.5 Evaluation of ITZ-loaded nanoemulsions containing OSAPS

3.3.2.5.1 Droplet size, zeta potential and polydispersity index (PDI) analysis

Each nanoemulsion was diluted with distilled water to be 1/1000 and measured for size distribution and zeta potential, using a Dynamic Light Scattering (DLS) particle size analyzer (Zetasizer Nano-ZS, Malvern Instrument, Worcestershire, UK) with a 4mW He-Ne laser at a scattering angle of 173°. PDI was calculated as the ratio of square of standard deviation of the particle size distribution and square of average hydrodynamic particle diameter. All measurements were carried out in triplicate.

3.3.2.5.2 Rheological measurement

The rheological property of nanoemulsion formulations was measured by Rheometer (Kinexus, Malvern instruments Ltd., UK) using plate upper geometry (PU diameter = 20 mm and gap=1). The measurements were carried out as

mentioned in section *3.3.2.2.2*. The high determination coefficient (R^2) was used as a parameter to evaluate the best fit to power law model.

3.3.2.5.3 Drug content determination in nanoemulsions

The drug content in nanoemulsions was determined by dissolving nanoemulsion in diluent such as isopropanol to be 1 in 10. It was shaken using vortex mixer and sonicated for about 5 min. The wavelength of 263 nm was used for drug content by HPLC as mentioned in section *3.3.2.1*.

3.3.2.6 In vitro drug release

The *in vitro* dissolution test of intact ITZ and prepared nanoemulsions were carried out using USP dissolution test apparatus type II (paddle) (Model DT70, Erweka, Germany). Two grams of ITZ-loaded nanoemulsion equivalent to 0.738 mg of ITZ was added to each vessel containing 900 ml of freshly prepared simulated gastric fluid (SGF) at pH 1.2 as dissolution medium. The dissolution temperature was controlled at 37°C and stirred at 100 rpm. The samples were withdrawn at 0, 5, 15, 30, 45, 60 and 120 min and replaced with a fresh SGF to maintain a constant volume of sink condition. To analyze the percent drug release, the samples were extracted with isopropanol at a ratio of 1:1 and filtered using Whatman (0.45µm) nylon filters. The samples were then analyzed by HPLC at 263 nm as mentioned in above section *3.3.2.1* and cumulative % drug release was calculated at each time point and analyzed using analysis of variance (ANOVA). The *in vitro* drug release data were fitted to models including first, Higuchi and Weibull using DDsolver program and high determination coefficient (R^2) was used as a parameter to evaluate the best fit to a specific model. The applied equations are as follows (Zhang et al., 2010):

$$F = 100.(1 - e^{-K1.t}) \quad (10)$$

$$F = K_H.t^{0.5} \quad (11)$$

$$F = F_{max}.\left[1 - e\frac{(t-Ti)^{\beta}}{\alpha}\right] \quad (12)$$

where F is the fraction (%) of drug released in time (t), F_{max} is the maximum fraction of the drug released infinite time, K_1 and K_H are release constant of first order and

Higuchi, respectively and β is shape parameter, α is scale parameter and T_i is location parameter for Weibull model.

The dissolution profiles were also statistically assessed by using the non-parametric bootstrap method to evaluate the similarity of dissolution profiles for each sample pair according to the following equation:

$$\hat{f}_2 = 50.\log\left\{[1 + \frac{1}{p}\sum_{i=1}^{p}(\bar{X}_{Ri} - \bar{X}_{Ti})^2]^{-0.5} \times 100\right\} \quad (13)$$

where $\bar{X}_{Ri}, \bar{X}_{Ti}$ are the mean dissolution values of the reference and test profiles respectively at the i-th time point and P is the number of sampling points. In this method, the 90% confidence interval of f_2 was estimated, where the lower and upper limits are the 5% (i.e. Bootstrap 5% percentiles) and 95% percentiles of the $\hat{f}_2$ values, respectively. Two dissolution profiles are considered similar, at 0.05 significance level, when the 90% lower confidence limit of f_2 is greater than 50 (Ocaña, Frutos, & Sánchez O, 2009). In this study, DDsolver: an Add-In program was used for modeling and comparison of drug dissolution profiles.

3.3.2.7 Stability studies

The selected nanoemulsions were subjected to accelerated stablility test for three months and six cycles of temperature cycling test. The effect of temperature on accelerated stability was studied by storing at 4°C ± 2°C and 25°C ± 2°C for 14 days, 30 days and 90 days. Six cycles of heating-cooling between temperature 4°C ± 2°C for 24 h and 40°C ± 2°C for 24 h was also conducted and investigated for changes in droplet size, PDI and %creaming of selected nanoemulsions. All measurements were carried out in triplicate.

3.3.2.7.1 Droplet size and PDI analysis

The droplet size and PDI were analysed as mentioned in above section *3.3.2.5.1.*

3.3.2.7.2 %Creaming measurement

%Creaming of the nanoemulsions was calculated using the following equation (10):

$$\%Creaming = \frac{V_H - V_l}{V_H} \times 100 \quad (14)$$

where V_H is the whole volume (mL) of the sample, and V_l is the lower layer volume (mL) (Burapapadh et al., 2010).

3.3.2.8 Optimization of ITZ-loaded nanoemulsions

In this study, three independent variables were selected for fractional factorial CCF design based on the results of preliminary screening using one-factor-at-a-time. RSM was used to study the effects of independent variables such as the concentration of OSAPS (X_1), the concentration of polysorbate 80 (X_2) and homogenization time (X_3) on droplet size (Y_1), PDI (Y_2), viscosity (Y_3) and *in vitro* drug release (%) within 15 mins (Y_4) as well as to optimize the ITZ-loaded nanoemulsions. Each of independent variables contained three different levels of -1, 0 and +1 shown in **Table 9**. The design consists of four factorial points, six axial points and five repetitions at central points and the total 15 runs were randomly carried out according to CCF design with coded and experimental values displayed in **Table 10**. The results were analyzed by ANOVA. The CCF design was employed along with linear and quadratic model. The second order polynomial equation was used to fit the responses as a function of independent variables which have been mentioned in above equation (1). For three independent variables, the following equation can be used to express the responses as follows (Bezerra et al., 2008):

$$Y = \beta_0 + \beta_1 X_1 + \beta_2 X_2 + \beta_3 X_3 + \beta_{11} X_1^2 + \beta_{22} X_2^2 + \beta_{33} X_3^2 + \beta_{12} X_1 X_2 + \beta_{13} X_1 X_3 + \beta_{23} X_2 X_3 \quad (15)$$

where Y represents the responses variables, β_0 is intercept and β_i, β_{ii} and β_{ij} are the coefficients of linear, quadratic and interaction parameters, respectively. The regression coefficients were analyzed using Design-Expert® software package (version 8.0.7.1; Stat-Ease, Inc., USA). The r^2 and RMSE were used for evaluating the polynomial model. The extra four experiments were also conducted for external validation. The desirability function approach was used for the optimization of multiple response processes (Myers et al., 2009).

Table 9 Fractional factorial CCF design employed for ITZ-loaded nanoemulsion preparation.

Independent variables	Symbols	Levels		
		-1	0	+1
OSAPS (%w/w)	X_1	1	2	3
Polysorbate 80 (%w/w)	X_2	15	17.5	20
Homogenization time (min)	X_3	20	25	30
Responses variables				
Droplet size	Y_1			
PDI	Y_2			
Viscosity	Y_3			
In vitro drug release (%) within 15 mins	Y_4			

Table 10 Fractional factorial CCF design of coded and experimental values of three independent variables for ITZ-loaded nanoemulsion preparation.

Std	Runs	Coded values			Experimental values		
		X_1	X_2	X_3	OSAPS (%w/w)	Polysorbate 80 (%w/w)	Homogenization time (min)
1	5	1	1	-1	3	20	20
2	2	1	-1	1	3	15	30
3	8	-1	1	1	1	20	30
4	4	-1	-1	-1	1	15	20
5	15	-1	0	0	1	17.5	25
6	10	1	0	0	3	17.5	25
7	7	0	-1	0	2	15	25
8	1	0	1	0	2	20	25
9	11	0	0	-1	2	17.5	20
10	13	0	0	1	2	17.5	30

11	6	0	0	0	2	17.5	25
12	14	0	0	0	2	17.5	25
13	12	0	0	0	2	17.5	25
14	3	0	0	0	2	17.5	25
15	9	0	0	0	2	17.5	25

3.3.2.9 Statistical analysis

The results were analyzed by ANOVA using SPSS version 23 for windows (SPSS Inc., USA), based on Levene statistics for homogeneity of variances. The *Post hoc* test of multiple comparisons was conducted at 95% confidence interval (p<0.05) by Tukey HSD.

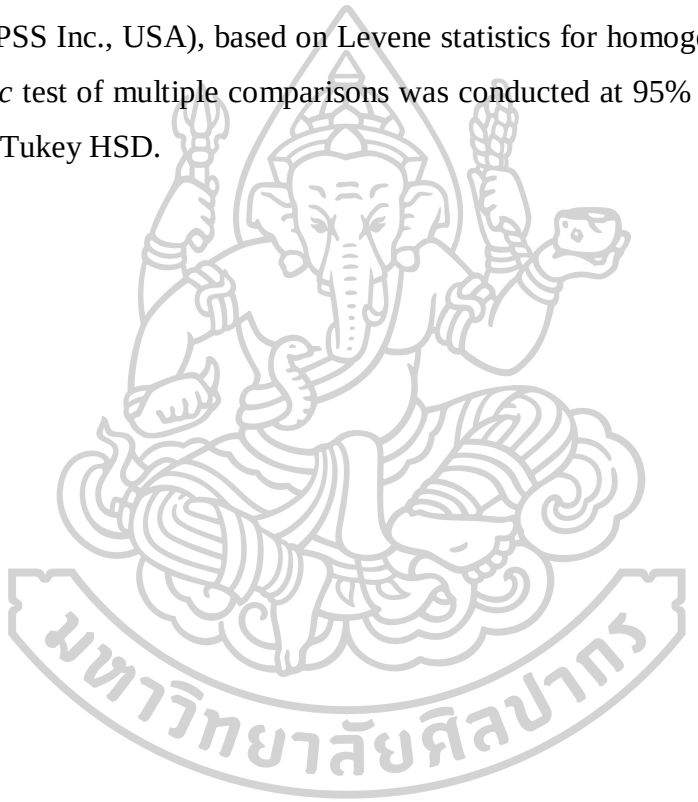

Chapter 4

Results and discussion

4.1 Part I: Optimization of reaction conditions of OSAPS using fractional factorial CCF design

4.1.1 Optimization OSA synthesis conditions of pineapple starch

The pineapple starch was analyzed by the Cassava and Starch Technology Research Unit through methods of AOAC (Helrich, 1990). It is composed of amylose (21.85%) and amylopectin (78.15%). Starch content was 90.22 % and protein, fat, crude fiber, and moisture contents were 1.25%, 0.14%, 0.40% and 5.57%, respectively. **Figure 9** shows the effect of OSA concentration on DS and RE under the following conditions: starch concentration of 30%w/w, pH 8, reaction temperature of 35 ℃, and reaction time of 5 h. An increase in OSA concentration resulted in an increase in DS and a decrease in RE. Similar trend was also reported by Hui et al (Hui et al., 2009). The effects of OSA concentration, pH, reaction temperature, and reaction time on DS were preliminarily investigated using a one-factor-at-a-time method. Finally, OSA concentrations of 1-30%w/w at pH 7–9 and reaction temperatures of 25-50 ℃ for a 2–5 h reaction time were selected as independent variables for pineapple starch modification using RSM. A fractional factorial CCF design of 21 experimental runs with the independent variables and the observed responses is summarized in **Table 11**.

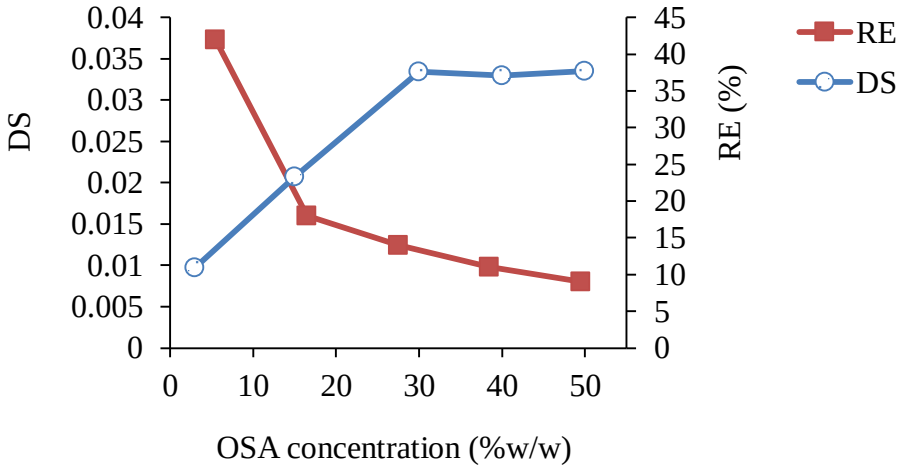

Figure 9 Effect of OSA concentration on DS and RE under the following conditions: starch concentration = 30%w/w, pH 8, reaction temperature = 35°C, and reaction time = 5 h.

4.1.1.1 DS model

The DS values of OSAPS from experiments ranged from 0.0006 to 0.0311, and RE ranged from 7 to 37%, as summarized in **Table 11**. The experimental data were used to determine the relation between the independent variables and DS. RSM was employed to produce a regression equation for the DS model as follows:

$$DS = -0.3629 + 0.0026 * OSA\ concentration + 0.1003 * pH + 0.0014 * Temperature - 0.0269 * Time - 0.0002 * OSA\ concentration * Time - 0.0002 * pH * Temperature + 0.0032 * pH * Time + 0.0001 * Temperature * Time - 0.00002 * OSA\ concentration * OSA\ concentration - 0.0068 * pH * pH \quad (16)$$

Table 11 A fractional factorial CCF design with independent variables and observed responses of OSAPS synthesis.

Runs	Independent variables				Responses								
	X_1	X_2	X_3	X_4	DS	RE (%)	Peak viscosity (mPa·s)	Surface tension (mN/m)	%Crystallinity	Gelatinization temperatures			Enthalpy (J/g starch)
										T_0	T_p	T_e	
1	30	7	50	5	0.0301	13	23	56.28	26	73.56	79.1	88.21	3.1201
2	1	9	50	5	0.0006	8	12	68.04	29	83.79	86.87	92.75	2.8623
3	15.5	7	37.5	3.5	0.0212	18	21	61.49	30	74.92	82.4	89.6	2.5664
4	15.5	8	50	3.5	0.0270	23	23	57.48	28	79.50	84.29	90.71	1.9522
5	15.5	9	37.5	3.5	0.0085	7	15	60.09	21	82.59	85.89	91.26	2.3744
6	1	9	25	5	0.0013	16	13	67.81	31	83.15	86.34	92.17	2.5056
7	30	7	25	5	0.0161	7	18	59.78	26	80.81	84.79	89.39	1.3217
8	15.5	8	37.5	3.5	0.0262	22	28	55.00	28	78.83	83.47	89.45	1.2212
9	30	9	50	2	0.0162	7	27	56.05	26	74.15	76.98	81.12	4.4990
10	1	7	50	2	0.0024	31	21	67.67	26	83.83	86.76	90.98	2.3016
11	1	8	37.5	3.5	0.0019	26	18	68.54	32	83.86	86.57	90.62	2.0220
12	15.5	8	37.5	3.5	0.0236	20	19	55.47	29	79.38	83.61	89.38	1.5422
13	15.5	8	25	3.5	0.0108	9	21	60.17	26	81.59	85.24	90.62	2.1626
14	15.5	8	37.5	2	0.0247	21	21	55.86	27	80.47	83.99	89.11	1.0497
15	15.5	8	37.5	3.5	0.0244	20	16	55.83	23	79.76	84.5	89.94	1.4281
16	1	7	25	2	0.0028	37	12	67.14	23	83.64	86.88	91.92	2.4479
17	30	8	37.5	3.5	0.0311	13	19	56.64	26	80.36	85.07	89.44	2.1027
18	15.5	8	37.5	5	0.0262	22	22	58.67	26	78.05	84.36	91.35	2.6088
19	15.5	8	37.5	3.5	0.0244	20	20	56.23	22	79.56	84.05	89.5	1.1911
20	15.5	8	37.5	3.5	0.0246	21	18	55.05	28	79.2	83.94	91.19	2.0815
21	30	9	25	2	0.0227	10	24	53.12	23	82.77	85.78	90.76	2.3304

X_1: octenyl succinic anhydride (OSA) concentration (%w/w), X_2: pH, X_3: temperature, X_4: time (h), T_o: onset temperature, T_p: Peak temperature and T_e: end temperature.

The ANOVA results for the response surface models are summarized in **Table 12**. The full model was reduced by excluding the non-significant interaction terms. The *p*-value was used as a tool to examine the significance of each variable, mutual interactions, and regression model. The DS model was significant according to an *F*-test value of 12.45 and $p<0.05$. The r^2 value was 0.9256 and the RMSE was 0.0028. The individual effect of OSA concentration, pH, and quadratic terms of OSA concentration*OSA concentration and pH*pH were the significant factors affecting DS while the other terms of temperature and time were non-significant. The contour plots **(Figure 10(a_1-f_1))** and 3D response surface plots **(Figure 10(a_2-f_2))** show the combined effect of OSA concentration, pH, temperature and time on DS**. Figure 10(a_1) & (a_2)** of contour and 3D response surface plots show the combined effects of the OSA concentration and pH on the DS of OSAPS. The reaction temperature and time were fixed at 37.5 °C and 3.5 h, respectively. It can be clearly observed that the DS value increased with increasing OSA concentration. It was similar to Wang et al (Wang et al., 2011). This may be due to the fact that the OSA molecule is insoluble in water and the dispersed OSA molecules can enter immobile hydroxyls at the carbon-2, 3, and 6 positions along the starch chains when the OSA concentration is increased. At a high OSA concentration (30% w/w), the maximum DS value was obtained when the optimum pH was at 8, as shown in **Figure 10(a_1) and (a_2)**. This indicates the interaction effects of OSA and pH on DS (Abiddin et al., 2015). When the pH was increased to 9, DS slightly decreased. The similar trend has been reported that pH > 8 promotes undesired side reactions (Rutenberg & Solarek, 1984), whereas pH<7.5 does not sufficiently activate the hydroxyls of starch for a nucleophillic attack by anhydride moieties, leading to decreased DS (Hui et al., 2009; Song et al., 2006).

Table 12 ANOVA results for the response surface models of OSAPS synthesis.

Source	**Model**	**df**	**Sum square**	**Mean square**	***F*-value**	***P*-value**	r^2	**RMSE**
DS-model	Quadratic	10	0.00206	0.000206	12.45	0.0002	0.9256	0.0028
Residual		10						
Total		20						
Surface tension-model	Quadratic	9	487.56	54.17	16.87	<0.0001	0.9324	1.297
Residual		11						
Total		20						
Enthapy-model	Quadratic	9	10.5	1.17	7.18	0.0017	0.8544	0.2919
Residual		11						
Total		20						

df: degrees of freedom; RMSE: root-mean-square error

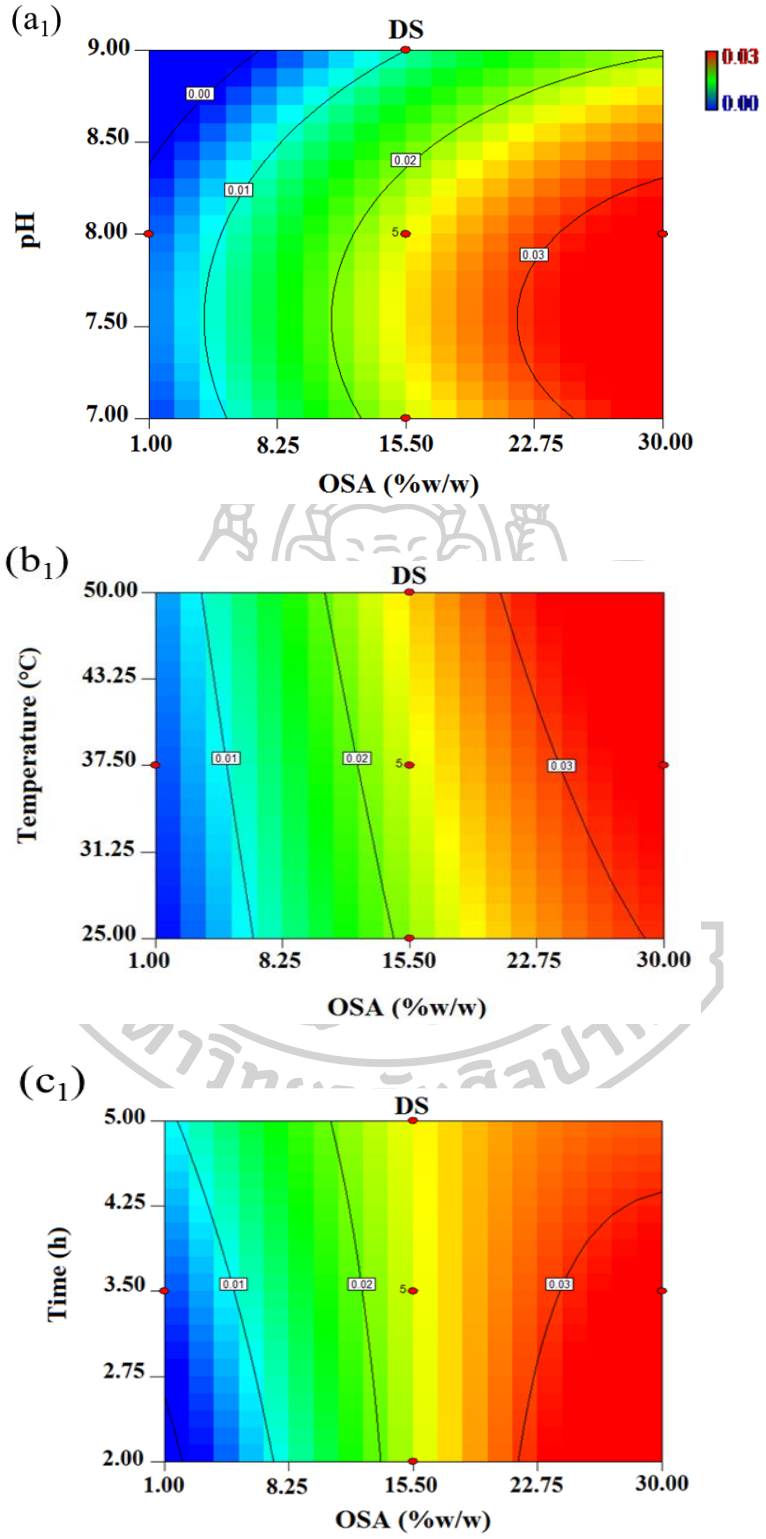
(a1)
DS
9.00
8.50
8.00
7.50
7.00
pH
0.03
0.00
0.00
0.01
0.02
0.03
5
1.00
8.25
15.50
22.75
30.00
OSA (%w/w)
(b1)
DS
50.00
43.25
37.50
31.25
25.00
Temperature (°C)
0.01
0.02
0.03
5
1.00
8.25
15.50
22.75
30.00
OSA (%w/w)
(c1)
DS
5.00
4.25
3.50
2.75
2.00
Time (h)
0.01
0.02
0.03
5
1.00
8.25
15.50
22.75
30.00
OSA (%w/w)

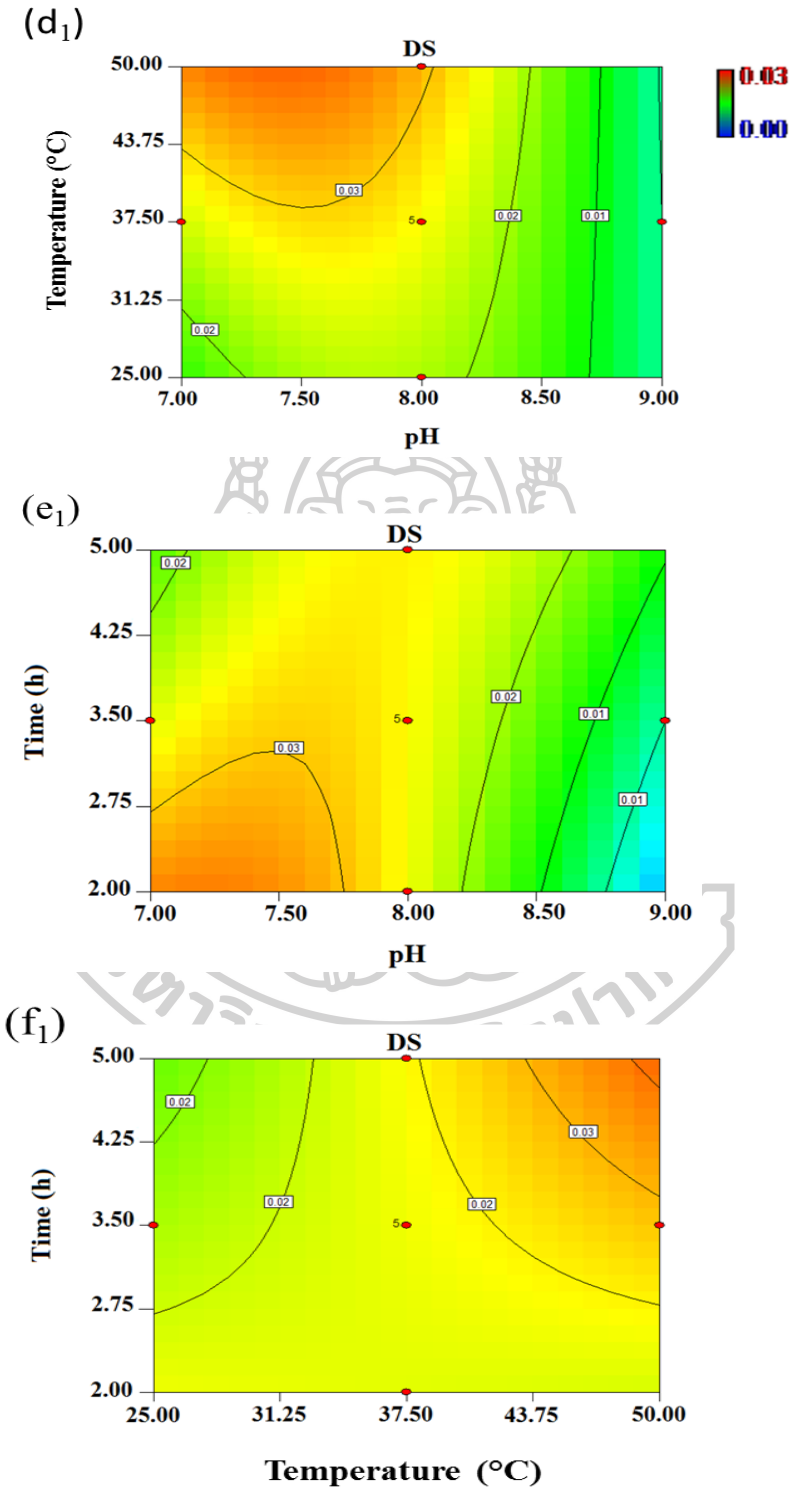
(d1)
DS
50.00
43.75
37.50
31.25
25.00
Temperature (°C)
7.00
7.50
8.00
8.50
9.00
pH
0.03
0.00
0.03
0.02
0.02
0.01
5
(e1)
DS
5.00
4.25
3.50
2.75
2.00
Time (h)
7.00
7.50
8.00
8.50
9.00
pH
0.02
0.03
0.02
0.01
0.01
5
(f1)
DS
5.00
4.25
3.50
2.75
2.00
Time (h)
25.00
31.25
37.50
43.75
50.00
Temperature (°C)
0.02
0.02
0.03
0.02
5

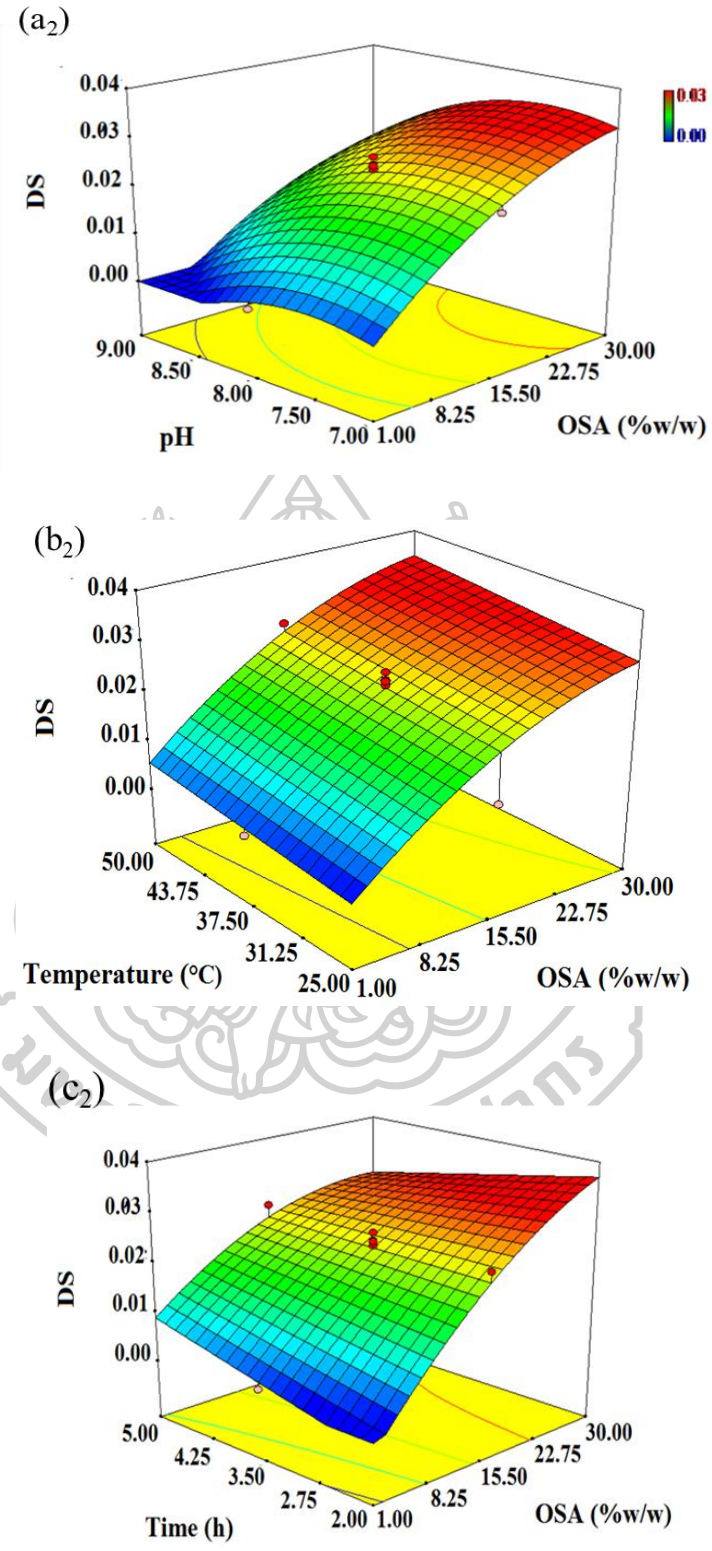
(a2)
DS
0.04
0.03
0.02
0.01
0.00
0.03
0.00
9.00
8.50
8.00
7.50
7.00
pH
1.00
8.25
15.50
22.75
30.00
OSA (%w/w)
(b2)
DS
0.04
0.03
0.02
0.01
0.00
50.00
43.75
37.50
31.25
25.00
Temperature (°C)
1.00
8.25
15.50
22.75
30.00
OSA (%w/w)
(c2)
DS
0.04
0.03
0.02
0.01
0.00
5.00
4.25
3.50
2.75
2.00
Time (h)
1.00
8.25
15.50
22.75
30.00
OSA (%w/w)

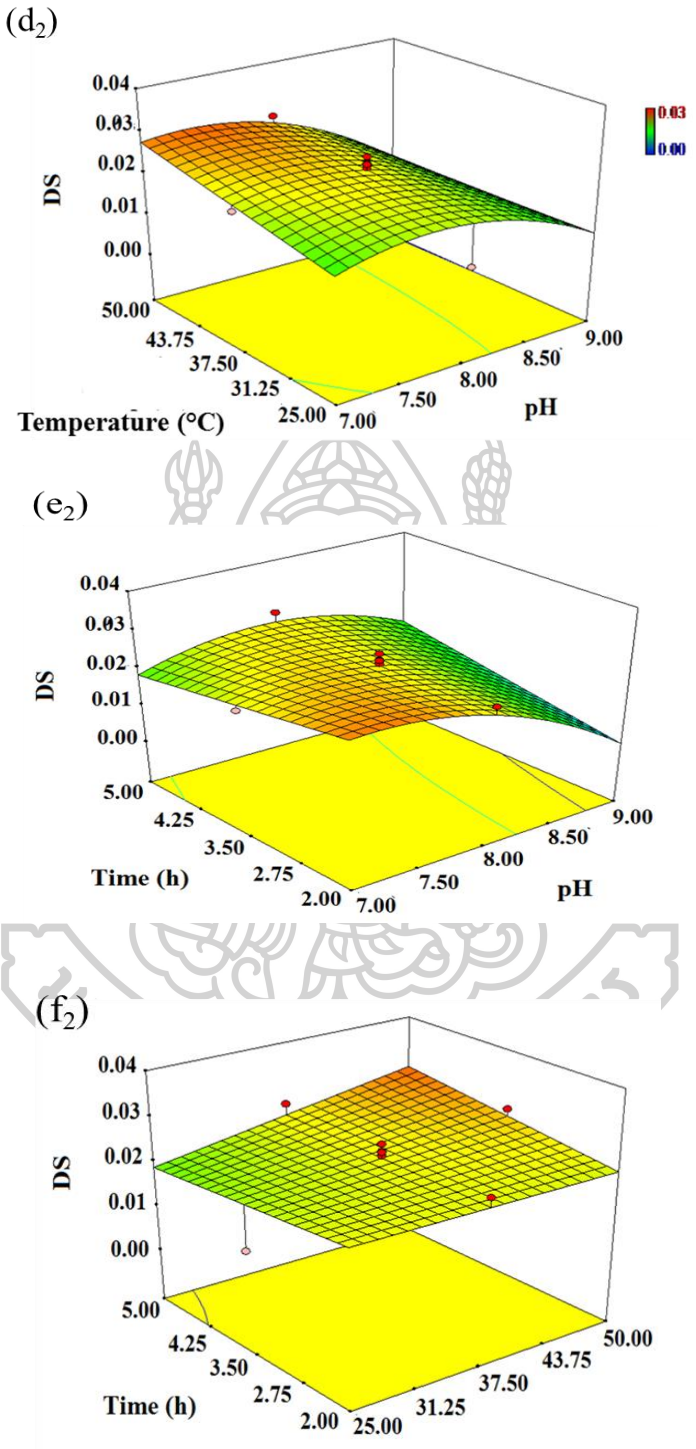

Figure 10 Contour (a_1-f_1) and 3D response surface plots (a_2-f_2) showing the combined effect of OSA concentration, pH, temperature and time on DS.

4.1.1.2 Surface tension model

The surface tension data of OSAPS from experiments ranged from 53.12 to 68.54 mN/m, as summarized in **Table 12**, whereas the surface tension of NPS was 69.8 mN/m. All surface tension values of OSAPS were decreased when compared with the NPS. It may be due to an increase in hydrophobicity after esterification with OSA. The similar pattern was demonstrated by the significantly decreased water sorption capacity of OSA-modified cassava starch (Prochaska, Kedziora, Le Thanh, & Lewandowicz, 2007). The significant quadratic model for surface tension is summarized in **Table 12**. The model terms were significant ($P<0.05$), and the model exhibited a good fit to the experimental data. The r^2 and RMSE value were 0.9324 and 1.297, respectively. The regression equation of the surface tension model can be expressed as follows:

$$Surface\ tension = +223.4526 - 0.99646 * OSA\ concentration - 39.45107 * pH - 0.35337 * Temperature + 6.28208 * Time + 0.0613 * pH * Temperature - 0.044867 * Temperature * Time + 0.01939 * OSA\ concentration * OSAconcentration + 2.27671 * pH * pH - 0.5548 * Time * Time \quad (17)$$

The ANOVA results indicated that the OSA concentration, the quadratic terms of OSA x OSA and pH x pH were the significant factors affecting the surface tension of OSAPS while other terms such as individual effect of pH, temperatue, time and interaction effects of pH*temperature, temperature*time and quadratic effects of OSA*OSA and time*time showed non-significant. The contour plots **(Figure 11(a_1-f_1))** and 3D response surface plots **(Figure 11(a_2-f_2))** display the combined effect of OSA concentration, pH, temperature and time on surface tension. **Figure 11(a_1) & (a_2)** shows the effects of OSA concentration and reaction pH on surface tension, with reaction temperature and reaction time fixed at 37.5˚C and 3.5 h, respectively. It was clearly observed that the surface tension of OSAPS decreased when the OSA concentration was increased to 30% shown in **Figure 11(a_1) & (a_2)**. This may be due to the fact that increasing hydrophobicity of starch modified by OSA lead to adsorb air-water interface, thereby decreasing air-water surface tension of OSAPS. This finding was complied with Prochaska et al (Prochaska et al., 2007). On

the contrary, the surface tension increased at 8<pH<7.5 with respect to lower OSA concentration shown in **Figure 11(a_1) & (a_2)**. These results correspond with those of DS model. This indicates that pH is a critical factor affecting DS and surface tension of OSAPS.

(a_1)

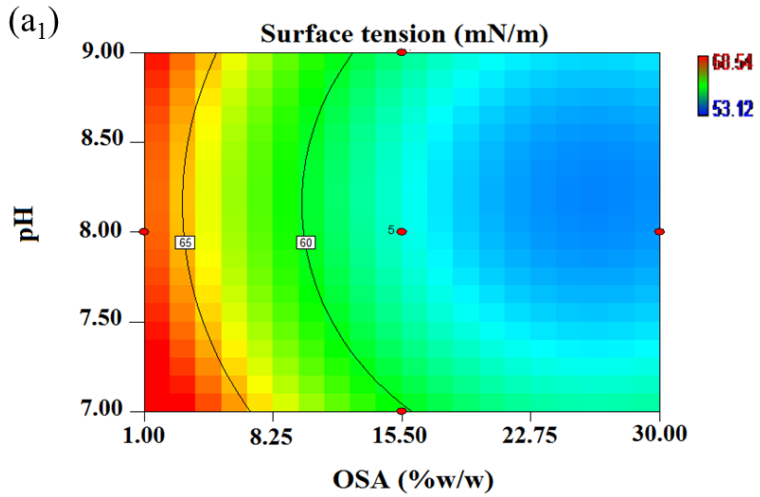

(b_1)

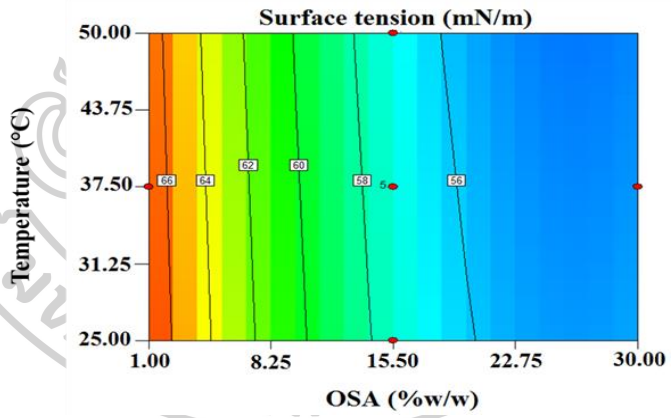

(c_1)

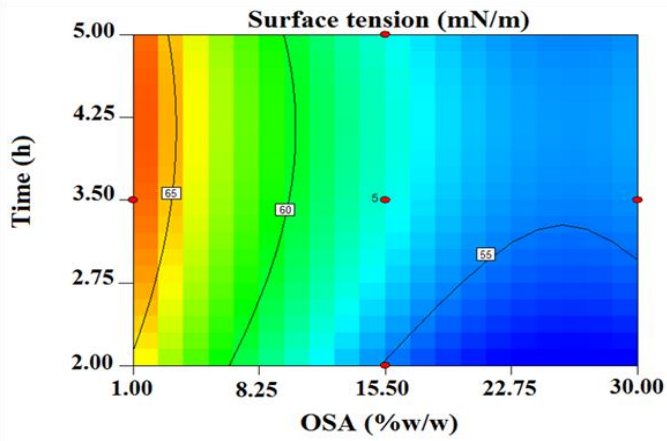

(d_1)

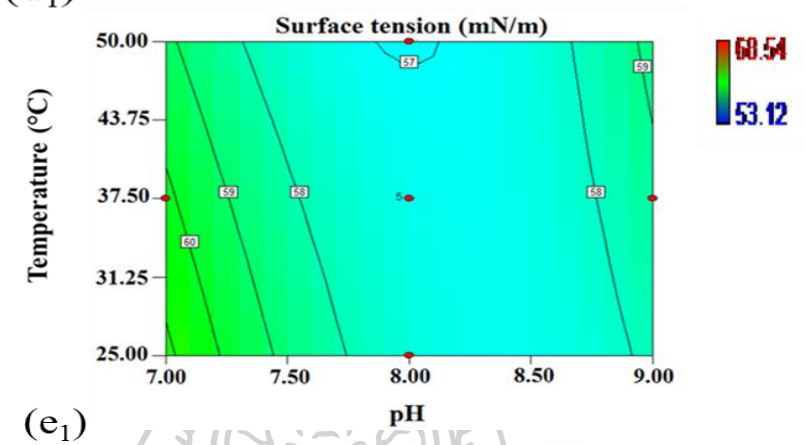
Surface tension (mN/m)
60.54
53.12
Temperature (°C)
50.00
43.75
37.50
31.25
25.00
7.00
7.50
8.00
8.50
9.00
pH

(e_1)

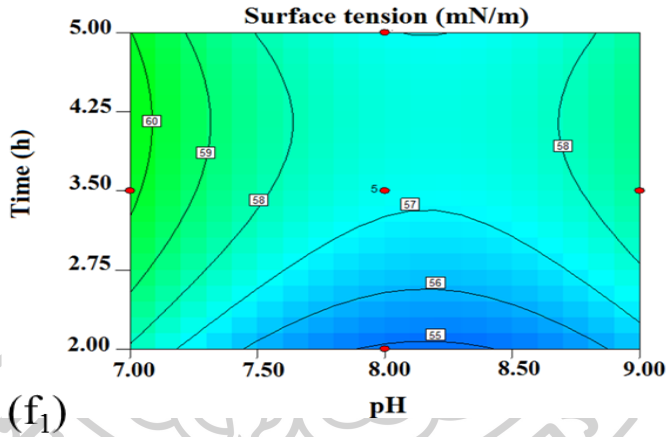
Surface tension (mN/m)
Time (h)
5.00
4.25
3.50
2.75
2.00
7.00
7.50
8.00
8.50
9.00
pH

(f_1)

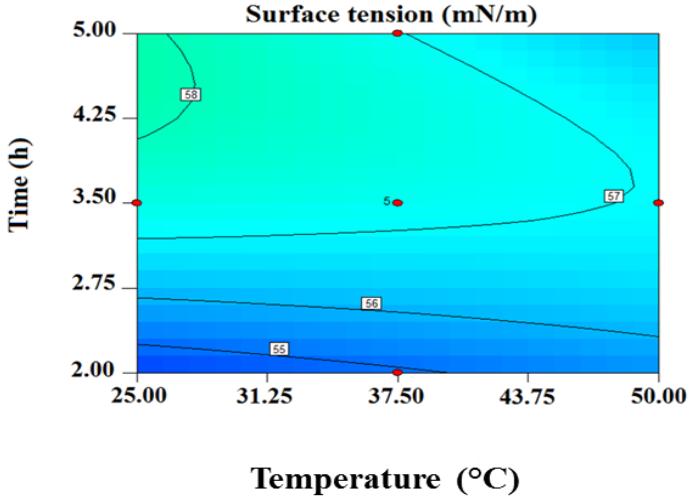
Surface tension (mN/m)
Time (h)
5.00
4.25
3.50
2.75
2.00
25.00
31.25
37.50
43.75
50.00
Temperature (°C)

(a_2)

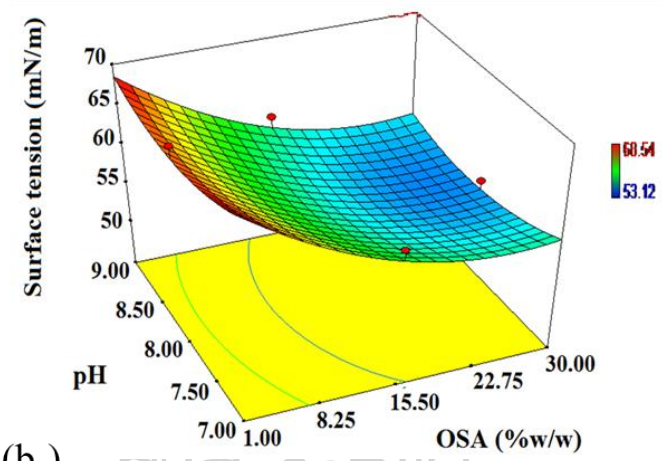
Surface tension (mN/m)
70
65
60
55
50
60.54
53.12
9.00
8.50
8.00
7.50
7.00
pH
1.00
8.25
15.50
22.75
30.00
OSA (%w/w)

(b_2)

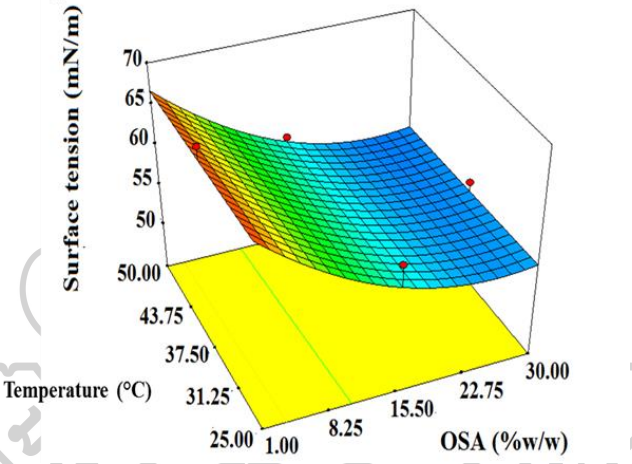
Surface tension (mN/m)
70
65
60
55
50
50.00
43.75
37.50
31.25
25.00
Temperature (°C)
1.00
8.25
15.50
22.75
30.00
OSA (%w/w)

(c_2)

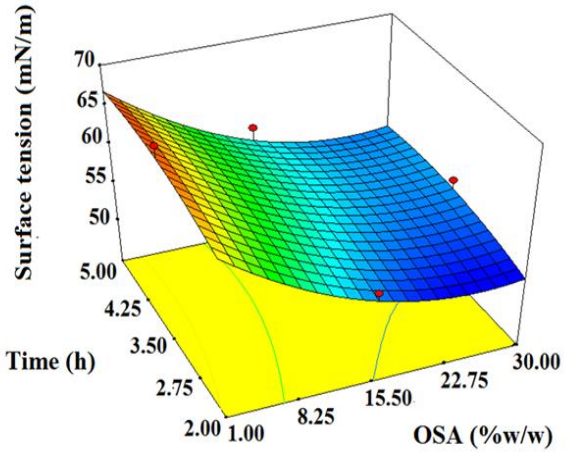
Surface tension (mN/m)
70
65
60
55
50
5.00
4.25
3.50
2.75
2.00
Time (h)
1.00
8.25
15.50
22.75
30.00
OSA (%w/w)

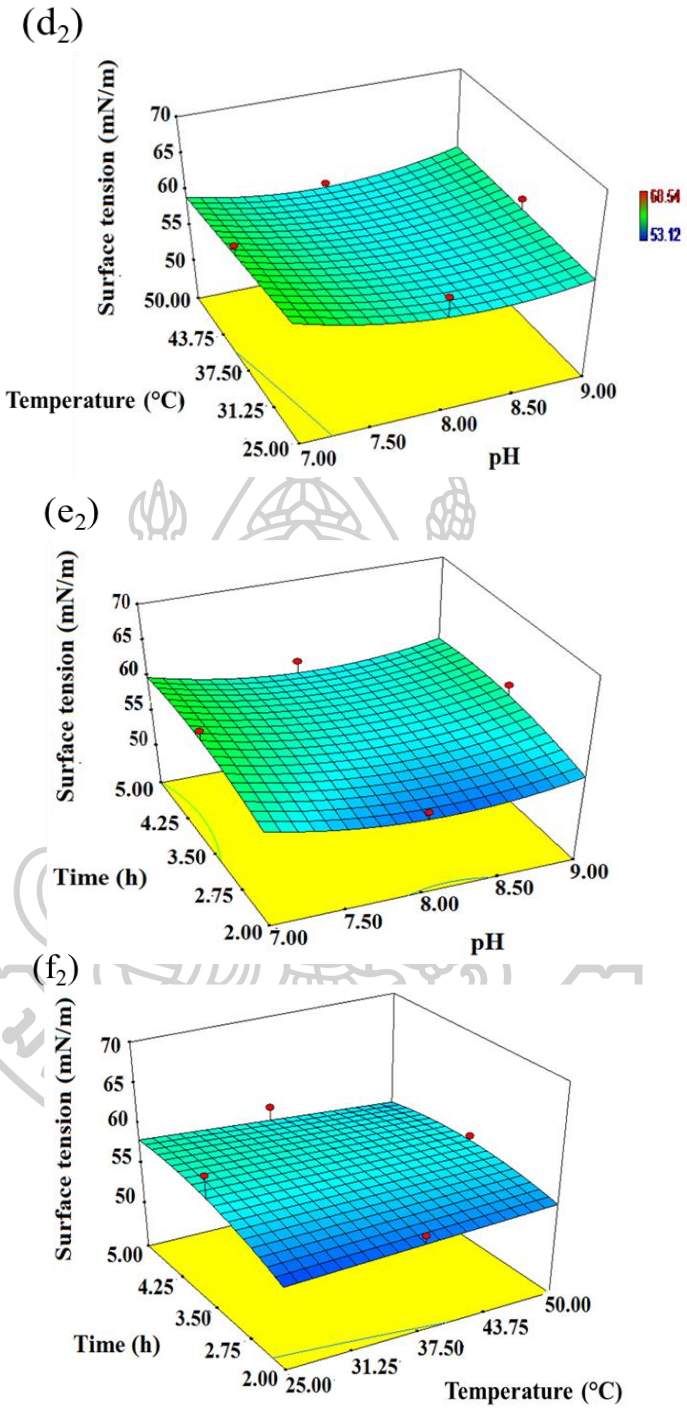

Figure 11 Contour (a_1-f_1) and 3D response surface plots (a_2-f_2) showing the combined effect of OSA concentration, pH, temperature and time on surface tension.

4.1.1.3 Enthalpy model

Enthalpy (ΔH_g) of gelatinization by DSC represents a net sum of all endothermic processes that take place during heating. Since the enthalpy is the factor indicating the efficiency on polymer swelling and one mechanism of emulsifying agent involved with the decrease in surface tension which related to high DS (Sweedman, Tizzotti, et al., 2013). The gelatinization temperature such as T_o, T_p, and T_e characterized by DSC are summarized in **Table 11**. The gelatinization temperature was 84.36 °C for OSAPS and 87.11°C for NPS. The enthalpy value of OSAPS was in the range 1.0497–4.499 J/g starch and that of NPS was 4.5939 J/g starch. It was found that the enthalpy values of OSAPS samples were lower than that of NPS, indicating that OSAPS did not require high energy to gelatinize after modification with OSA. It may be possible that the OSA groups weaken the interactions between starch macromolecules, thereby the starch granules swell and easily gelatinize at low temperature (Bello-Flores et al., 2014). The enthalpy model yielded a significant quadratic fit, and the obtained regression equation for enthalpy model is expressed as follows:

$$Enthalpy = \ + 53.044 - 0.6072 * OSA\ concentration - 12.289pH - 0.0084 * Temperature + 0.8559 * Time + 0.0690 * OSA\ concentration * pH + 0.0026 * OSA\ concentration * Temperature - 0.0217 * OSA\ concentration * Time + 0.0014 * OSA\ concentration * OSA\ concentration + 0.6952 * pH * pH \quad (18)$$

Among the model terms, the reaction temperature, reaction time, and their interaction effects such as OSA concentration*pH, OSA concentration*temperature, and quadratic effect of pH*pH, were significant model terms for the enthalpy model. The individual effect of OSA concentration, pH, interaction effect of OSA concentration*time and quadratic effect of OSA concentration*OSA concentration were non-significant. The correlation between the actual and predicted values based on the experimental data yielded an r^2 value of 0.8544 and an RMSE value of 0.2918 (**Table 12**). **Figure 12(a_1) & (a_2)** shows the interaction effect of OSA concentration and pH on the enthalpy while the other two factors such as temperature and time kept at 37.5°C and 3.5 h, respectively. It was

observed that low enthalpy was produced at low OSA concentration and pH ≥ 8. It might be due to the fact that starch swell at high alkaline pH and small number of OSA can enter the starch molecules and decrease in enthalpy after modification with OSA. However, an increase in OSA concentration and pH lead to increase in enthalpy. It may be due to undesirable side reaction derived from sodium hydroxide reacted with OSA molecules, thereby increasing enthalpy value approximately about 3 J/g starch shown in **Figure 12(a_1) & (a_2)** by green color region. Moreover, **Figure 12(b_1) & (b_2)** show the effect of OSA concentration and temperature on the enthalpy with pH and time fixed at 8 and 3.5 h, respectively. It was found that an increase in OSA concentration at low temperature produced low enthalpy value of OSAPS, indicating that OSA modification make the starch gelatinize easily at low temperature due to disruption of OSA groups on starch chains. Furthermore, **Figure 12(f_1) & (f_2)** demonstrates the effects of the reaction temperature and time on the enthalpy, with OSA concentration and pH fixed at 15.5%w/w and 8, respectively. The increase in the reaction time and temperature slightly affected the enthalpy of OSAPS. The contour plots **(Figure 12(a_1-f_1))** and 3D response surface plots **(Figure 12(a_2-f_2))** display the combined effect of OSA concentration, pH, temperature and time on enthalpy.

(a_1)

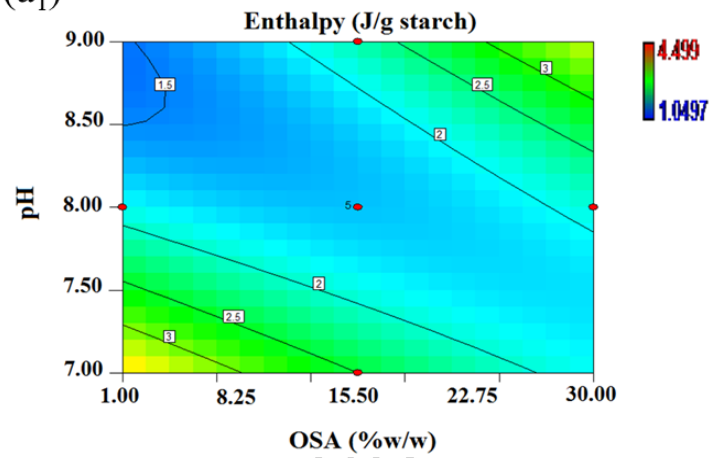
Enthalpy (J/g starch)
4.499
1.0497
pH
9.00
8.50
8.00
7.50
7.00
1.00
8.25
15.50
22.75
30.00
OSA (%w/w)

(b_1)

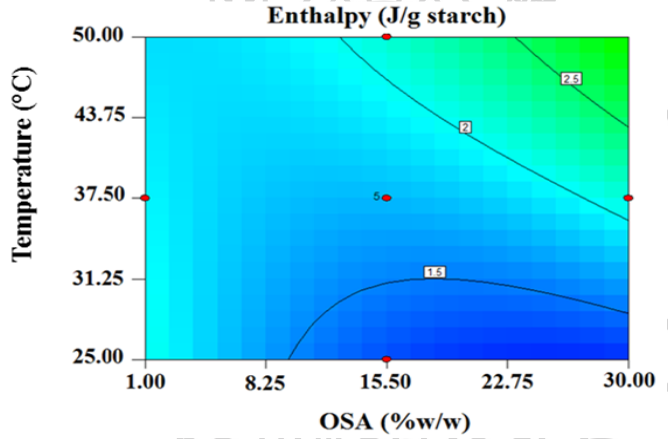
Enthalpy (J/g starch)
Temperature (°C)
50.00
43.75
37.50
31.25
25.00
1.00
8.25
15.50
22.75
30.00
OSA (%w/w)

(c_1)

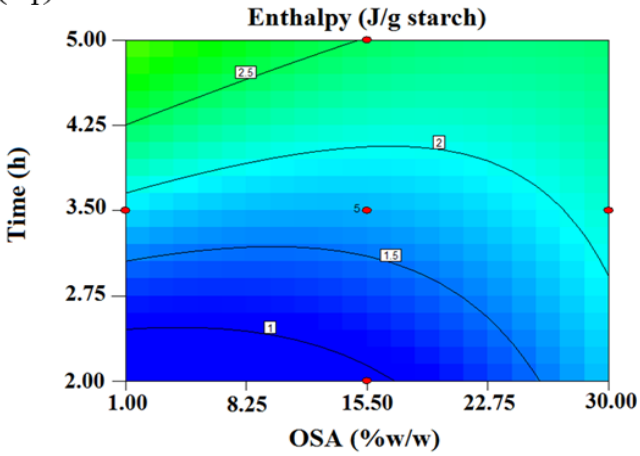
Enthalpy (J/g starch)
Time (h)
5.00
4.25
3.50
2.75
2.00
1.00
8.25
15.50
22.75
30.00
OSA (%w/w)

(d_1)

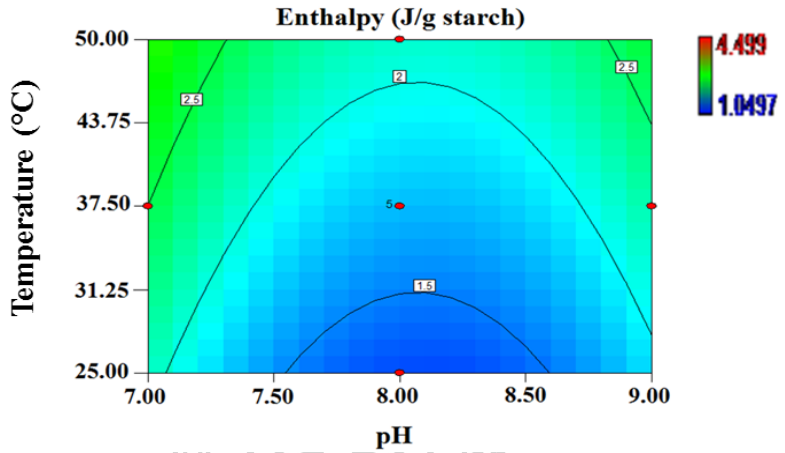
Enthalpy (J/g starch)
4.499
1.0497
Temperature (°C)
50.00
43.75
37.50
31.25
25.00
7.00
7.50
8.00
8.50
9.00
pH

(e_1)

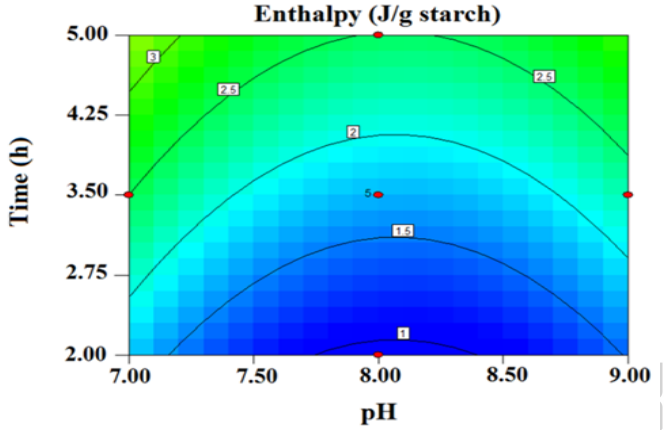
Enthalpy (J/g starch)
Time (h)
5.00
4.25
3.50
2.75
2.00
7.00
7.50
8.00
8.50
9.00
pH

(f_1)

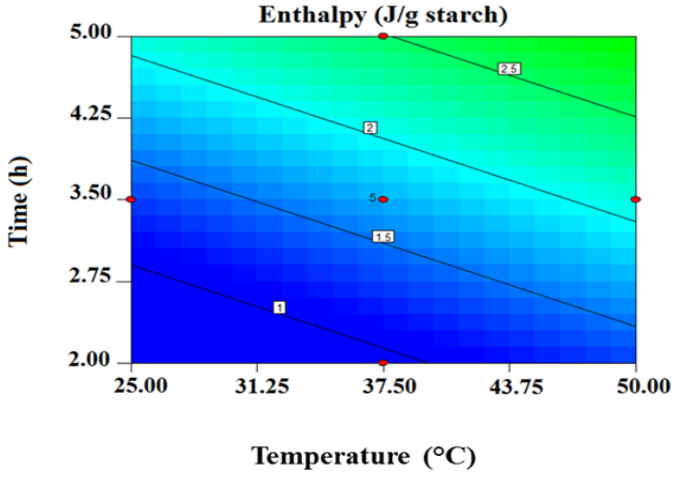
Enthalpy (J/g starch)
Time (h)
5.00
4.25
3.50
2.75
2.00
25.00
31.25
37.50
43.75
50.00
Temperature (°C)

(a_2)

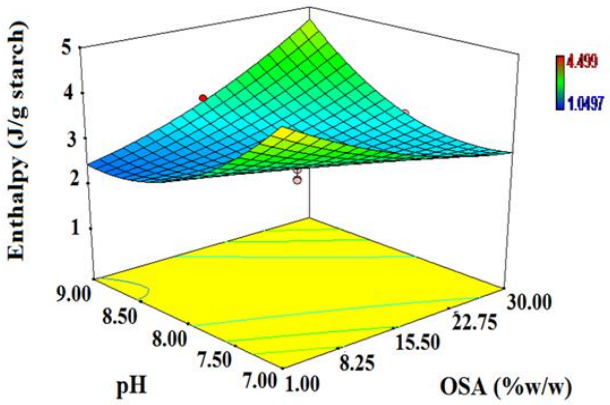
Enthalpy (J/g starch)
5
4
3
2
1
4.499
1.0497
9.00
8.50
8.00
7.50
7.00
pH
1.00
8.25
15.50
22.75
30.00
OSA (%w/w)

(b_2)

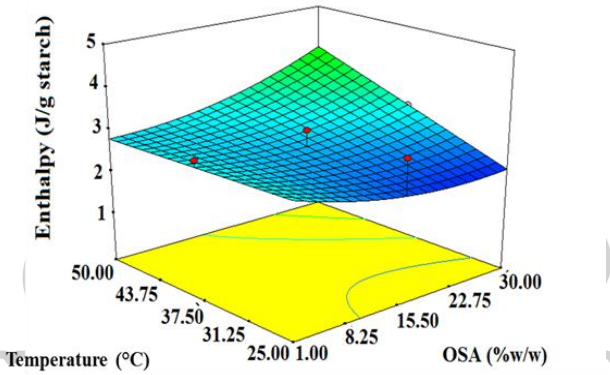
Enthalpy (J/g starch)
5
4
3
2
1
50.00
43.75
37.50
31.25
25.00
Temperature (°C)
1.00
8.25
15.50
22.75
30.00
OSA (%w/w)

(c_2)

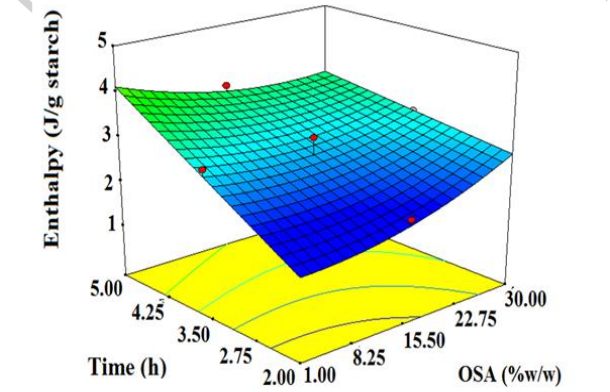
Enthalpy (J/g starch)
5
4
3
2
1
5.00
4.25
3.50
2.75
2.00
Time (h)
1.00
8.25
15.50
22.75
30.00
OSA (%w/w)

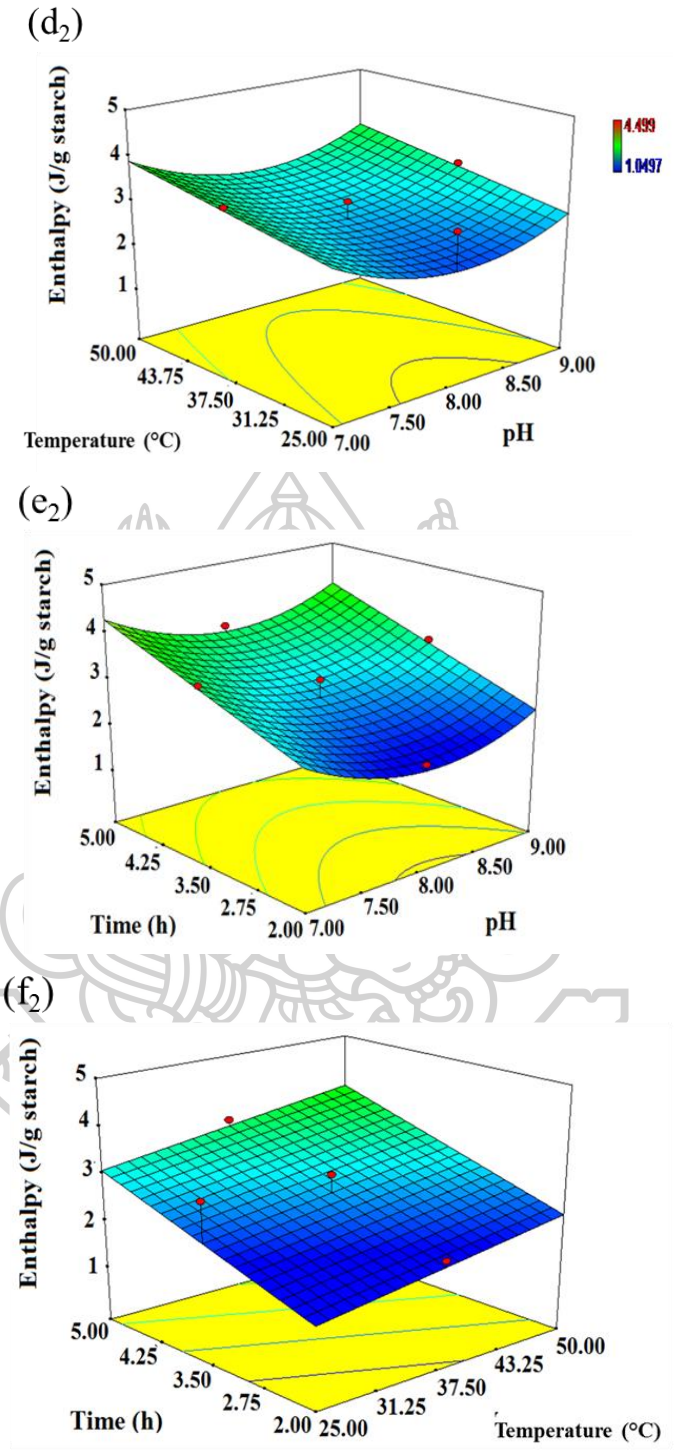

Figure 12 Contour (a_1-f_1) and 3D response surface plots (a_2-f_2) showing the combined effect of OSA concentration, pH, temperature and time on enthalpy.

4.1.1.4 Optimization model

The predictive ability of each model was validated by a set of four compounds that were not included in the training dataset. The predicted and experimental values for DS, surface tension, and enthalpy were well correlated with the standard predicted errors of 0.0132, 2.2297, and 1.395, respectively. Thus, it was suggested that the obtained model could exhibit good performance for predicting the DS, surface tension, and enthalpy values. To obtain design space for multiple responses, graphical optimization was performed by specify the desired response limits. In this study, modified pineapple starch with high DS, low surface tension and low enthalpy were required for effective emulsifying property. **Figure13 (a), (b) & (c)** shows the graphical optimization, which displays the area of feasible response values in the factor space. The area that satisfies the constraints is indicated in yellow, whereas the area that does not meet the criteria is indicated in gray. The optimum conditions were OSA =24%w/w, pH 7.8, reaction temperature = 37.5°C, and reaction time = 2 h, with a predicted DS value of 0.03, surface tension of 53.49 mN/m, enthalpy of 1.3417 J/g starch, and desirability value of 0.97.

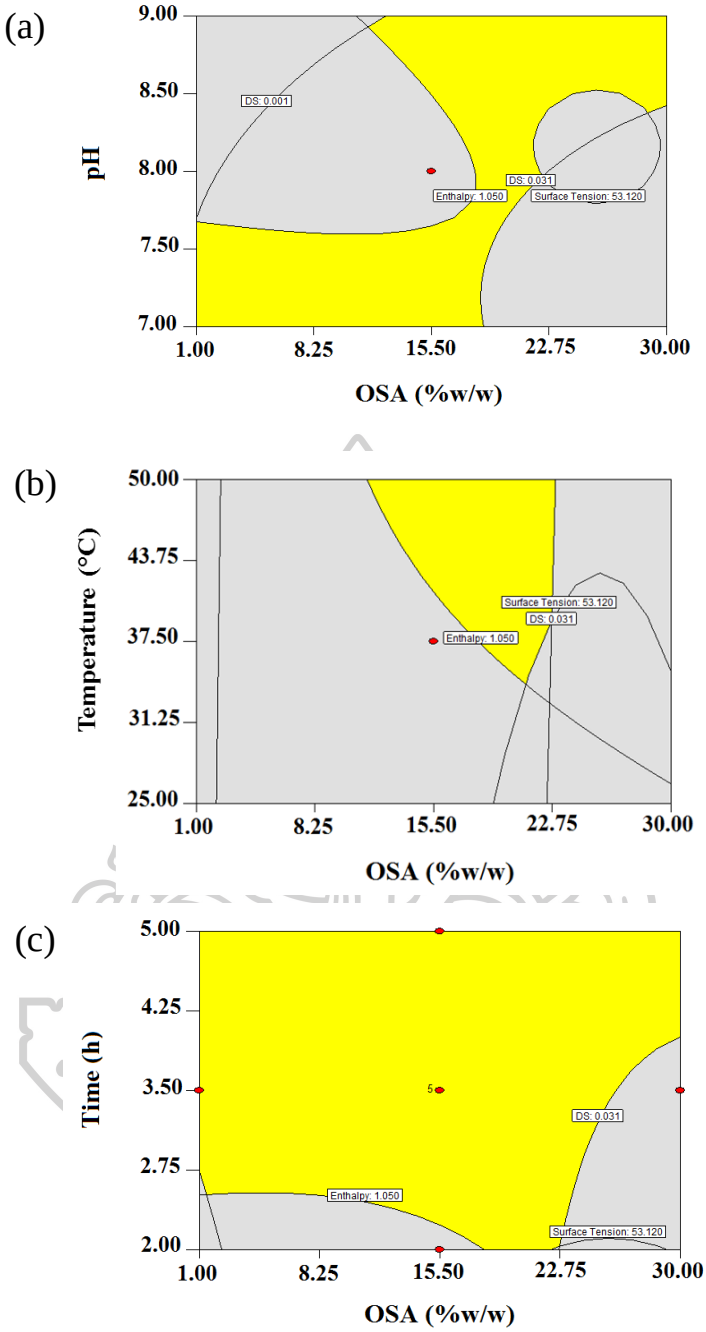

Figure 13 Overlay plots of graphical optimization displaying the area of feasible response values in the factor space for OSA synthesis condition between (a) OSA concentration and pH, (b) OSA concentration and temperature and (c) OSA concentration and time while other two factors kept at center points (Yellow color satisfies the constraints whereas grey color indicates for the area which does not meet the optimum criteria).

4.1.2 Viscosity

The effect of DS on the pasting profiles OSAPS is shown in **Figure 14**. After modification, the pasting temperature decreased, whereas the peak viscosity (at 90°C), final viscosity (at 30°C), and breakdown values increased compared with NPS. The viscosity of OSAPS increased with increasing DS. It may be possible that the hydrophobic groups of OSA being octenyl moieties disrupt hydrogen bonding along starch chains which make the starch chains more easily water-soluble. A similar pattern was found for OSA-modified plantain starch (Bello-Flores et al., 2014).

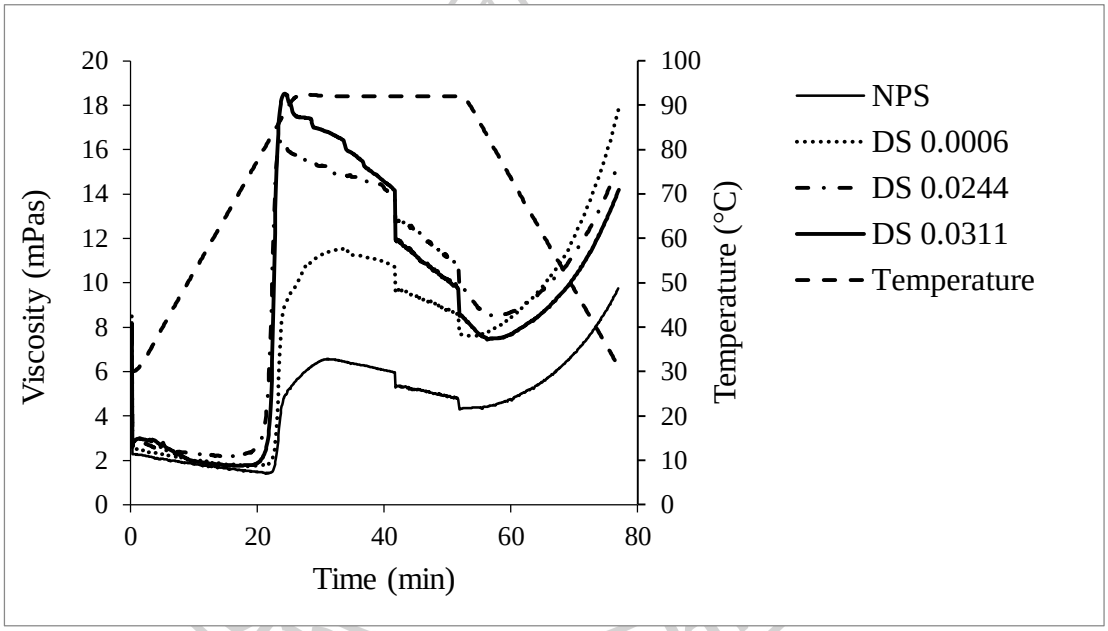

Figure 14 Effect of DS on the pasting profiles of OSAPS.

4.1.3 Crystallinity

Figure 15 shows the XRD patterns of NPS and OSAPS. The %crystallinity of OSAPS is listed in **Table 11**. Both NPS and OSAPS exhibit crystalline A-type XRD patterns, as shown by the strong reflections at approximately 15.1°, 17.5°, and 23°. The diffraction pattern of OSAPS did not change up to a DS value of 0.0311 because esterification primarily occurred in the amorphous region (Wang et al., 2011)

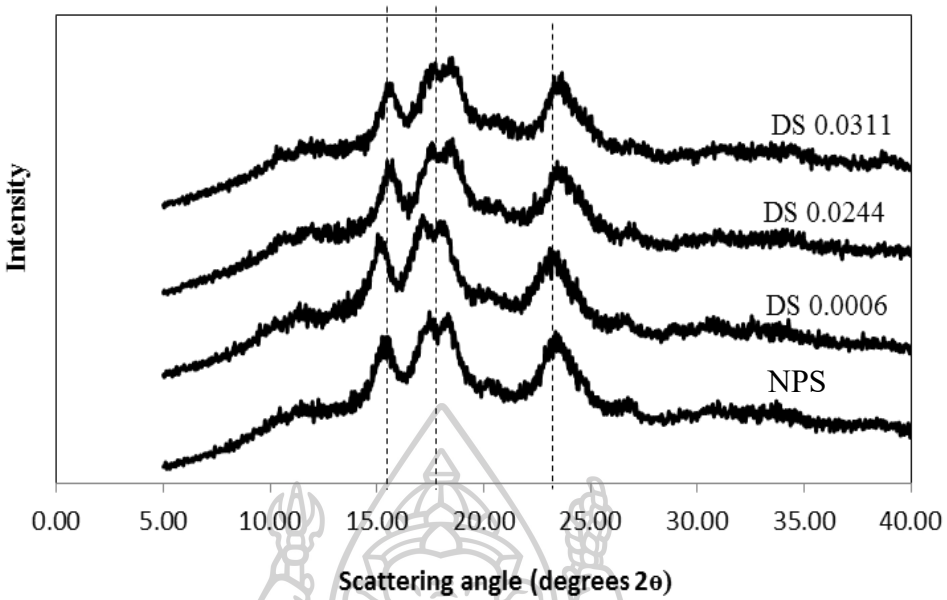

Figure 15 XRD patterns of NPS and OSAPS with DS of 0.0006, 0.0244, and 0.0311.

4.1.4 Morphology

The SEM results reveal that pineapple starch exhibited Y-shaped granules, with the granule sizes of 5–10 µm. The clustering of granules increased with increasing DS as shown in **Figure 16**. This could be due to the swelling and disruption of the starch particles during the reaction (Wang et al., 2011). Similar to potato starch, OSA modification moderately changed the morphology of starch (Hui et al., 2009; Wang et al., 2011).

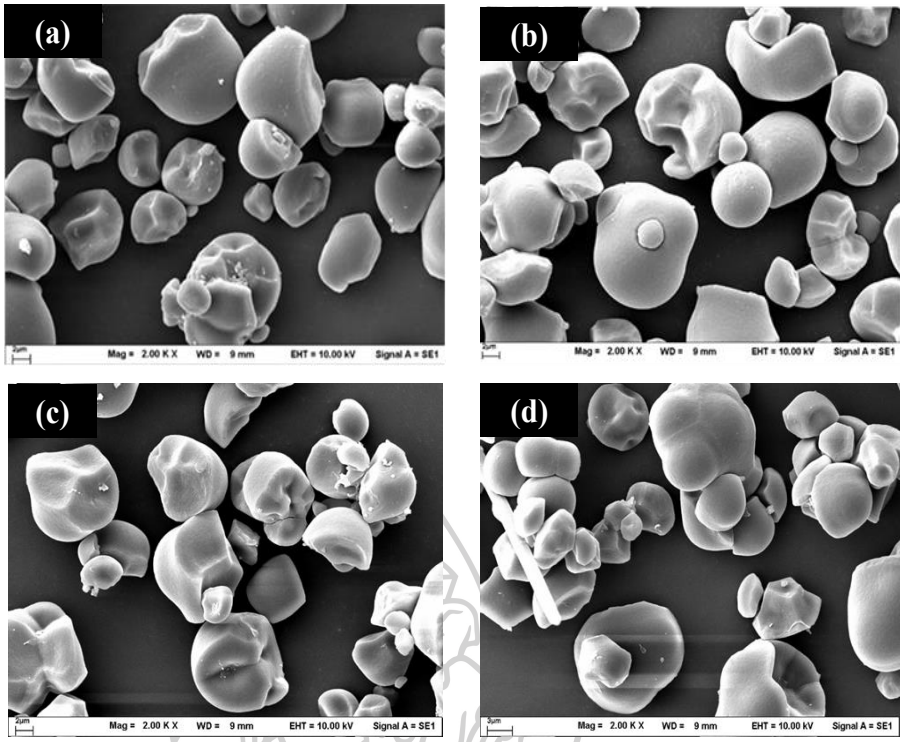

Figure 16 SEM images of (a) NPS and OSAPS granules with DS of (b) 0.0006, (c) 0.0244, and (d) 0.0311. The magnification was 2000×.

4.1.5 FTIR spectra

Figure 17 illustrates the FTIR spectra of NPS and OSAPS having different DS. The five absorption peaks of finger print regions were observed between 800-1200 cm^{-1} which are attributed to C-O bond stretching. The bands approximately appeared at 2928 cm^{-1} and 3417 cm^{-1} are characteristics of C-H stretching vibration of glucose unit and O-H stretch vibration of starch, respectively (Hui et al., 2009). The band occurred at 1646 cm^{-1} was due to residual bound water (Chang et al., 2014). Compared with NPS, a new peak was found at 1716 cm^{-1} for OSAPS, which can be attributed to the formation of ester carbonyl groups (Chang et al., 2014; Hui et al., 2009). In the modification process, sodium octenyl succinate starch was formed under alkaline conditions, leading to the appearance of a new peak at 1568 cm^{-1} that can be attributed to the asymmetric stretching vibration of carboxylate (Hui et al., 2009). The absorption peaks' intensity at 1716 and 1568 cm^{-1} increased with increasing DS (Chang et al., 2014).

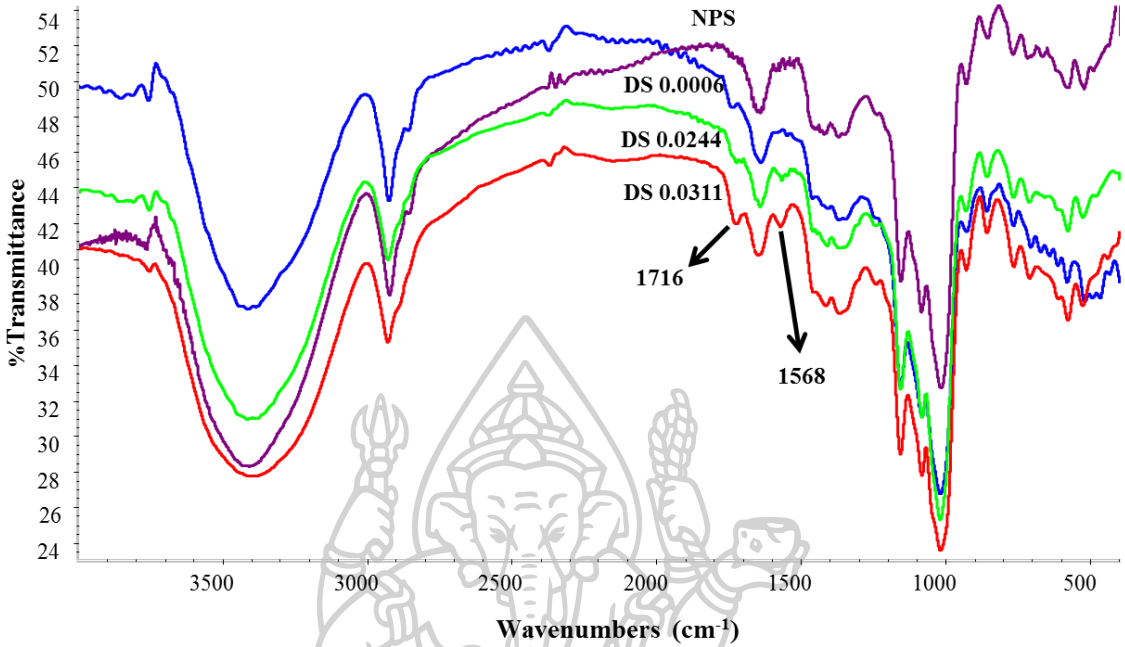

Figure 17 FTIR spectra of NPS and OSAPS.

4.2 Part II: Evaluation of OSAPS as nanoemulsion stabilizer and optimization of ITZ-loaded nanoemulsions

4.2.1 Solubility of ITZ

The solubility tests were conducted to select the suitable oil phase for ITZ nanoemulsions. **Figure 18(a)** shows the solubility of ITZ in different types of oil. Among the oils, castor oil and oleic acid showed the high solubility of 0.54±0.05 mg/mL and 0.46±0.01 mg/mL respectively whereas the other types of oil provided the solubility in the range of 0.12-0.20 mg/mL. Therefore, the solubility of ITZ was subsequently conducted in a combination system of castor oil and oleic acid (1:0.33, 1:0.5, 1:1, 1:2 and 1:3) because high molecular weight of castor oil (927 g/mol) and oleic acid (282.46 g/mol) may increase the solubility of lipophilic ITZ. Moreover, mixing of oils can solubilize the poorly water soluble drugs and oleic acid itself is solubilizing agent for water insoluble drug (Kalepu, Manthina, & Padavala, 2013). **Figure 18(b)** shows the effect of the combination of castor oil and oleic acid in various ratios on ITZ solubility. It was found that the combination of castor oil and oleic acid at the ratio of 1:1 displayed the highest loading of ITZ (1.23±0.21 mg/mL) as compared to other ratios. Therefore, it was chosen as the oil phase for the preparation of nanoemulsions.

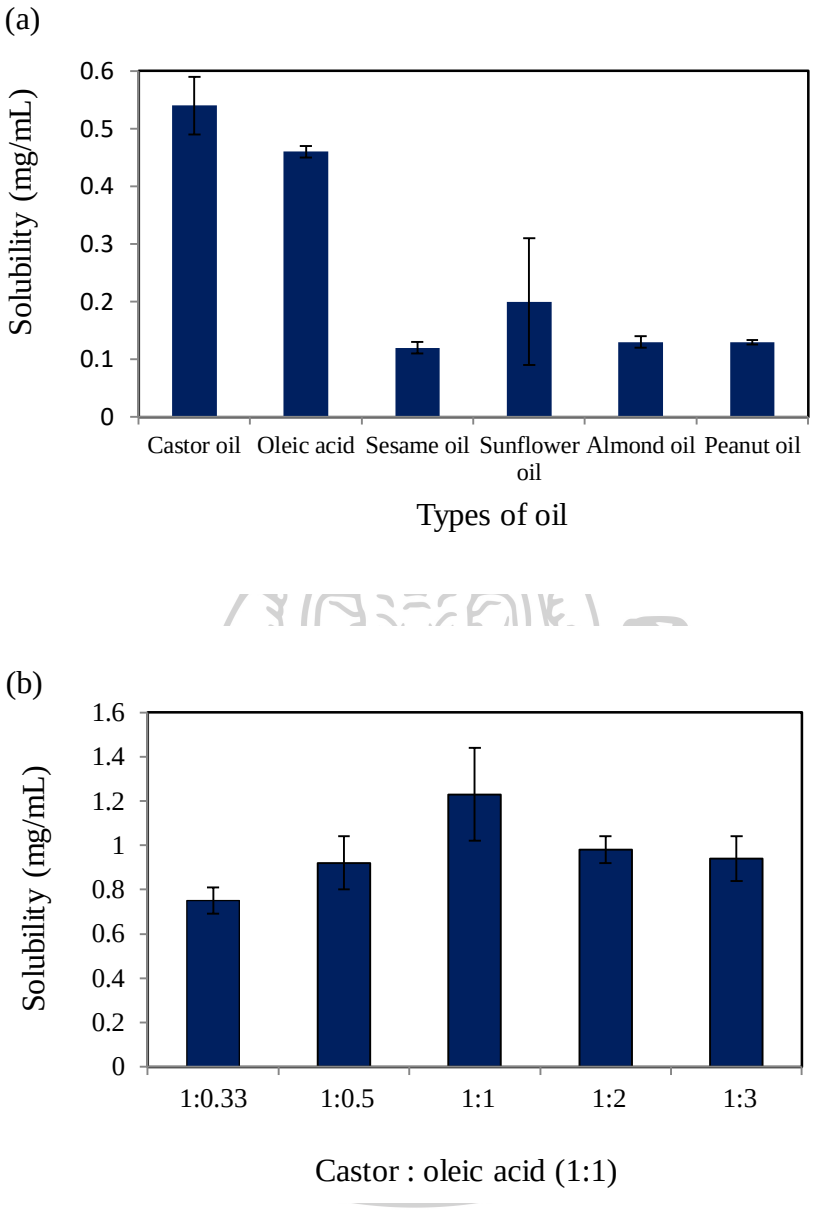

Figure 18 Solubility of itraconazole in: (a) different types of oil and (b) the combination of castor oil and oleic acid in various ratios. Data expressed as mean ± SD (*n*=3).

4.2.2 Functional properties of OSAPS

4.2.2.1 Surface and interfacial tension of OSAPS

The effect of NPS and OSAPS concentrations (0.5%, 1%, 3% and 5%w/w) having different DS 0.001, 0.02 and 0.03 on surface tension and interfacial tension were studied at air/water and oil/water system, respectively. The surface and interfacial tension measurement of the concentration 10% was limited and thus it was discontinued for the present work. The surface tension results ranged from 51.33-71.89 mN/m. The effect of DS on surface tension was obviously noticed at high DS when starch concentration was increased to 5% as shown in **Figure 19(a)**. The surface tension of NPS was statistically different from OSAPS when the starch concentration was 0.5% and 1%w/w (p<0.05). The surface tension of OSAPS having high DS 0.02 and 0.03 was not different at 0.5%-1%w/w. However, the surface tension of OSAPS having high DS was slightly decreased when compared with NPS and OSAPS with DS 0.001. The surface tension of OSAPS having DS 0.001 was statistically different from NPS and OSAPS having high DS at those concentrations (0.5-1%). At higher concentration of starch 3% and 5%, the surface tension of OSAPS having DS 0.02 and DS0.03 indicated significant difference when compared with NPS and OSAPS with low DS, indicating that different DS of OSAPS affected surface tension property. It may be due to an increase in hydrophobicity after esterification with OSA. Hydrophobic groups of OSA starches are oriented toward the air and hydrophilic starch are extended to the water when they are dissolved in water, thereby forming a boundary layer, leads to lower surface tension due to migration of macromolecules to air/water interface (Sweedman, Tizzotti, et al., 2013). Therefore, OSA starches have extreme surface active property which was positively related to DS (Shogren & Biresaw, 2007). Efficiency of emulsifiers not only relates with efficient lowering surface tension but also depends on adsorption kinetics to prevent shear induced coalescence for stabilization after droplet formation (Mason et al., 2006). Therefore, interfacial property was also tested in this study.

The effect of concentration of NPS and OSAPS (0.5-5%w/w) on interfacial tension at oil-water interface was examined against the combination of castor and oleic acid (1:1). In this study, interfacial tension results ranged from 11.7-16.95 mN/m. The increase in OSAPS concentration led to a decrease in interfacial

tension. This finding was in agreement with the previous research (Abbas et al., 2014; Hategekimana et al., 2015; Zhao et al., 2017). At starch concentration 0.5%, the interfacial tension of OSAPS was not different but lower than that of NPS. When the starch concentration was increased from 1-5%, OSAPS having high DS 0.03 showed a significant decrease in interfacial tension as shown in **Figure 19(b)**. The results suggested that OSAPS have capability in reduction of interfacial tension due to adsorption at oil-water interface. Since the interfacial property is considered as a critical factor in preparation of emulsion, therefore, it had potential to use as emulsifier.

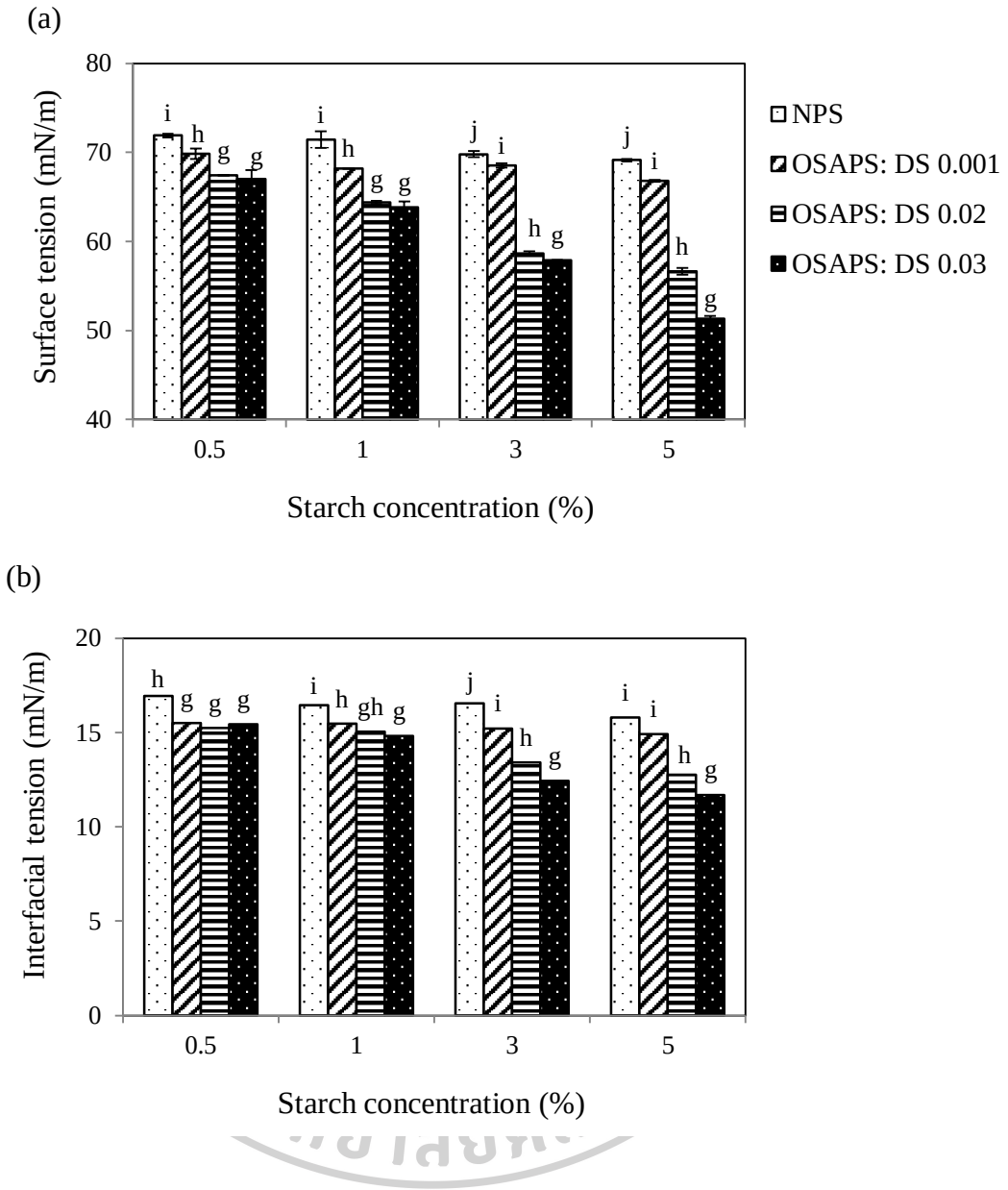

Figure 19 Effect of concentration of NPS and OSAPS with different DS on: (a) surface tension (b) interfacial tension. g-jDifferent alphabet letters in the same category show statistically different (p<0.05) by Tukey HSD.

4.2.2.2 Rheological property of OSAPS

The rheological properties of NPS and OSAPS gel solutions at various concentrations were summarized in **Table 13**. The results of consistency indices (K) ranged from 0.004 to 0.5455 Pa.s. Comparison of means by a Tukey HSD test indicated that the K values of OSAPS were increased when the starch

concentration was increased from 0.5 to 5%. The similar finding was corresponded with Dokic et al (Dokić et al., 2012). For NPS, the consistency index was not statistically different at 0.5-3% (p>0.5). It was found that an increase DS tended to increase the consisitency indices and showed significant difference (p<0.5) shown in **Table 13**. The K values of NPS and OSAPS having DS 0.001 were not significantly different at five percent of starch concentration whereas those of OSAPS having high DS were significantly different. The flow behavior indices (n) of NPS and OSAPS having DS 0.001 and 0.02 were significant different when starch concentration was increased from 0.5-5%. It was observed that n values of OSAPS having high DS 0.03 was not statistically different at 0.5-5%. However, the n values of NPS and OSAPS were smaller than 1 (n<1) as resulted from power law model fit. This indicated non-newtonian behavior with shear thinning and pseudoplastic flow characteristics (Dokić et al., 2012; Sharif et al., 2017).

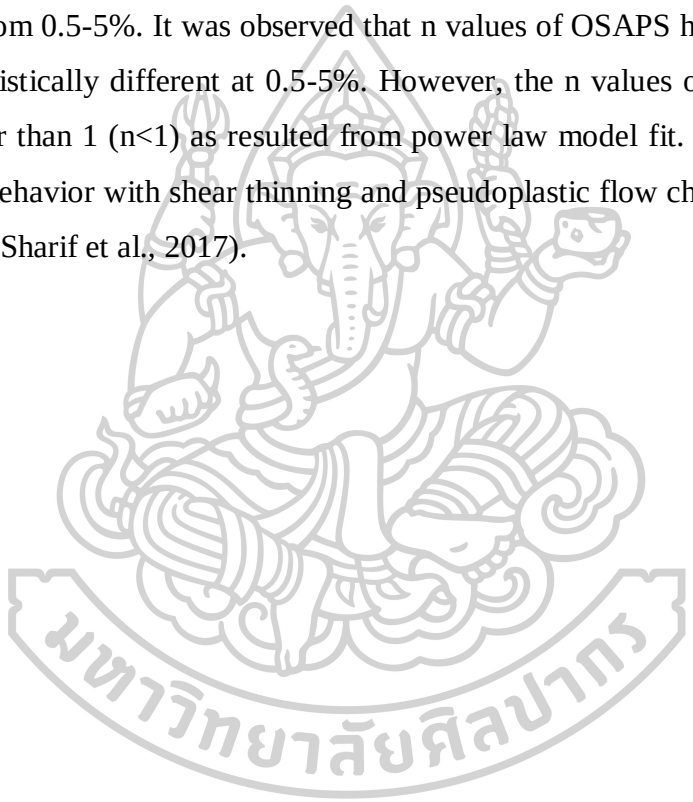

Table 13 Rheological properties of NPS and OSAPS gel solutions at different concentrations* (n=3).

Starch	DS	Concentration (%)	Flow parameters	
			K (Pa.s)	n
NPS	0	0.5	0.0040±0.00^{a}	0.5756±0.20^{bcd}
		1	0.0053±0.00^{a}	0.5855±0.06^{bcd}
		3	0.0333±0.00^{a}	0.7686±0.02^{d}
		5	0.1367 ± 0.03^{c}	0.7508 ± 0.03^{cd}
OSAPS	0.001	0.5	0.0065±0.00^{a}	0.3032±0.06^{a}
		1	0.0083±0.00^{a}	0.531±0.14^{abc}
		3	0.0431±0.02^{ab}	0.6629±0.11^{bcd}
		5	0.1501±0.02^{c}	0.7164±0.07^{bcd}
OSAPS	0.02	0.5	0.0067±0.00^{a}	0.6706±0.05^{bcd}
		1	0.0082±0.00^{a}	0.7495±0.03^{cd}
		3	0.1177±0.01b^{ab}	0.7550±0.01^{cd}
		5	0.4381±0.08^{d}	0.4888±0.01^{ab}
OSAPS	0.03	0.5	0.0148±0.00^{a}	0.5781±0.04^{bcd}
		1	0.0225±0.00^{a}	0.6489±0.04^{bcd}
		3	0.1349±0.02^{c}	0.6949±0.02^{bcd}
		5	0.5455±0.06^{e}	0.6159±0.02^{bcd}

K=consistency index, n=flow behavior index; *Data were expressed as mean ± standard deviation (SD).$^{a\text{-}e}$Different superscript letters in the same column indicate statistically difference (p<0.05) by Tukey HSD.

4.2.2.3 Emulsifying property

The EAI of emulsions containing OSAPS was higher than that of emulsion containing NPS as shown in **Figure 20**. The EAI was relatively increased with increasing DS of OSAPS. It is possible that OSA group increases hydrophobicity of pineapple starch and decreases in interfacial tension of emulsion. This was similar to that observed by Miao et al (Miao et al., 2014). Therefore, it could be possible to further study the application of OSAPS as effective co-emulsifier.

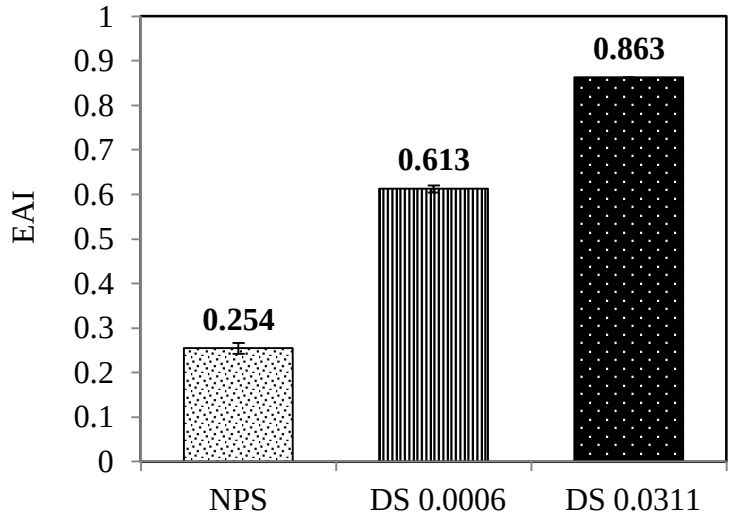

Figure 20 EAI of emulsions containing NPS and OSAPS with DS of 0.0006 and 0.0311.

4.2.3 Effect of different parameters on droplet size of ITZ-loaded nanoemulsions

Based on the functional properties of OSAPS having different DS studied in part I, OSAPS having high DS 0.03 was selected and preliminary studies was performed to investigate the effects of different parameters on droplet size of ITZ-loaded nanoemulsions using a one-factor-at-a-time.

4.2.3.1 Effect of homogenization speed

Homogenization speed is one of the important influence factor on droplet size of the nanoemulsion. Smaller droplet size of nanoemulsions can be formed by high speed homogenization. Its dimmution principle to disrupt the droplets is use of the hydrodynamic shear force which produces vigorous turbulent flow and powerful heat energy, thereby leading to increase temperature. Subsequently, the elevated temperature can cause a decrease in viscosity of the dispersed phase and facilitate to get small size of droplets (Scholz & Keck, 2015). Hence, the effect of homogenization speed on droplet size of ITZ-loaded nanoemulsion was first studied under the conditions of 1%w/w OSAPS concentration, 20%w/w polysorbate 80 concentration, 30%w/w castor : oleic acid oil (1:1) and homogenization time of 25

mins as shown in **Figure 21(a)**. The droplet size of ITZ-loaded nanoemulsions sharply decreased with increasing homogenization speed (16000-20000 rpm). At 16,000 rpm, the nanoemulsions showed droplet size of 1144 ± 5.03 nm. When homogenization speed was increased to 18000 rpm, the droplet size of ITZ-loaded nanoemulsions decreased to 645 ± 8.39 nm. Further increasing of homogenization speed (20000 rpm) provided nanoscale droplet size (393 ± 0.58 nm). It was within the range of nanodroplet size (<500 nm) (Debnath et al., 2011; Gupta et al., 2016). The droplet size of nanoemulsions displayed downward trend with an increase in homogenization speed. This finding was in agreement with Li, et al (Li et al., 2017). In order to consider the comprehensive influence on the nanoscale-droplet size, the homogenization speed 20000 rpm was selected and fixed for further study.

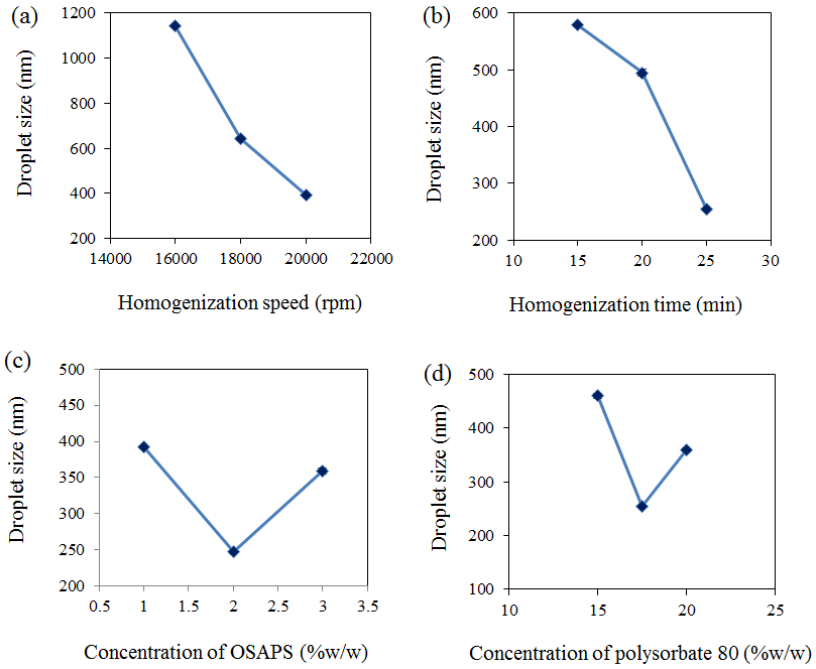

Figure 21 Effect of different parameters (a) homogenization speed (b) homogenization time (c) concentration of OSAPS and (d) concentration of polysorbate 80 on droplet size using a one-factor-at-a-time. Average data from triplicate are presented as mean ± standard deviation (SD) of the mean, (n=3).

4.2.3.2 Effect of homogenization time

Besides homogenization speed, the effect of homogenization time on droplet size was also investigated under the conditions of OSAPS concentration of 3%, polysorbate 80 concentration of 20% and homogenization speed of 20000 rpm as shown in **Figure 21(b)**. When the time was increasing from 15 min to 25 min, the droplet size of ITZ-loaded nanoemulsion was relatively decreased from 579 ± 1.00 nm to 255 ± 1.82 nm. This downward trend was related with homogenization speed effect as mentioned above. The similar finding was in agreement with Li et al (Li et al., 2017). The longer the time treatment, the smaller the droplet size was reported by Calligaris et al (Calligaris et al., 2016). Homogenization speed as well as the time had a strong influence on the droplet size of the nanoemulsion (Scholz & Keck, 2015).

4.2.3.3 Effect of OSAPS concentration

Most polysaccharides in the continuous phase perform as emulsion stabilizer and influence on droplet size of nanoemulsion due to its higher viscosity (Arancibia, Navarro-Lisboa, Zúñiga, & Matiacevich, 2016; Li et al., 2017). Therefore, the effect of OSAPS concentration (1-3%) on droplet size of nanoemulsion was investigated under the conditions of polysorbate 80 at the concentration of 20%w/w, homogenization speed of 20,000 rpm, homogenization time of 25 min as shown in **Figure 21(c)**. Studies of OSAPS concentration more than 3% was limited due to higher viscosity of OSAPS gel concentration as mentioned in above section *4.2.2.2*. At 1% of OSAPS concentration, the nanoemulsions showed droplet size (393 ± 0.58 nm) and then decreased rapidly when starch concentration was increased to 2% (248 ± 1.62 nm). Further increasing to 3% OSAPS concentration resulted a slight increase in droplet size (359 ± 4.0 nm). It might be due to raised viscosity of nanoemulsion containing the combination of 3%w/w OSAPS and 20%w/w polysorbate 80. However, an increase in starch concentration leads to increase in droplet size. The similar trend was in agreement with the one observed by Li, et al (Li et al., 2017).

4.2.3.4 Effect of polysorbate 80 concentration

The ITZ-loaded nanoemulsions were prepared by varying concentration of polysorbate 80 (15-20%) while other factors are kept at constant conditions of 3%w/wOSAPS, homogenization speed of 20000 rpm and time of 25 min and studied the effect of polysorbate 80 concentration on droplet size of the nanoemulsions as displayed in **Figure 21(d)**. At low concentration of polysorbate 80 (15%), the nanoemulsions showed droplet size 460 ± 4.35 nm. Then, the droplet size was sharply decreased (255 ± 1.82 nm) when polysorbate 80 concentration was increased to 17.5 %. It might be due to lowering interfacial tension of Polysorbate 80. The similar finding was reported by Mehmood, et al (Mehmood, Ahmad, Ahmed, & Ahmed, 2017). Further increasing polysorbate 80 concentration leads to a slight increase in droplet size about 359 ± 4.00 nm. It might be possible that higher concentration of polysorbate 80 and OSAPS concentration result in increasing viscosity of nanoemulsions and being difficult in the droplet breaking into smaller size. The result was corresponded with Mehmood, et al and Li, et al (Li et al., 2017; Mehmood et al., 2017).

4.2.4 ITZ-loaded nanoemulsions containing OSAPS using CCF design

ITZ-loaded nanoemulsions were prepared by simple homogenization method to avoid high pressure and using mixtures of emulsifier and surfactant to rupture the droplets effectively. Extreme shear is one of the factors controlling to rupture microscale droplets into nanodroplets. However, to prevent shear-induced coalescence, the continuous phase requires a significant excess of surfactant. They can easily and quickly adsorb onto the surfaces of newly fresh created droplets (Mason et al., 2006). In this study, a fractional factorial CCF design was conducted to determine the relationship between independent variables and response variables. Three parameters such as OSAPS concentration of 1-3%w/w, polysorbate 80 concentration of 15-20%w/w and homogenization time 20-30 min were selected as independent variables to optimize the preparation conditions of ITZ-loaded nanoemulsion using RSM, based on the results of the single factor test studied in preliminary screening. A fractional factorial CCF design of 15 experimental runs with the independent variables and the observed responses such as droplet size, PDI, zeta

potential, drug content, flow parameters including consistency index, flow behavior index and determination coefficient and *in vitro* drug release (%) within 15 min of the prepared ITZ-loaded nanoemulsions is summarized in **Table 14**.

It was found that smaller nanodroplet size and PDI of ITZ-loaded nanoemulsion is dependent upon the concentration of OSAPS and polysorbate 80. In this study, droplet size values ranged from 246 to 319 nm. The minimum droplet size 246 nm and PDI 0.25 corresponded to high percent of OSAPS (3%w/w) and polysorbate 80 (20%w/w) of Run 5 nanoemulsion as shown in **Table 14**. It might be due to the fact that the combination of OSAPS and polysorbate 80 can effectively adsorb oil-water interface and decrease interfacial tension. An increase amount of surfactant can easily and quickly adsorb onto the surface of newly fresh created droplet (Mason et al., 2006). The similar finding was observed by Kumar et al (Kumar et al., 2009) who reported that higher content of polysorbate 80 led to reduce in globule size. In addition, it has been reported that the droplet size decreased with respect to an increase in surfactant concentration due to availability of surfactant molecules around the freshly created oil droplets (Nagi et al., 2017).

Table 14 Fractional factorial CCF design with independent variables and observed responses of ITZ loaded nanoemulsions

Independent variables				Observed responses							
Runs	X_1	X_2	X_3	Droplet size (nm)	Polydispersity index	Zeta potential (mV)	Drug content (%)	Flow parameters			*In vitro* drug release (%) within 15 mins
								K (Pa.s)	n	R^2	
1	2	20	25	248 ± 1.62^{a}	0.27 ± 0.01^{ab}	-37.80 ± 0.36^{bcd}	101 ± 1.95	371 ± 3.74^{k}	0.1222 ± 0.00^{b}	0.9634 ± 0.01^{bc}	37 ± 3.04^{abc}
2	3	15	30	297 ± 0.25^{cd}	0.39 ± 0.03^{de}	-41.87 ± 0.35^{a}	104 ± 1.68	260 ± 6.37^{i}	0.1444 ± 0.01^{bc}	0.9702 ± 0.01^{c}	36 ± 0.71^{abc}
3	2	17.5	25	319 ± 1.97^{e}	0.42 ± 0.04^{e}	-37.47 ± 0.47^{bcd}	104 ± 3.66	182 ± 5.16^{de}	0.1474 ± 0.01^{bcd}	0.9973 ± 0.00^{c}	55 ± 1.25^{de}
4	1	15	20	306 ± 10.14^{de}	0.55 ± 0.04^{f}	-37.63 ± 1.16^{bcd}	106 ± 1.86	3 ± 0.14^{a}	0.7519 ± 0.00^{g}	0.9990 ± 0.00^{c}	105 ± 2.68^{g}
5	3	20	20	246 ± 2.48^{a}	0.25 ± 0.02^{a}	-39.07 ± 0.90^{b}	102 ± 2.10	517 ± 2.23^{l}	0.1299 ± 0.01^{bc}	0.9220 ± 0.03^{b}	61 ± 6.63^{e}
6	2	17.5	25	298 ± 6.74^{cd}	0.34 ± 0.03^{bcde}	-38.43 ± 0.40^{bc}	103 ± 2.67	193 ± 4.27^{ef}	0.1495 ± 0.01^{bcd}	0.9962 ± 0.00^{c}	53 ± 11.7^{cde}
7	2	15	25	281 ± 3.91^{b}	0.42 ± 0.02^{e}	-38.50 ± 0.35^{bc}	103 ± 1.41	120 ± 1.71^{c}	0.1811 ± 0.00^{e}	0.9941 ± 0.00^{c}	82 ± 8.13^{f}
8	1	20	30	274 ± 2.48^{b}	0.29 ± 0.01^{abc}	-36.73 ± 0.90^{bcd}	103 ± 1.76	202 ± 6.37^{fg}	0.1749 ± 0.01^{de}	0.9926 ± 0.00^{c}	44 ± 2.99^{bcd}
9	2	17.5	25	303 ± 7.55^{d}	0.32 ± 0.04^{abcd}	-38.83 ± 0.49^{bc}	103 ± 2.00	214 ± 3.74^{gh}	0.1383 ± 0.00^{bc}	0.9928 ± 0.00^{c}	42 ± 6.14^{bcd}
10	3	17.5	25	255 ± 1.82^{a}	0.27 ± 0.01^{ab}	-36.53 ± 1.91^{cd}	103 ± 3.10	331 ± 2.48^{j}	0.0718 ± 0.01^{a}	0.8067 ± 0.04^{a}	31 ± 10.76^{ab}
11	2	17.5	20	317 ± 1.70^{e}	0.42 ± 0.02^{e}	-35.37 ± 0.12^{d}	106 ± 1.09	178 ± 2.90^{de}	0.1441 ± 0.01^{bc}	0.9955 ± 0.00^{c}	28 ± 1.74^{ab}
12	2	17.5	25	297 ± 5.46^{cd}	0.38 ± 0.02^{de}	-35.47 ± 0.40^{d}	104 ± 2.60	205 ± 4.57^{fg}	0.1504 ± 0.00^{bcd}	0.9962 ± 0.00^{c}	34 ± 1.80^{ab}
13	2	17.5	30	297 ± 6.17^{cd}	0.37 ± 0.04^{cde}	-37.53 ± 1.19^{bcd}	105 ± 0.12	226 ± 5.26^{h}	0.1322 ± 0.01^{bc}	0.9890 ± 0.00^{c}	32 ± 6.44^{ab}
14	2	17.5	25	279 ± 4.45^{b}	0.32 ± 0.02^{abcd}	-43.20 ± 0.44^{a}	105 ± 2.25	204 ± 8.29^{fg}	0.1550 ± 0.00^{cde}	0.9901 ± 0.00^{c}	24 ± 2.70^{a}
15	1	17.5	25	285 ± 4.35^{bc}	0.38 ± 0.05^{de}	-35.80 ± 0.69^{d}	105 ± 1.77	60 ± 7.23^{b}	0.3582 ± 0.026^{f}	0.9858 ± 0.00^{c}	44 ± 1.83^{bcd}

X_1: octenyl succinic anhydride (OSA) modified pineapple starch concentration (%w/w), X_2: polysorbate 80 concentrtion (%w/w), X_3: Homogenization time (min); K: Viscosity index; n: Consistency index; R^2: Correlation coefficients. All data are presented as mean ± SD, (n=3). $^{a-l}$Different superscript letters in the same column statistically difference ($p<0.05$) by Tukey HSD.

Moreover, lower PDI was obtained at higher concentration of OSAPS and polysorbate 80, suggesting that the effect of OSAPS and polysorbate 80 concentration on droplet size of nanoemulsion was the same trend on size distribution, represented by PDI. However, the prepared ITZ-loaded nanoemulsions showed narrower size distribution, ranged from (0.25-0.55). The similar finding was reported by Tan, et al (Tan et al., 2016).

When homogenization time was increased from 20 to 30 min, the droplet size of ITZ-loaded nanoemulsions reduced from 317 nm to 297 nm depending on homogenization time at constant level of OSAPS and polysorbate 80 as shown in **Table 14**. This finding was corresponded with (Calligaris et al., 2016; Li et al., 2017; Scholz & Keck, 2015). It has been reported that the longer the time treatment, the smaller the droplet size is observed (Calligaris et al., 2016). In this study, the droplet size of prepared ITZ-loaded nanoemulsions was found to be less than 500 nm (Debnath et al., 2011; Gupta et al., 2016). Homogenization time had a negative effect on PDI in this study.

Zeta potential is an important parameter for stability of emulsion. In the present study, the prepared nanoemulsions showed negative zeta potential and ranged from -35.37 to -43.20 mV. It might be due to the presence of negatively charged (carboxylic) groups on OSA starch molecules. This finding was corresponded with (Abbas et al., 2014; Woitiski, Veiga, Ribeiro, & Neufeld, 2009). According to HPLC analysis, all prepared nanoemulsions showed 100% drug content.

In this study, OSAPS, polysorbate 80 and homogenization time had a positive effect on viscosity of ITZ-loaded nanoemulsions. The viscosity results ranged from 3-517 Pa.s. Run 4 containing 1%w/w OSAPS plus 20%w/w polysorbate 80 showed low viscosity of 3 Pa.s while Run 5 containing 3%w/w OSAPS and 20%w/w polysorbate 80 showed the maximum viscosity (517 Pa.s) as shown in **Table 14**. An increase in OSAPS concentration and polysorbate 80 concentration raised the viscosity of ITZ-loaded nanoemulsion. Moreover, an increase in homogenization time from 20 to 30 min at constant level of other two factors tended to elevate the viscosity of nanoemulsions (Run 11, 12 and 13), showing 178, 205 and 226 Pa.s, respectively. The viscosity results of the prepared nanoemulsions were significantly different

(p<0.05) except Run 12 and 14, where the viscosity results of 205 and 204 Pa.s were not statistically different (p>0.05) shown in **Table 14**.

Nevertheless, the viscosity of nanoemulsions containing OSAPS were higher than that of control having 1 Pa.s and ITZ-loaded nanoemulsion containing NPS having 58 pa.s. It can be explained by the fact that starch after modification with OSA increased the viscosity of native starch due to disruption of hydrogen bonding along the starch chain by OSA group (Bello-Flores et al., 2014). Therefore, the rheological property of oil-in-water emulsion containing OSA starch was increased with respect to OSA starch concentration (Dokić et al., 2012). In this study, OSAPS having high DS of 0.03 exhibited higher viscosity than that of NPS (Latt et al., 2019). Moreover, it has been reported that increasing concentration of emulsifier and surfactant resulted in raised viscosity of nanoemulsions (Li et al., 2017; Mehmood et al., 2017). Therefore, the prepared ITZ-loaded nanoemulsions exhibited increased viscosity property with respect to increasing concentration of OSAPS and polysorbate 80.

The flow behavior index (n) of the prepared nanoemulsions ranged from 0.0718 to 0.7519. n values of all nanoemulsions displayed less than 1, indicating that they had shear thinning behavior and followed pseudoplastic characteristics. This finding was in agreement with some researches (Dokić et al., 2012; Sharif et al., 2017). Furthermore, the prepared nanoemulsions showed determination coefficient (R^2) 0.92-0.99 except Run 10 formulation containing OSAPS (3%) and polysorbate 80 (17.5%) (R^2=0.8067). It might be due to raised viscosity of nanoemulsion which make the flow behavior difficult to fit the power law model (99%). However, the prepared nanoemulsions well fitted to power law model according to high R^2 (0.81-0.99).

4.2.5 In vitro drug release

Dissolution studies of ITZ was conducted to compare the release of ITZ from the prepared nanoemulsions against the intact ITZ. **Figure 22** exhibits the results of comparative drug release profiles of all ITZ-nanoemulsions and intact ITZ. It was found that the drug release from ITZ-nanoemulsions was much faster and higher in SGF than intact ITZ**.** Among the prepared nanoemulsions, Run 4 containing the combination of 1%w/w OSAPS and 15%w/w polysorbate 80 and Run 7 containing

the combination of 2%w/w OSAPS and 15%w/w polysorbate 80 exhibited faster dissolution rate and high drug release of (105%) and (82 %) within 15 min as shown in **Figure 22** and the droplet size were 306 nm and 281 nm respectively **(Table 14)**, indicating that nanoscale droplet size (<500 nm) leads to high surface area and ITZ dissolve fast (Chhabra et al., 2011; Parveen et al., 2011). However, Run 5 containing 3%w/w OSAPS and 20%w/w polysorbate 80 showed drug release of 61% within 15 min in spite of the smallest droplet size (246 nm). It might be due to highest viscosity of 517 nm, indicating that the nanoemulsion droplet is slowly dissolved, thereby leading to a decrease in drug release as shown in **Table 14**. This finding was in agreement with Bhattacharjee, et al (Bhattacharjee et al., 2017). Control containing 17.5%w/w polysorbate 80 in the absence of polymer and nanoemulsion containing 2%w/w NPS and 17.5%w/w polysorbate 80 also showed fast dissolution and high drug release of (94%) and (87%) within 15 min as displayed in **Figure 22** and **Appendix (4)**. It might be due to low viscosity of nanoemulsions. This finding was corresponded with those reported by Parveen, et al (Parveen et al., 2011).

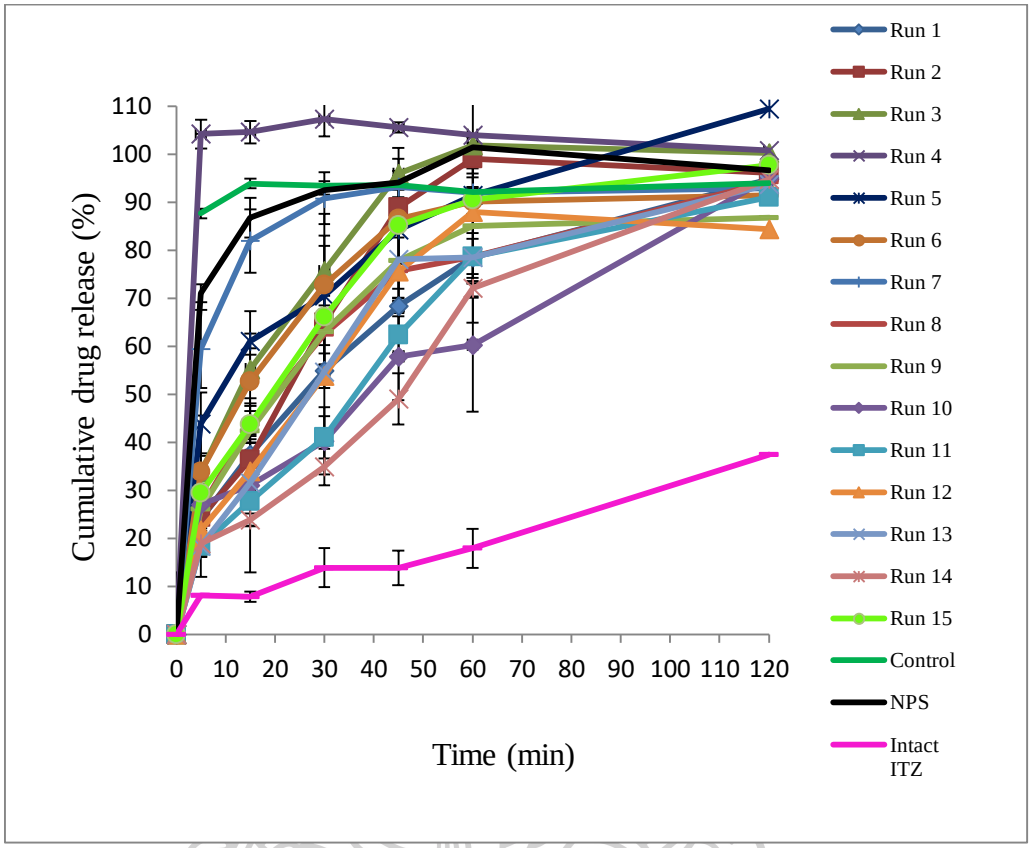

Figure 22 Drug release profiles of ITZ-loaded nanoemulsions in various conditions based on fractional factorial CCF and intact ITZ.

The prepared ITZ-loaded nanoemulsions having high viscosity such as Run 1, Run5 and Run 10 showed slow drug release, suggesting that the nanoemulsion droplet is slowly dissolved. It may be due to increased concentration of OSAPS and polysorbate 80 concentration which might delay drug release. The similar finding was agreed with Bhattacharjee et al (Bhattacharjee et al., 2017). However, the prepared nanoemulsions showed the drug release more than 60% after 30 min except Run 10, Run 11 and Run 14 and the results were significantly different (p<0.05) except (76% and 78%) drug release of Run 8 and Run 9 as well as (96%) of Run 3 and (93%) of Run 7, (94%) of control and NPS were not statistically different (p>0.05) as displayed in **appendix (4)**.

Then, drug release data were fitted to drug kinetics models such as First, Higuchi or Weibull model, where coefficient of determination (R^2) parameter was used as a tool to select the order of drug release for a specific model (Koester, Ortega,

Mayorga, & Bassani, 2004; Zhang et al., 2010). The prepared ITZ-loaded nanoemulsions followed Weibull model due to best fit with highest R^2 among the studied models as shown in **Table 15.** In addition, one important parameter of Weibull such as shape parameter, β, characterizes the curve as exponential if β=1, S-shaped with upward curvature followed by a turning point if β>1 or curve with steeper initial slope if β<1 (Koester et al., 2004). In this study, Weibull shape parameter, β values of the prepared nanoemulsions were greater than 1 except control, Run 4 and Run 8 nanoemulsions, where β value of Run 8 was close to 1 (β=0.83) and it was found that its curve was not steep too much. However, β values of control (β=-0.708) and Run 4 (β=0.113) were relatively less than 1. Therefore, these two formulations showed curve with steeper initial slope, indicating that dissolution shape curves of control and Run 4 were different from other formulations as shown in **Figure 22**. The trend of these two formulations (control and Run 4) showing steeper curve was corresponded with faster drug dissolution and high drug release among the prepared ITZ-nanoemulsions.

Moreover, the dissolution profiles comparison was also investigated using a non-parametric bootstrap method. The results showed that non-similarity was observed between dissolution profiles of pure ITZ and prepared ITZ-nanoemulsions, since the bootstrap 5% percentiles (90% confidence lower limit) are below 50 (Koester et al., 2004; Zhang et al., 2010) except 9 pairs of dissolution profiles such as Run 1 x Run 8, Run 1 x Run 10, Run 1 x Run 13, Run 2 x Run 15, Run 8 x Run 9, Run 8 x Run 13, Run 8 x Run 15, Run 11 x Run 14 and control x NPS, as displayed in **Table 16**. However, the dissolution and release of ITZ from nanoemulsions in SGF media was higher than that of intact ITZ.

Table 15 Comparative parameters, determination coefficients and release kinetics of ITZ-loaded nanoemulsions.

Runs	First order		Higuchi		Weibull	
	K_1	R^2	K_H	R^2	β	R^2
1	0.028	0.9435	9.470	0.9843	1.468	0.9992
2	0.040	0.9242	10.794	0.7796	3.252	0.9865
3	0.058-	0.9484	11.758	0.6081	2.270	0.9887
4	-	-	-	-	-0.708	0.6853
5	0.059	0.6884	11.608	0.5963	1.012	0.9653
6	0.053	0.8966	10.757	0.3462	2.536	0.9938
7	-	-	-	-	1.349	0.9462
8	0.033	0.9193	9.890	0.8568	0.830	0.9941
9	0.035	0.8593	9.810	0.6905	2.225	0.9927
10	0.020	0.7343	8.353	0.8309	1.284	0.9398
11	0.022	0.9597	8.720	0.9341	2.865	0.9929
12	0.029	0.8622	9.406	0.7640	2.844	0.9654
13	0.028	0.9452	9.532	0.8682	2.001	0.9752
14	0.018	0.9241	8.185	0.9198	2.378	0.9800
15	0.040	0.9516	10.689	0.8052	2.154	0.9926
Control	-	-	-	-	0.113	0.7626
NPS	0.228	0.5664	-	-	1.440	0.9160

K_1 and K_H: release constant; β : shape parameter; R^2: determination coefficient

Table 16 Statistical Bootstrap at 5% percentile results for each comparison of dissolution profiles.

Comparisons	Bootstrap 5% percentiles	Similarity	Comparisons	Bootstrap 5% percentiles	Similarity
Run 1 x Run 2	38.816	No	Run3 x Run 8	38.867	No
Run 1 x Run 3	33.384	No	Run3 x Run 9	36.051	No
Run 1 x Run 4	13.449	No	Run3 x Run 10	22.560	No
Run 1 x Run 5	30.609	No	Run3 x Run 11	27.230	No
Run 1 x Run 6	34.638	No	Run3 x Run 12	32.101	No
Run 1 x Run 7	23.593	No	Run3 x Run 13	32.440	No
Run 1 x Run 8	**56.980**	**Yes**	Run3 x Run 14	23.796	No
Run 1 x Run 9	46.889	No	Run3 x Run 15	45.952	No
Run 1 x Run 10	**58.532**	**Yes**	Run3 x control	26.750	No
Run 1 x Run 11	48.516	No	Run3 x NPS	33.086	No
Run 1 x Run 12	47.366	No	Run3 x ITZ	8.985	No
Run 1 x Run 13	**51.046**	**Yes**	Run 4 x Run 5	19.391	No
Run 1 x Run 14	40.608	No	Run 4 x Run 6	16.995	No
Run 1 x Run 15	43.903	No	Run 4 x Run 7	28.020	No
Run 1 x control	19.168	No	Run 4 x Run 8	15.367	No
Run 1 x NPS	22.140	No	Run 4 x Run 9	14.143	No
Run 1 x ITZ	15.304	No	Run 4 x Run 10	9.535	No
Run 2 x Run 3	43.714	No	Run 4 x Run 11	10.780	No
Run 2 x Run 4	15.101	No	Run 4 x Run 12	12.499	No
Run 2 x Run 5	35.794	No	Run 4 x Run 13	12.496	No
Run 2 x Run 6	41.568	No	Run 4 x Run 14	9.386	No
Run 2 x Run 7	26.206	No	Run 4 x Run 15	16.740	No
Run 2 x Run 8	42.936	No	Run 4 x control	41.126	No
Run 2 x Run 9	40.652	No	Run 4 x NPS	35.886	No
Run 2 x Run 10	26.095	No	Run 4 x ITZ	1.908	No
Run 2 x Run 11	32.924	No	Run 5 x Run 6	40.161	No
Run 2 x Run 12	37.859	No	Run 5 x Run 7	34.160	No
Run 2 x Run 13	40.214	No	Run 5 x Run 8	35.321	No
Run 2 x Run 14	27.941	No	Run 5 x Run 9	31.670	No
Run 2 x Run 15	**52.226**	**Yes**	Run 5 x Run 10	23.372	No
Run 2 x control	20.516	No	Run 5 x Run 11	25.461	No
Run 2 x NPS	24.596	No	Run 5 x Run 12	29.433	No
Run 2 x ITZ	10.542	No	Run 5 x Run 13	29.772	No
Run3 x Run 4	20.383	No	Run 5 x Run 14	22.602	No
Run3 x Run 5	42.954	No	Run 5 x Run 15	40.009	No
Run3 x Run 6	45.815	No	Run 5 x control	26.472	No
Run3 x Run 7	34.494	No	Run 5 x NPS	31.101	No

Comparisons	Bootstrap 5% percentiles	Similarity	Comparisons	Bootstrap 5% percentiles	Similarity
Run 5 x ITZ	8.266	No	Run 9 x control	19.831	No
Run 6 x Run 7	29.945	No	Run 9 x NPS	23.235	No
Run 6 x Run 8	41.006	No	Run 9 x ITZ	12.791	No
Run 6 x Run 9	38.905	No	Run 10 x Run 11	42.174	No
Run 6 x Run 10	24.620	No	Run 10 x Run 12	31.920	No
Run 6 x Run 11	27.507	No	Run 10 x Run 13	33.934	No
Run 6 x Run 12	33.448	No	Run 10 x Run 14	42.594	No
Run 6 x Run 13	32.668	No	Run 10 x Run 15	28.073	No
Run 6 x Run 14	24.297	No	Run 10 x control	14.288	No
Run 6 x Run 15	46.382	No	Run 10 x NPS	15.953	No
Run 6 x control	23.473	No	Run 10 x ITZ	18.878	No
Run 6 x NPS	27.806	No	Run 11 x Run 12	42.029	No
Run 6 x ITZ	10.230	No	Run 11 x Run 13	43.794	No
Run 7 x Run 8	26.746	No	**Run 11 x Run 14**	**51.516**	**Yes**
Run 7 x Run 9	25.318	No	Run 11 x Run 15	35.118	No
Run 7 x Run 10	17.406	No	Run 11 x control	15.638	No
Run 7 x Run 11	19.267	No	Run 11 x NPS	18.005	No
Run 7 x Run 12	22.581	No	Run 11 x ITZ	17.855	No
Run 7 x Run 13	21.936	No	Run 12 x Run 13	46.297	No
Run 7 x Run 14	17.056	No	Run 12 x Run 14	36.088	No
Run 7 x Run 15	29.023	No	Run 12 x Run 15	40.068	No
Run 7 x control	38.627	No	Run 12 x control	17.756	No
Run 7 x NPS	48.363	No	Run 12 x NPS	20.733	No
Run 7 x ITZ	6.652	No	Run 12 x ITZ	13.877	No
Run 8 x Run 9	**52.591**	**Yes**	Run 13 x Run 14	36.032	No
Run 8 x Run 10	33.896	No	Run 13 x Run 15	42.125	No
Run 8 x Run 11	41.095	No	Run 13 x control	17.638	No
Run 8 x Run 12	46.883	No	Run 13 x NPS	20.512	No
Run 8 x Run 13	**50.380**	**Yes**	Run 13 x ITZ	14.902	No
Run 8 x Run 14	35.509	No	Run 14 x Run 15	29.931	No
Run 8 x Run 15	**51.217**	**Yes**	Run 14 x control	14.104	No
Run 8 x control	21.412	No	Run 14 x NPS	16.198	No
Run 8 x NPS	24.959	No	Run 14 x ITZ	20.063	No
Run 8 x ITZ	14.330	No	Run 15 x control	22.807	No
Run 9 x Run 10	29.451	No	Run 15 x NPS	27.020	No
Run 9 x Run 11	36.669	No	Run 15 x ITZ	11.647	No
Run 9 x Run 12	44.609	No	**Control x NPS**	**50.453**	**Yes**
Run 9 x Run 13	43.338	No	Control x ITZ	5.327	No
Run 9 x Run 14	31.235	No	NPS x ITZ	5.192	No
Run 9 x Run 15	46.565	No	-	-	-

4.2.6 Storage stability studies

The three months stability studies as well as temperature cycling of six cycles were conducted to evaluate the stability of selected nanoemulsions of Run 5, Run 1, Run 15 containing OSAPS in the concentrations of 3%w/w, 2%w/w and 1%w/w, respectively and compared with control containing 17.5%w/w polysorbate 80 and 2%w/w NPS. The nanoemulsions were stored for 90 days under two different storage temperature (4˚C and 25˚C). Then, the changes on droplet size and PDI was evaluated as stability assessment. It was found that the droplet size and PDI of Run 1 and Run 5 nanoemulsions containing OSAPS were slightly increased over 90 days storage time at 4˚C **(Figure 23(a) and (b))** and 25˚C **(Figure 23(c) and (d))**. However, a slight increase in droplet size of Run 1, Run 5 and Run 15 was more distinct at 25˚C storage temperature than those stored at 4˚C after 90 days, and statistically different (p<0.05) as exhibited in **Figure 24(a) and (b).** The PDI value of Run 1 had no significant difference between 4˚C and 25˚C shown in **Figure 24(b).** Different storage temperature 4˚C and 25˚C had significant effect on PDI of Run 5 nanoemulsion till 30 & 90 days long storage (p<0.05)**,** indicating that the nanoemulsion Run 5 was more stable with smallest droplet size and PDI at 4˚C. This finding was similar to (Liang et al., 2013; Sharif et al., 2017). After 30 days storage at 25˚C, the PDI of control was highest (0.47 ± 0.03). However, there was not different in droplet size and PDI of control and NPS from the initial day 0 till 90 days at 4˚C and 25˚C storage.

For test of temperature cycling, the freshly prepared nanoemulsions containing the same concentration of 2%w/w OSAPS (Run 1) and 2%w/w NPS, respectively, were subjected to stability studies of temperature cycling each at 4˚C for 24 h and 40˚C for 24 h and then compared with control. After storage of temperature cycling six cycles, average droplet size and PDI of Run 1 increased 55 nm and 0.11, respectively and the values were nearly same to NPS, as exhibited in **Figure 25(a) and (b)** whereas the droplet size of control and NPS had no distinct change as shown in **Figure 4.20(a)**. It was corresponded with three months long storage. Moreover, PDI of three nanoemulsions were increased after temperature cycling storage. Among the ITZ-nanoemulsions Run 1, control and NPS, control showed highest PDI value before and after temperature cycling storage stability test, as displayed in **Figure**

25(b). It might be due to absence of starch polymer as stabilizer because PDI is affected by type and amount of constituents for freshly prepared nanoemulsions (Zorzi, Carvalho, von Poser, & Teixeira, 2015). In addition, PDI is a good indicator of stability and smaller PDI provide more stable nanoemulsion (Tan et al., 2016; Zorzi et al., 2015). Moreover, zeta potential is also an important parameter showing stability. After temperature six cycling, the zeta potential of Run 1, control and NPS were -37.57 mV, -37.13 and -34.53 mV, respectively. Moreover, accelerated stability for three months storage at 4˚C and 25˚C demonstrated that the zeta potential was -41.43 mV and -38.77 mV for Run 1, -41.83 mV and -36.27 mV for control and -35.47 mV and -36.27 mV for NPS, respectively based on each temperature. However, the ITZ-nanoemulsions Run 1, control and NPS had no distinct change in zeta potential after stability and showed stable and no obvious change in phase separation or creaming (100% creaming) after three months storage stability and temperature cycling storage stability test, and suggesting as thermodynamically stable of ITZ-loaded nanoemulsions.

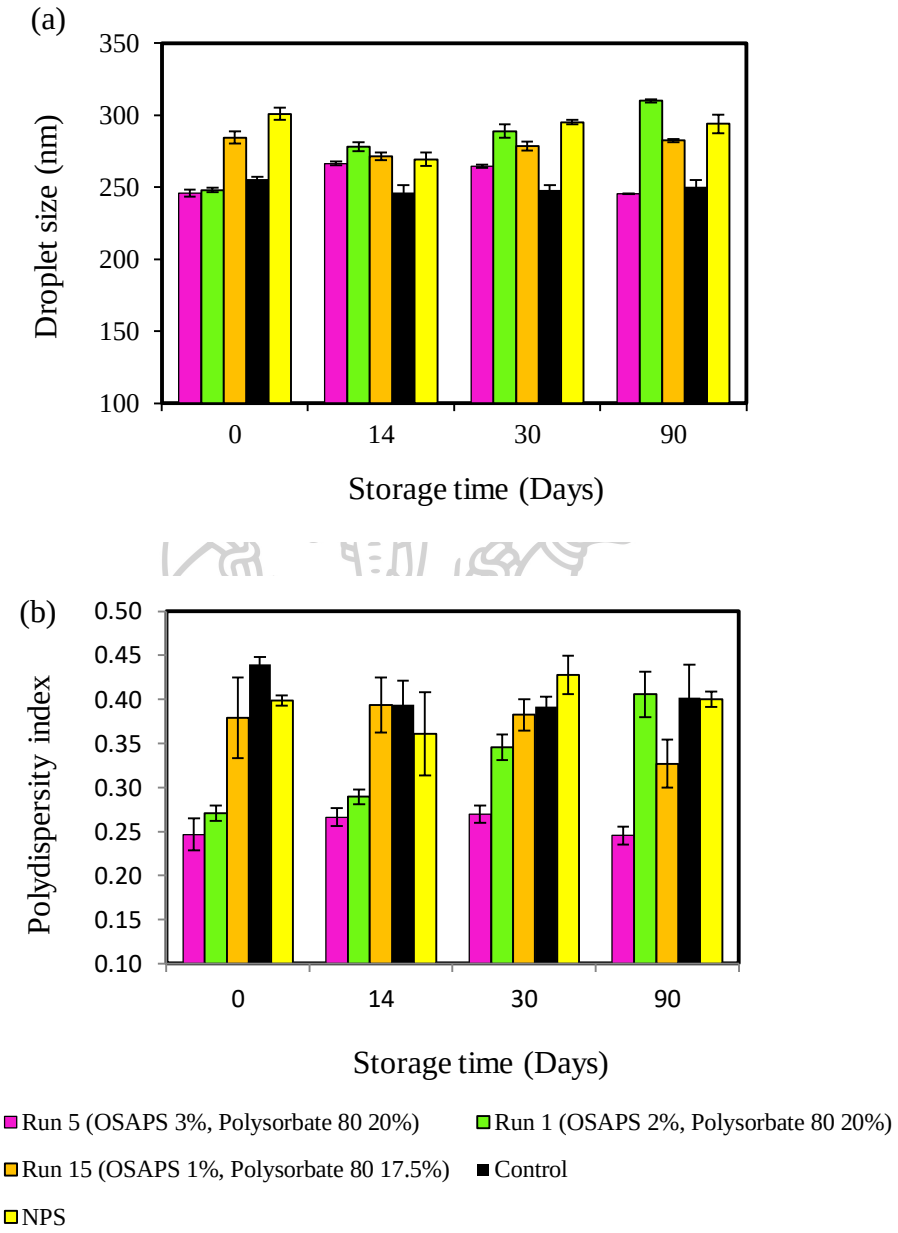
(a)
Droplet size (nm)
350
300
250
200
150
100
0
14
30
90
Storage time (Days)
(b)
Polydispersity index
0.50
0.45
0.40
0.35
0.30
0.25
0.20
0.15
0.10
0
14
30
90
Storage time (Days)
Run 5 (OSAPS 3%, Polysorbate 80 20%)
Run 1 (OSAPS 2%, Polysorbate 80 20%)
Run 15 (OSAPS 1%, Polysorbate 80 17.5%)
Control
NPS

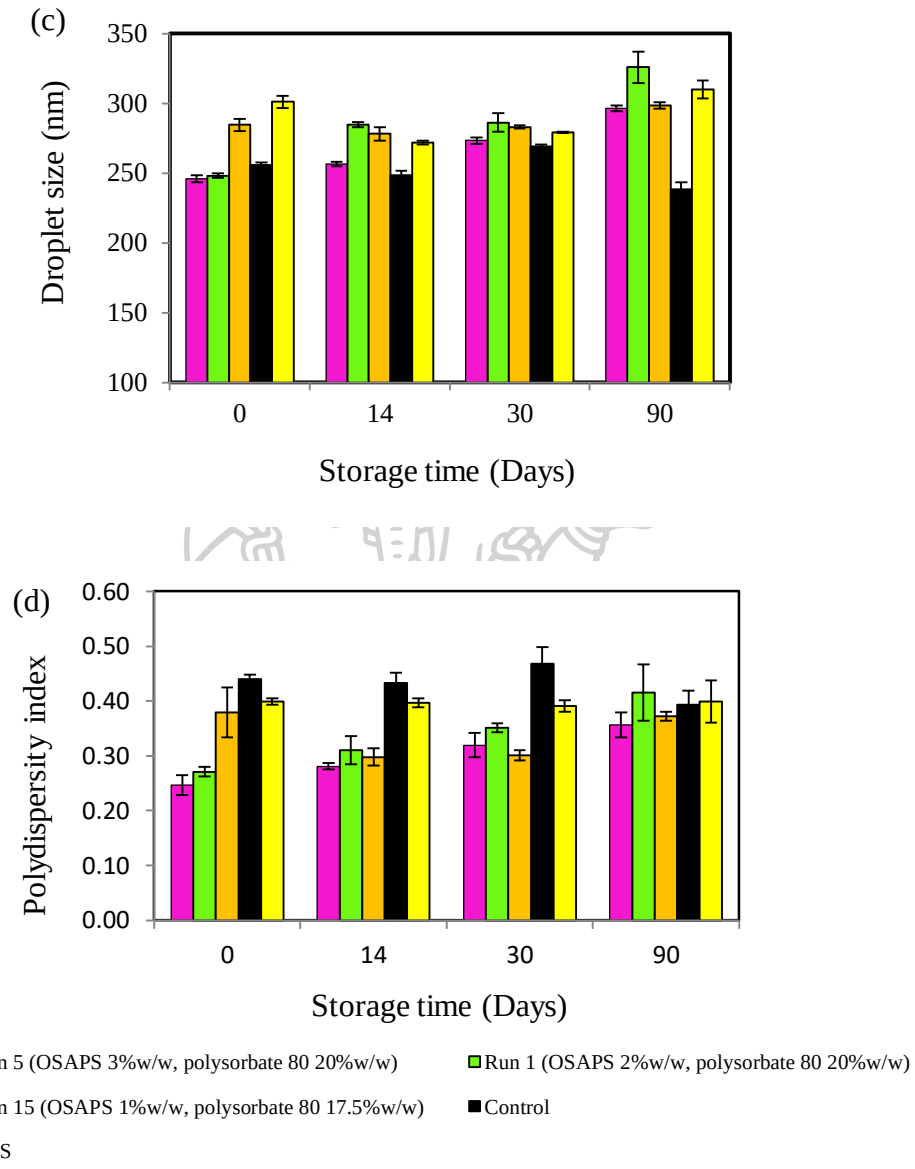

Figure 23 Three months-stability studies of nanoemulsions Run 5, Run 1, Run 15, control and NPS (a) droplet size at 4°C, (b) polydispersity index at 4°C, (c) droplet size at 25°C and (d) polydispersity index at 25°C.

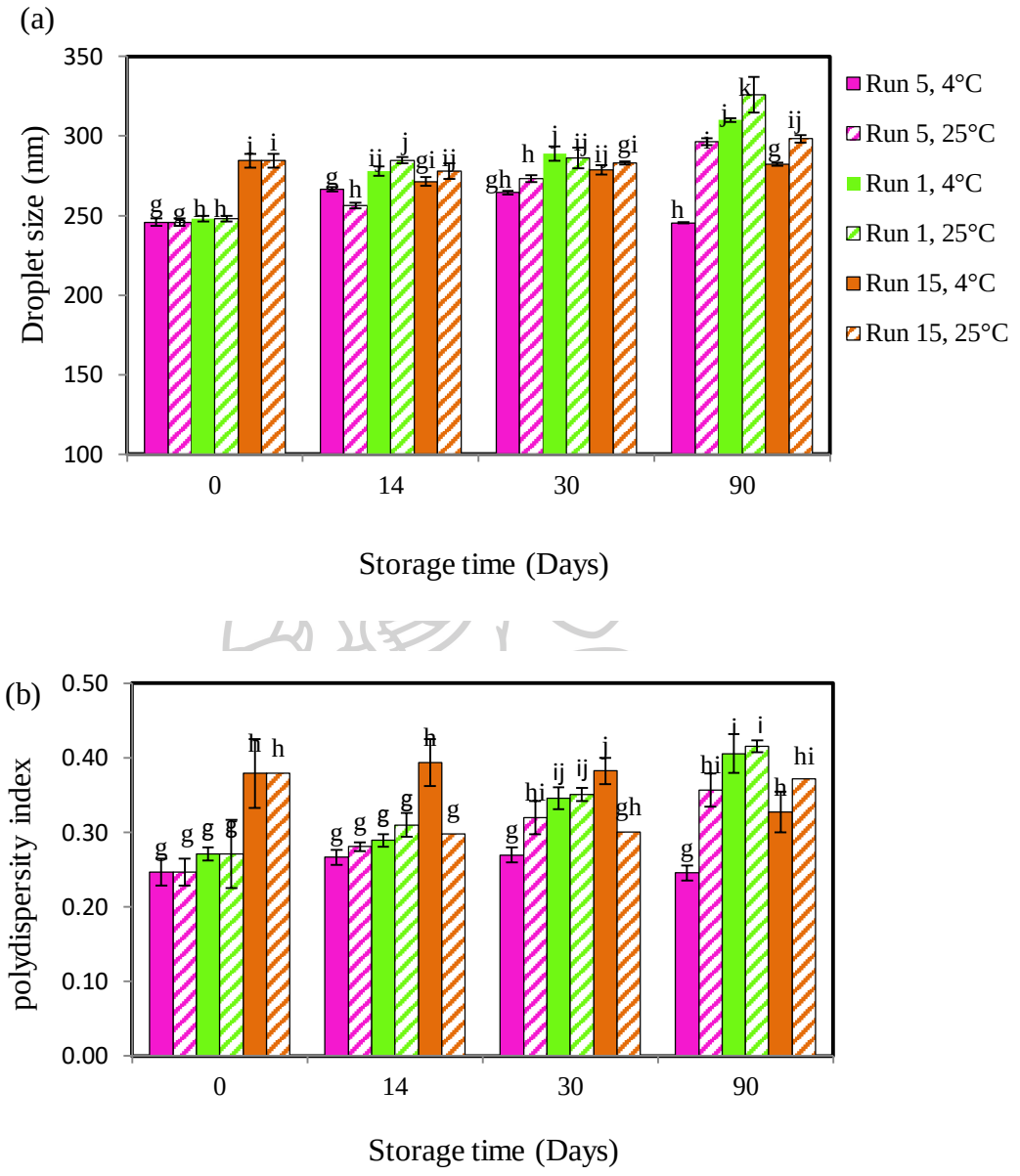

Figure 24 Droplet size (a) and polydisperisity index (b) of nanoemulsions Run 5, Run 1 and Run 15 against storage time at 4˚C and 25˚C. [g-k]Different alphabet letters in the same category show statistically different (p<0.05) by Tukey HSD.

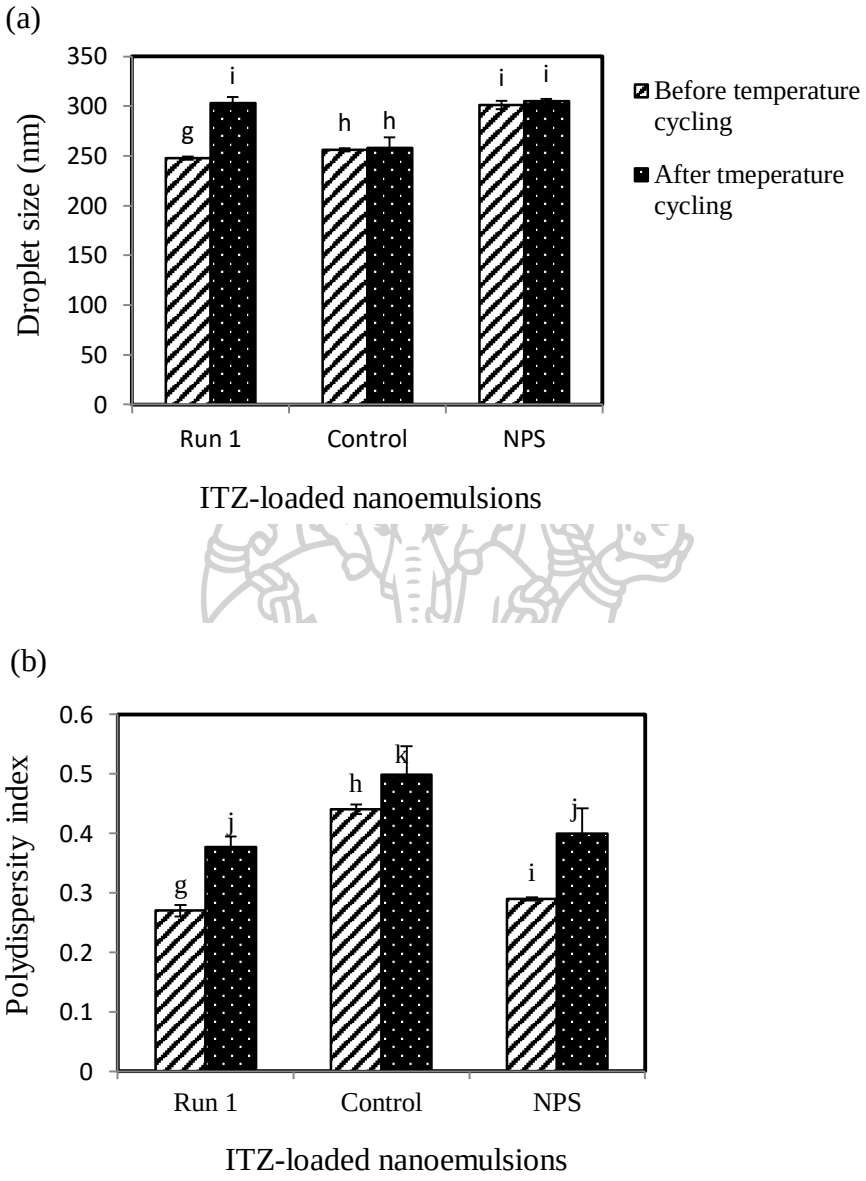

Figure 25 Temperature cycling stability studies of nanoemulsion Run 1, control and NPS (a) droplet size and (b) polydispersity index. $^{g\text{-}k}$Different alphabet letters in the same category show statistically different (p<0.05) by Tukey HSD.

4.2.7 Model analysis

RSM was used to analyze the effects of independent variables such as OSAPS concentration (X_1), polysorbate 80 concentration (X_2) and homogenization time (X_3) on response variables including droplet size (Y_1), PDI (Y_2), viscosity (Y_3) and *in vitro* drug release within 15 mins (Y_4), respectively. The experimental results of total 15 runs in the current fractional factorial CCF shown in **Table 14** were fitted to linear and quadratic model. ANOVA was conducted to test the significance of fitted linear and quadratic polynomial derived from the experimental data. The ANOVA results for each response surface model were exhibited in **Table 17** and regression coefficients of final reduced response surface models of ITZ-loaded nanoemulsion preparation were summarized in **Table 18**.

4.2.7.1 Droplet size model

Droplet size values of ITZ-loaded nanoemulsions ranged from 246 to 319 nm, as summarized in **Table 14**, whereas the droplet size of control and NPS were 256 and 301 nm respectively. The experimental data were used to determine the relation between the independent variables and droplet size. RSM was applied to produce a regression equation for the droplet size model as follows:

$$Droplet\ size = -133.824 + 52.48039 * OSAPS + 112.1726 * polysorbate\ 80 - 42.2098 * Homogenization\ time - 15.9118 * OSAPS * OSAPS - 3.42588 * polysorbate\ 80 * polysorbate\ 80 + Homogenization\ time * Homogenization\ time \quad (19)$$

ANOVA suggested to fit quadratic model for droplet size response variable. Then, the full quadratic model was reduced by excluding the non-significant interaction terms. *p*-value was used as a tool to investigate the significance of individual effect, two factor interactions, quadratic effects and regression model. Model *F*-value of 4.4 implied that the droplet size model was significant and the model terms were also significant according to value of "Prob>F" less than 0.05 ($p<0.05$). In addition, the lack of fit of F-value at 1.11 revealed that there was not significant relative to the pure error. The droplet size model fitted well according to non-significant lack of fit *p*-value = 0.4597. The r^2 value was 0.7674 and RMSE was

10.7574. The OSAPS concentration, polysorbate 80 concentration and quadratic terms of polysorbate 80 concentration*polysorbate 80 concentration and homogenization time x homogenization time were significant factors influencing the droplet size while individual effect of homogenization time and quadratic effect of OSAPS*OSAPS were non-significant terms. The contour plots **(Figure 26(a_1-c_1))** and 3D response surface plots **(Figure 26(a_2-c_2))** show the combined effect of OSAPS, polysorbate 80 and homogenization time on droplet size.

The 3D contour and response surface plots of **Figure 26(a_1) and (a_2)** show the combined effects of OSAPS concentration and polysorbate 80 concentration on droplet size of ITZ-loaded nanoemulsion under the condition of homogenization time kept at a mean level. It can be clearly observed that the droplet size sharply decreased with increasing concentration of OSAPS (3%w/w) and polysorbate 80 (20%w/w), resulting in minimum droplet size of 246 ± 2.48 nm. It can be explained by the fact that 3% of OSAPS can effectively reduce interfacial tension against oil as discussed in section *4.2.2.1* and higher concentration of polysorbate 80 can lower interfacial tension as well as adsorb onto freshly created oil droplets, thereby leading to decrease in droplet size. It was similar to the findings of Kumar et al and Nagi et al (Kumar et al., 2009; Nagi et al., 2017). Moreover, high amount of surfactant can easily and quickly adsorb onto freshly new oil droplets and protect shear-induced coalescence (Mason et al., 2006). In addition, it was found that the quadratic effects of polysorbate 80 and homogenization time on droplet size were significant (p<0.05). At low concentration of polysorbate 80 (15%w/w) with increasing homogenization time (30 mins), the droplet size tends to increase 297 nm of Run 2 formulation while at high level of polysorbate 80 (20%w/w), the droplet size was found to decrease to 274 nm of Run 8 formulation with an increase in time (30 mins) at constant level of other factor shown in **Table 14**, indicating the quadratic effects on droplet size. The similar finding was observed by Mehmood, et al (Mehmood et al., 2017).

(a_1)

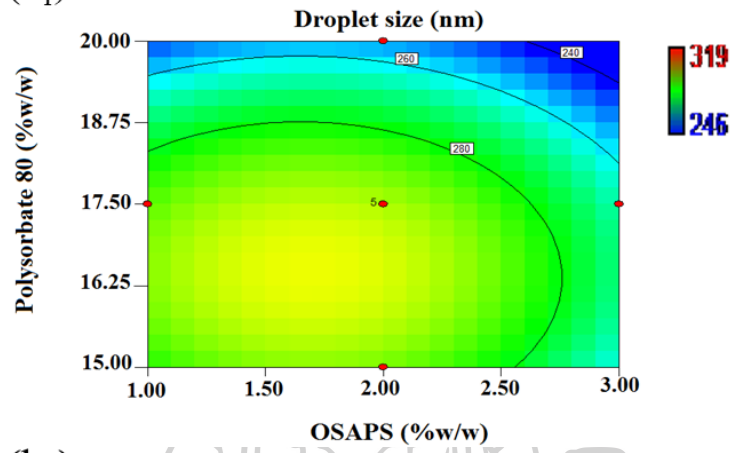
Droplet size (nm)
Polysorbate 80 (%w/w)
20.00
18.75
17.50
16.25
15.00
1.00
1.50
2.00
2.50
3.00
OSAPS (%w/w)
319
246
240
260
280
300

(b_1)

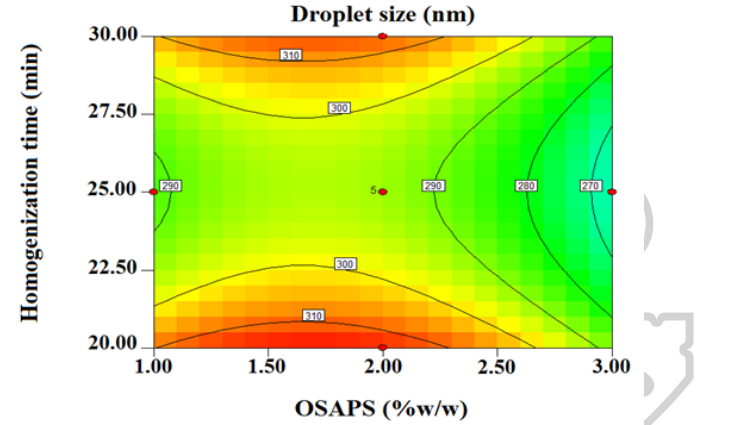
Droplet size (nm)
Homogenization time (min)
30.00
27.50
25.00
22.50
20.00
1.00
1.50
2.00
2.50
3.00
OSAPS (%w/w)
310
300
290
280
270

(c_1)

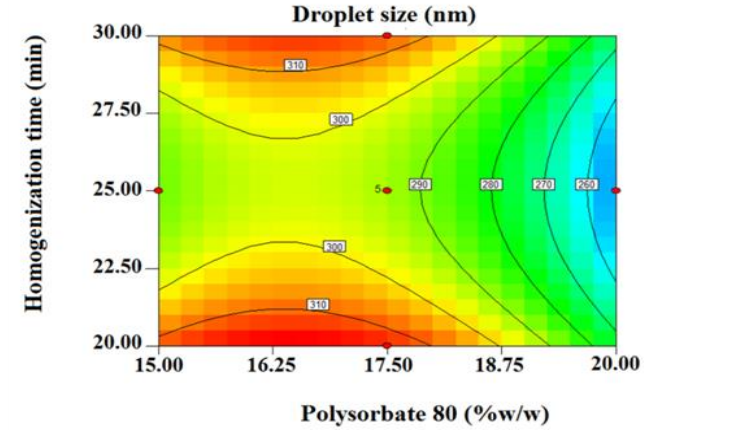
Droplet size (nm)
Homogenization time (min)
30.00
27.50
25.00
22.50
20.00
15.00
16.25
17.50
18.75
20.00
Polysorbate 80 (%w/w)
310
300
290
280
270
250

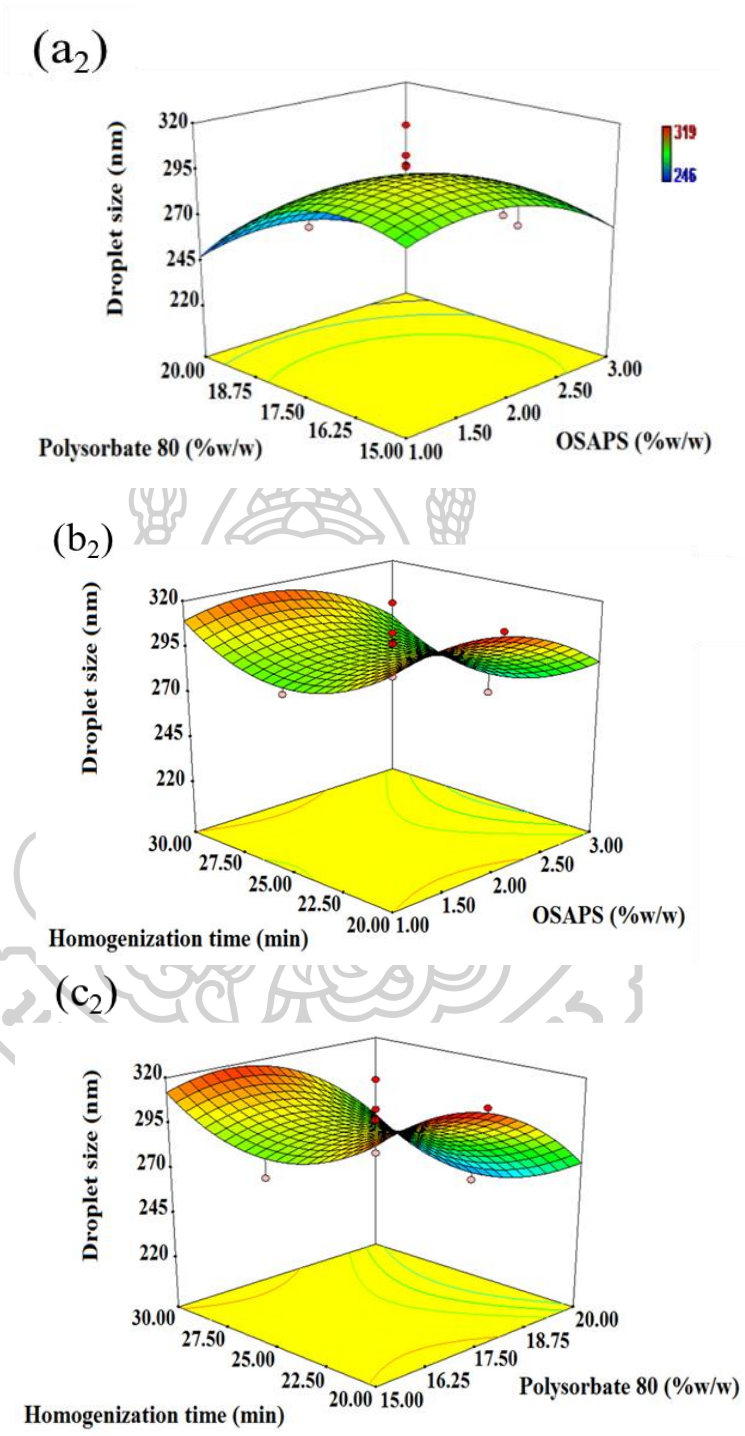

Figure 26 Contour (a_1-c_1) and 3D response surface plots (a_2-c_2) showing the combined effect of OSAPS, polysorbate 80 and homogenization time on droplet size.

4.2.7.2 PDI model

The PDI values of the prepared ITZ-loaded nanoemulsions ranged from 0.25-0.55 as summarized in **Table 14**, whereas the PDI values of control and NPS were 0.44 and 0.4, respectively. Among the total 15 runs in the current CCF, the PDI value of Run 4 (0.55) was slightly higher than NPS. It may be due to low concentration of polysorbate 80 (15%w/w) with shorter homogenization time (20 min) for Run 4, suggesting that low concentration of surfactant and minimum homogenization time was not enough to produce narrower size distribution. Therefore, droplet size distribution or PDI of Run 4 was wider than NPS, which was prepared under the conditions of mean level of all three independent variables such as 2%w/w NPS, 17.5%w/w polysorbate 80 and homogenization time of 25 min. However, the width of droplet size distribution varies from 0 to 1 (Zorzi et al., 2015). The current PDI results of ITZ-loaded nanoemulsions were within the range. The significant linear model for PDI was summarized in **Table 17**. The model and model terms were significant according to F-test value 18.34 and p<0.05, respectively. In addition, the model exhibited a good fit to the experimental data due to non-significant lack of fit p-value = 0.7942. The r^2 and RMSE were 0.8334 and 0.0308, respectively. The regression equation for response variable PDI can be described as follows:

$$PDI = +1.246 - 0.051667 * OSAPS - 0.036667 * polysorbate\ 80 - 0.00567 * Homogenization\ time \quad (20)$$

The ANOVA results showed that there was linear relationship between the independent variables and response PDI. It was similar to Tan et al (Tan et al., 2016). In this study, OSAPS concentration (p<0.05) and polysorbate 80 concentration (p<0.0001) had a strong effect on PDI according to smaller p-value. Homogenization time (p>0.05) had no significant effect on PDI of ITZ-loaded nanoemulsions. **Figure 27(a_1) and (a_2)** display the combined effects of OSAPS and polysorbate 80 on PDI. It was clearly observed that PDI of ITZ-nanoemulsions was relatively decreased at high concentration of OSAPS and polysorbate 80. On the contrary, PDI increased with respect to lower concentration of

OSAPS and polysorbate 80, shown in **Figure 27(a_1) and (a_2).** These results corresponded with droplet size model, indicating that OSAPS concentration and polysorbate 80 concentration are critical factors affecting the droplet size and size distribution (PDI) of ITZ-loaded nanoemulsions. The contour and 3D response surface plots showing the combined effect of OSAPS, polysorbate 80 and homogenization time on PDI were exhibited in **Figure 27(a_1-c_1) & (a_2-c_2)**.

(a_1)

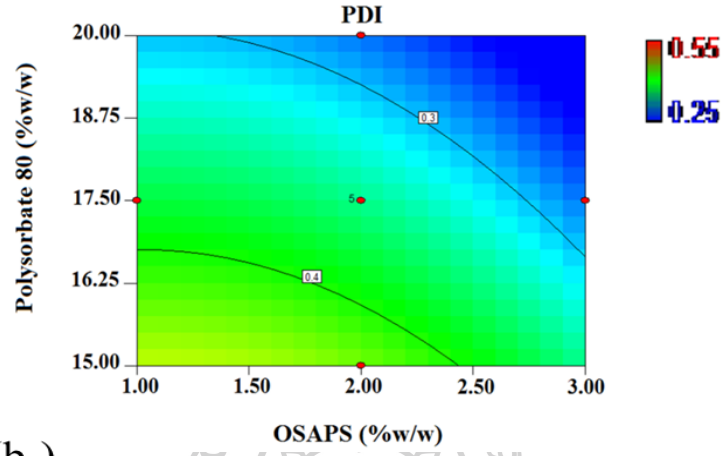
PDI
0.55
0.25
20.00
18.75
17.50
16.25
15.00
Polysorbate 80 (%w/w)
1.00
1.50
2.00
2.50
3.00
OSAPS (%w/w)
0.3
0.4
5

(b_1)

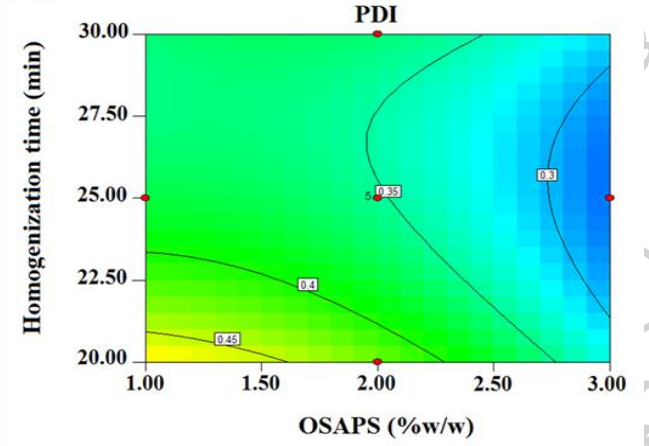
PDI
30.00
27.50
25.00
22.50
20.00
Homogenization time (min)
1.00
1.50
2.00
2.50
3.00
OSAPS (%w/w)
0.3
0.35
0.4
0.45
5

(c_1)

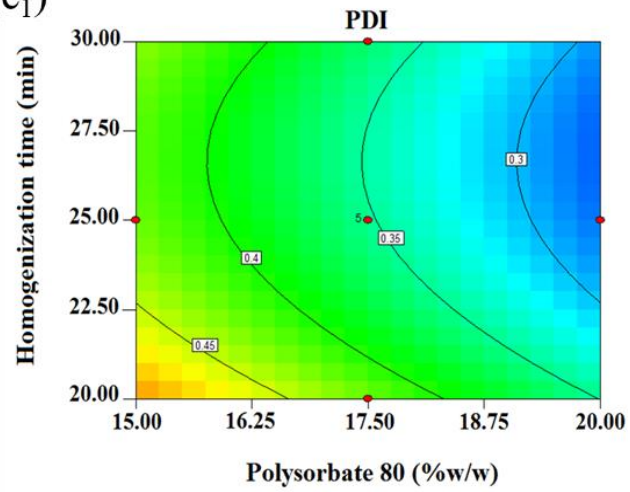
PDI
30.00
27.50
25.00
22.50
20.00
Homogenization time (min)
15.00
16.25
17.50
18.75
20.00
Polysorbate 80 (%w/w)
0.3
0.35
0.4
0.45
5

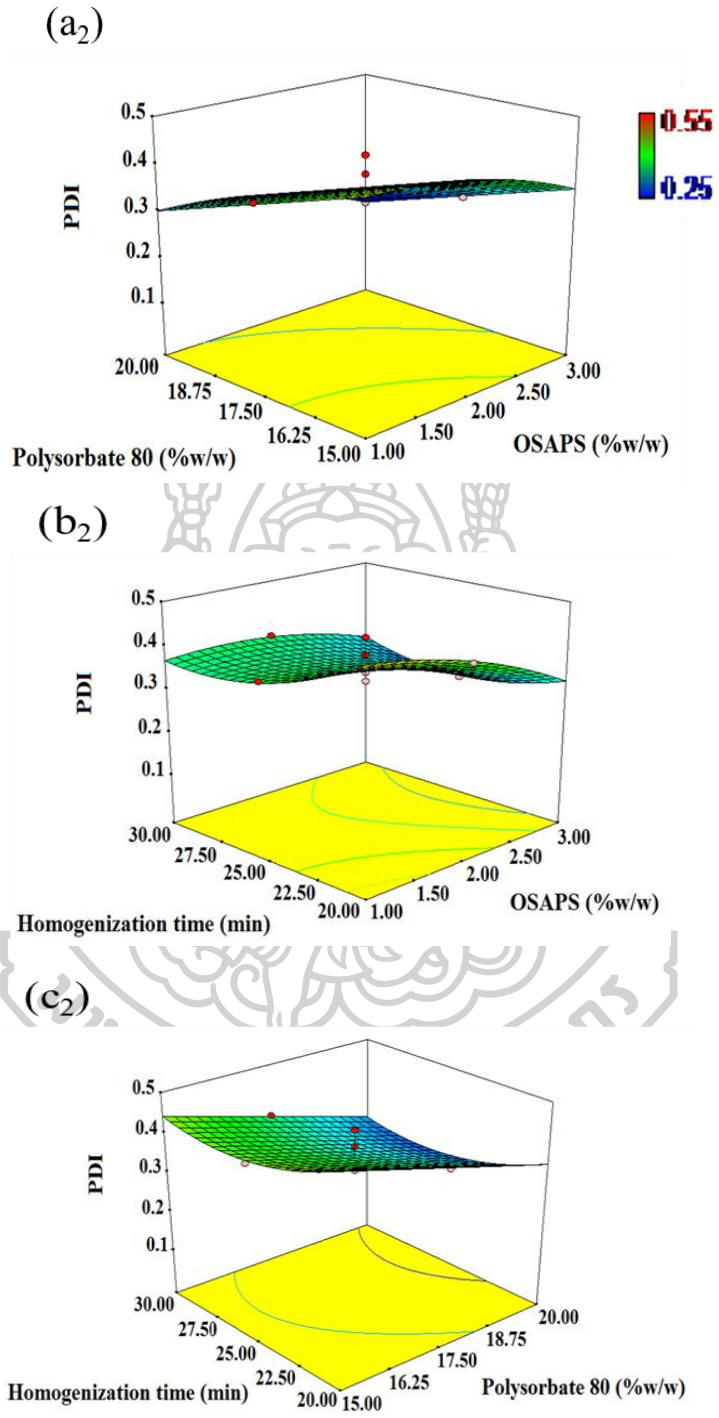

Figure 27 Contour (a_1-c_1) and 3D response surface plots (a_2-c_2) showing the combined effect of OSAPS, polysorbate 80 and homogenization time on PDI.

4.2.7.3 Viscosity model

The viscosity data of prepared ITZ-loaded nanoemulsions in CCF design was in the range 3.01-517.57 Pa.s, as depicted in **Table 14**, and those of control and NPS were 1.00 and 58.56 Pa.s, respectively. It was found that the viscosity of ITZ-nanoemulsions containing OSAPS was higher than that of NPS prepared under the condition of all factors kept at a mean level, indicating that the viscosity of pineapple starch after modification with OSA was improved (Latt et al., 2019) and use of OSAPS gel in the continuous phase raised the viscosity of nanoemulsion formulations. The larger F-value (324.17), the smaller *p*-value (p<0.0001) indicated that the viscosity model was significant and yielded the best quadratic fit according to lack of fit *p*-value (0.9582), meaning that non-significant lack of fit was observed for viscosity model and obtained regression equation for viscosity model is expressed as follows:

$$Viscosity = +1588.83333 - 191.5 * OSAPS - 224.75556 * polysorbate\ 80 + 10.7 * Homogenization\ time + 15.4 * OSAPS * polysorbate\ 80 + 2.3 * OSAPS * Homogenization\ time - 0.6 * polysorbate\ 80 * Homogenization\ time + 7.40444 * polysorbate\ 80 * polysorbate\ 80 \quad (21)$$

Among the model terms, the individual effect of OSAPS concentration (p<0.0001), polysorbate 80 concentration (p<0.0001), homogenization time (p<0.05), interaction effect of OSAPS concentration*polysorbate 80 concentration and quadratic effect of polysorbate 80 concentration* polysorbate 80 concentration were significant model terms whereas the interaction effects of OSAPS*homogenization time and polysorbate 80*homogenization time were non-significant terms for viscosity model. Contour and 3D response surface plots showing the combined effect of OSAPS, polysorbate 80 and homogenization time on viscosity were exhibited in **Figure 28(a_1-c_1) to (a_2) & (c_2)**. The correlation between actual and predicted values based on the experimental data provided an r^2 value of 0.9969 and RMSE value of 0.6707 (**Table 17**). **Figure 28(a_1) and (a_2)** demonstrate the interaction effect of OSAPS concentration and polysorbate 80 concentration with homogenization time fixed at a mean level of 25 min. The increase in OSAPS concentration and

polysorbate 80 concentration strongly affected the viscosity of ITZ-loaded nanoemulsions. The maximum viscosity (517.57 Pa.s) was seen in high concentration of OSAPS (3%w/w) and polysorbate 80 (20%w/w) as shown in contour and 3D response surface plots of **Figure 28(a_1) and (a_2),** respectively. It has been reported that an increase amount of emulsifier and surfactant resulted in high viscosity of nanoemulsions (Li et al., 2017; Mehmood et al., 2017).

(a$_1$)

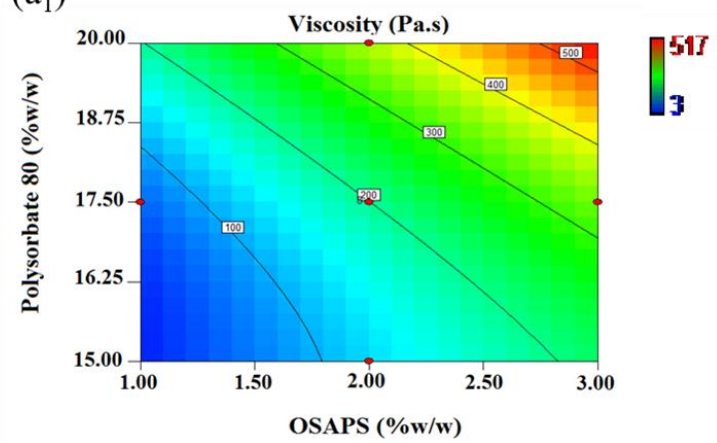
Viscosity (Pa.s)
517
3
500
400
300
200
100
20.00
18.75
17.50
16.25
15.00
Polysorbate 80 (%w/w)
1.00
1.50
2.00
2.50
3.00
OSAPS (%w/w)

(b$_1$)

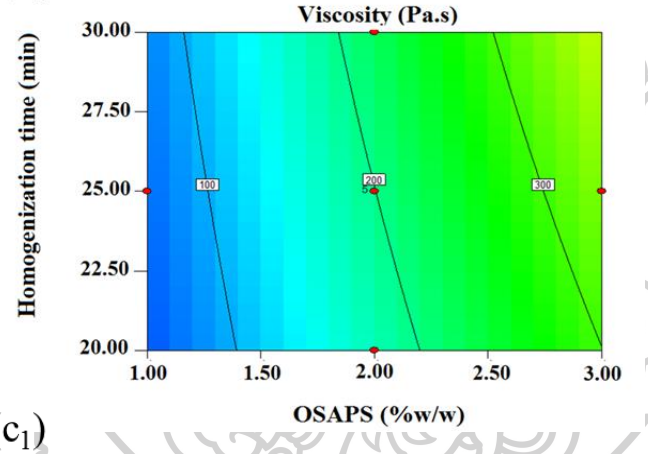
Viscosity (Pa.s)
30.00
27.50
25.00
22.50
20.00
Homogenization time (min)
100
200
300
1.00
1.50
2.00
2.50
3.00
OSAPS (%w/w)

(c$_1$)

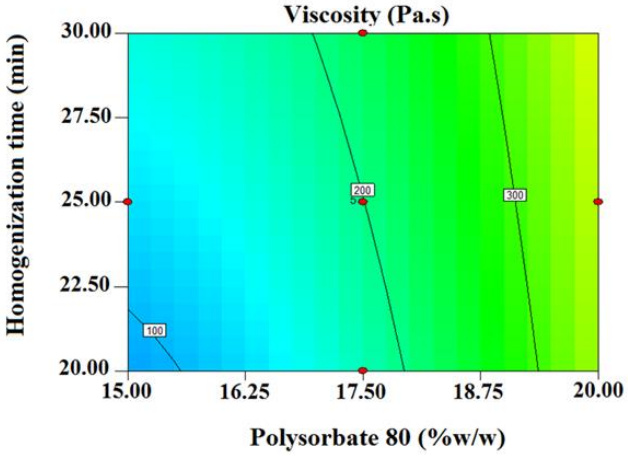
Viscosity (Pa.s)
30.00
27.50
25.00
22.50
20.00
Homogenization time (min)
100
200
300
15.00
16.25
17.50
18.75
20.00
Polysorbate 80 (%w/w)

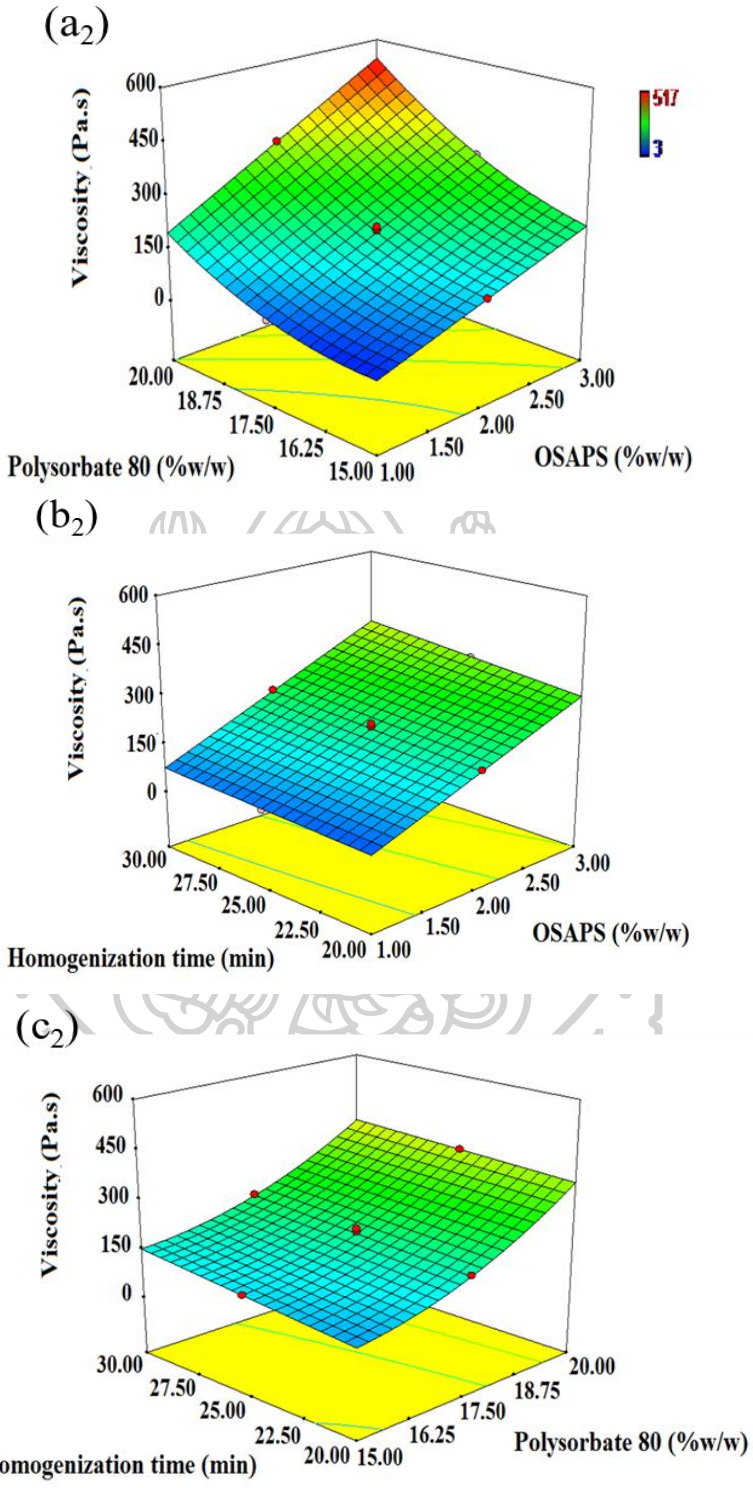

Figure 28 Contour (a_1-c_1) and 3D response surface plots (a_2-c_2) showing the combined effect of OSAPS, polysorbate 80 and homogenization time on viscosity.

4.2.7.4 In vitro drug release (%) within 15 mins model

In vitro drug release in 15 min data was summarized in **Table 14**. It was clearly observed that Run 4 and Run 7 nanoemulsions showed 100% and about 85% drug release in 5 min, respectively. That corresponds to low concentration of polysorbate 80 (15%). ANOVA results showed that the model was significant $p<0.05$. Moreover, model terms such as individual effect of OSAPS, polysorbate 80 and interaction effects of OSAPS*polysorbate 80 and the quadratic terms of polysorbate 80*polysorbate 80 were significant according to $p<0.05$ while the homogenization time and interaction effect of OSAPS*homogenization time were non-significant. **Figure 29** contour (a_1-c_1) and 3D response surface plots (a_2-c_2) show the combined effect of OSAPS, polysorbate 80 and homogenization time on %drug release within 15 mins. The polynomial regression equation can be expressed for the model of *in vitro* drug release within 15 mins as follows:

$$In\ vitro\ drug\ release\ within\ 15\ min = +1514.667 - 107.833 * OSAPS + 5.8 * Homogenization\ time + 9.4 * OSAPS * polysorbate\ 80 - 2.7 * OSAPS * Homogenization\ time + 3.63556 * polysorbate\ 80 * polysorbate\ 80 \quad (22)$$

According to ANOVA analysis, non-significant lack of fit *p*-value (0.8166) was obtained for drug release within 15 mins model, indicating that the model showed the best fit to the experimental data. According to correlation between actual and predicted values based on the experimental data, r^2 and RMSE were 0.8606 and 7.8827, respectively, as exhibited in **Table 17**. **Figure 29(a_1) and (a_2)** show the combined effect of OSAPS concentration and polysorbate 80 concentration (%) on *in vitro* drug release within 15 mins. An increase in concentration of OSAPS and polysorbate 80 caused a decrease in percent drug release which contribute to Run 5 nanoemulsion containing 3%w/w OSAPS and 20%w/w polysorbate 80. It means that the nanoemulsion droplet is slowly dissolved, suggesting that the release of drug entrapped inside the oil droplet was slow. It might be due to the fact that higher amount of OSAPS and polysorbate 80 might delay drug release. This finding was in agreement with (Bhattacharjee et al., 2017). However, the Run 5 nanoemulsion showed durg release of 60% within 15 mins. An increase in percent drug release was

achieved at low concentration of OSAPS and polysorbate 80, under which condition control and NPS also showed high percent drug release in 5 mins as in Run 4 and Run 7. In this study, OSAPS and polysorbate 80 concentraion factors had a positive effect on *in vitro* drug release within 15 mins while homogenization time had a negative effect on drug release within 15 mins.

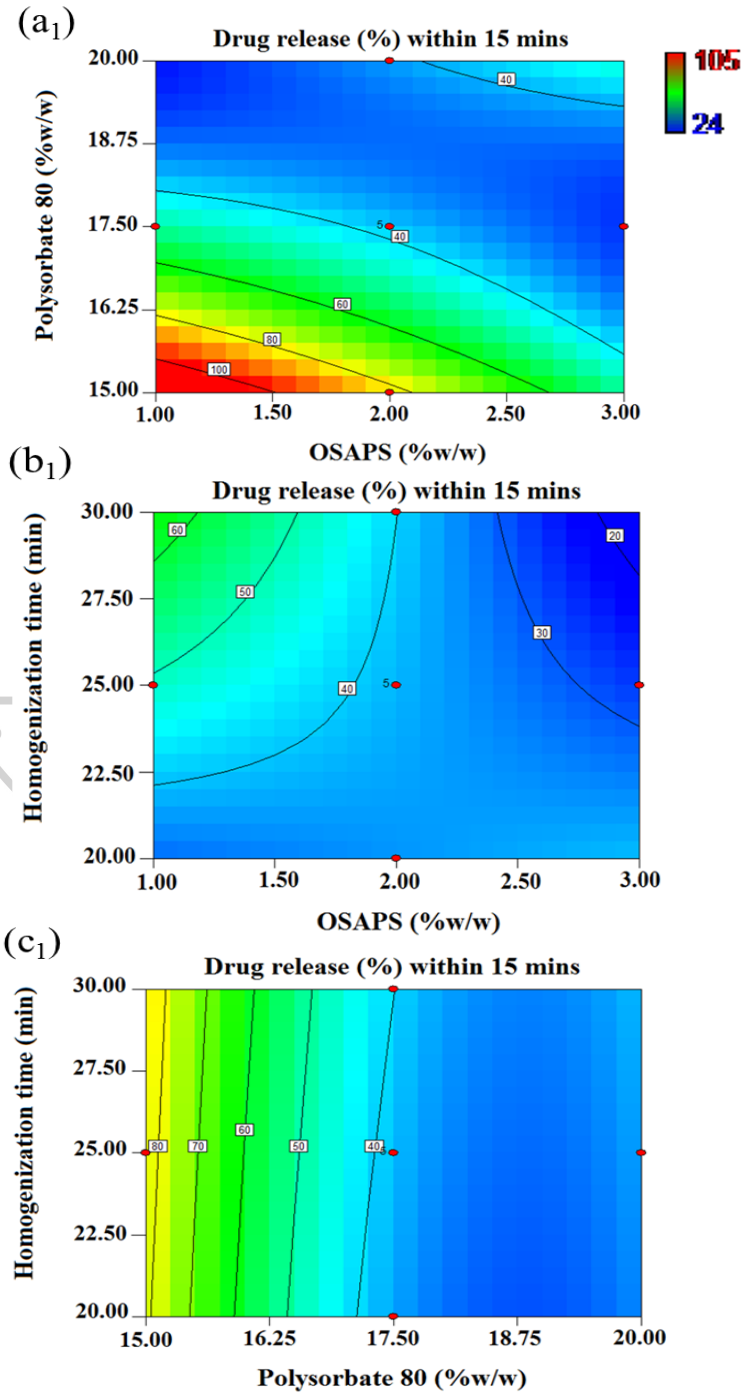

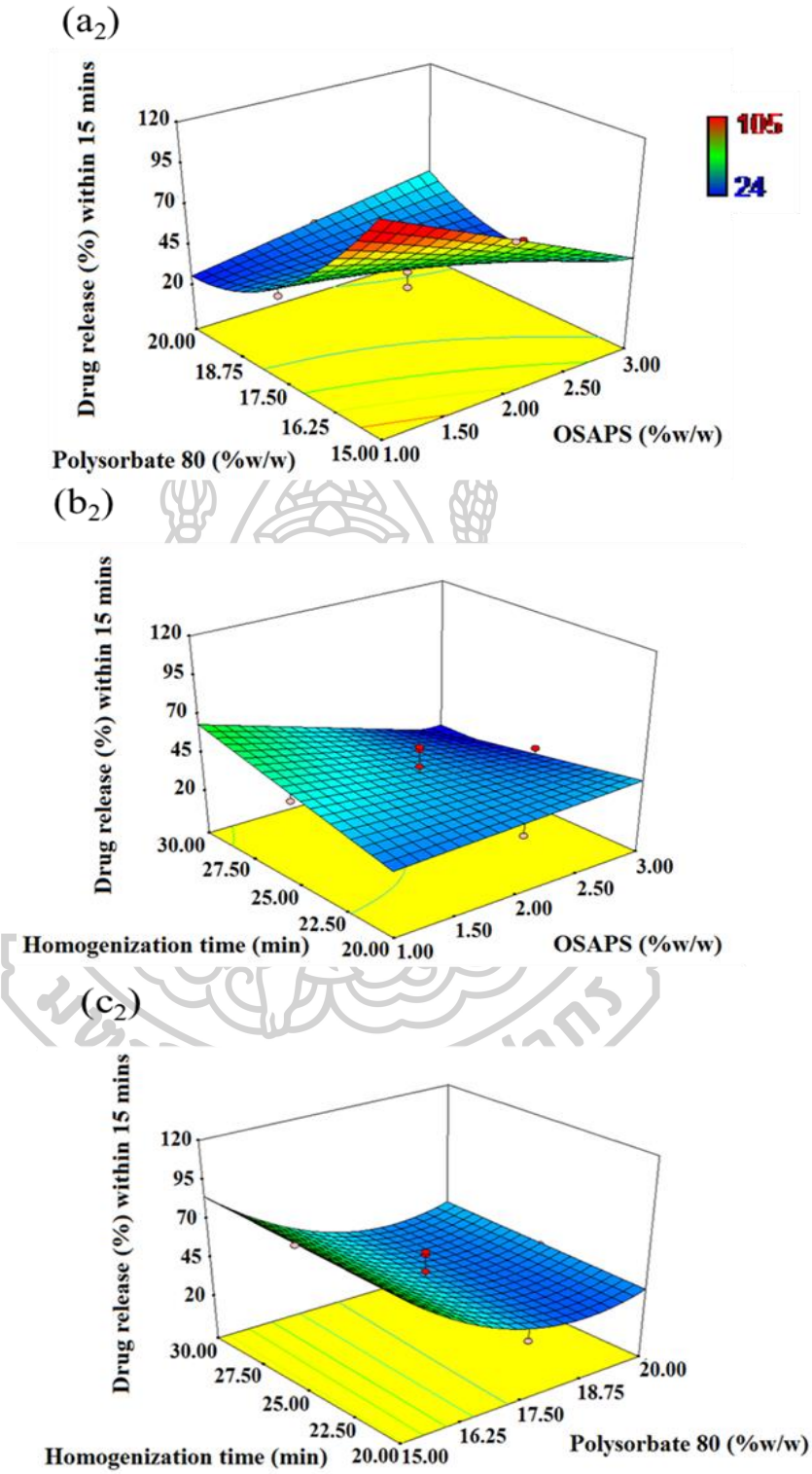

Figure 29 Contour (a_1-c_1) and 3D response surface plots (a_2-c_2) showing the combined effect of OSAPS, polysorbate 80 and homogenization time on drug release (%) within 15 mins.

4.2.7.5 Optimization model

A set of four compounds that were not included in the training dataset was conducted to validate and check the predictive ability of each model. The predicted and experimental values for droplet size, PDI, viscosity and *in vitro* drug release within 15 min were well correlated using predicted r^2 of 0.6188, 0.8525, 0.7123 and 0.8642, respectively, (**Table 19**), suggesting that the obtained model could exhibit good performance for predicting the values of droplet size, PDI, viscosity and *in vitro* drug release within 15 min. To obtain design space for multiple responses, graphical optimization was performed by specify the desired response limits. In this study, minimum droplet size, minimum PDI, lower and upper limit ranges for viscosity, and *in vitro* drug release within 15 min were set as goals for optimization of ITZ-loaded nanoemulsions. **Figure 30** shows the graphical optimization, which displays the area of feasible response values in the factor space for ITZ-loaded nanoemulsion preparation. The area that satisfies the constraints is indicated in yellow, whereas the area that does not meet the criteria is indicated in gray.

The optimum conditions were 3%w/w OSAPS, 19.8%w/w polysorbate 80 and 20 min homogenization time, with a predicted droplet size value of 250 nm, PDI of 0.25, viscosity of 500 Pa.s, and *in vitro* drug release (%) within 15 mins of 60% with desirability value of 0.98. The observed values of Run 5 nanoemulsion under the conditions of 3%w/w OSAPS, 20%w/w polysorbate 80, and 20 min homogenization time in the CCF design with droplet size of 246 nm, PDI 0.25, viscosity of 517 Pa.s, and *in vitro* drug release (%) within 15 mins of 61% were nearly the same to predicted values of optimum condition. The difference between experimental and predicted values of optimum condition was reported as % error which was found to be minimal, as exhibited in **Table 20.** After analyzing the comparison of experimental and predicted values of optimum condition by graphical optimization, Run 5 nanoemulsion was determined and selected as optimum formula in this study, due to low %error, it can be said as Run 5 nanoemulsion meets the optimum criteria.

(a)

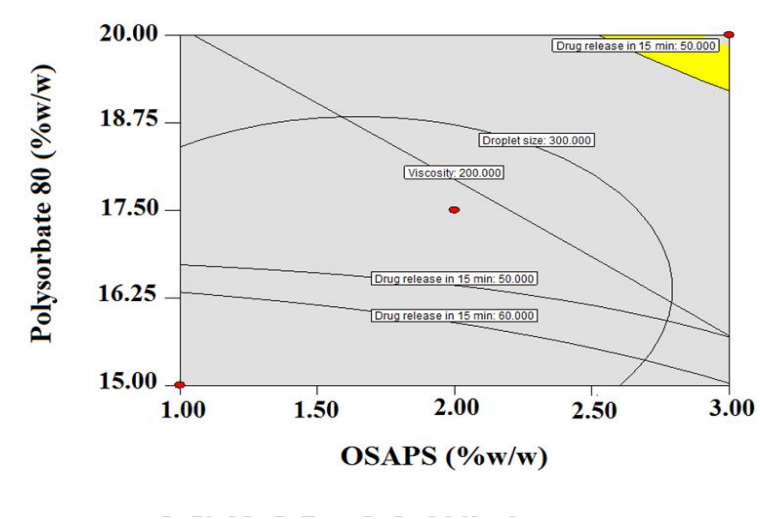

(b)

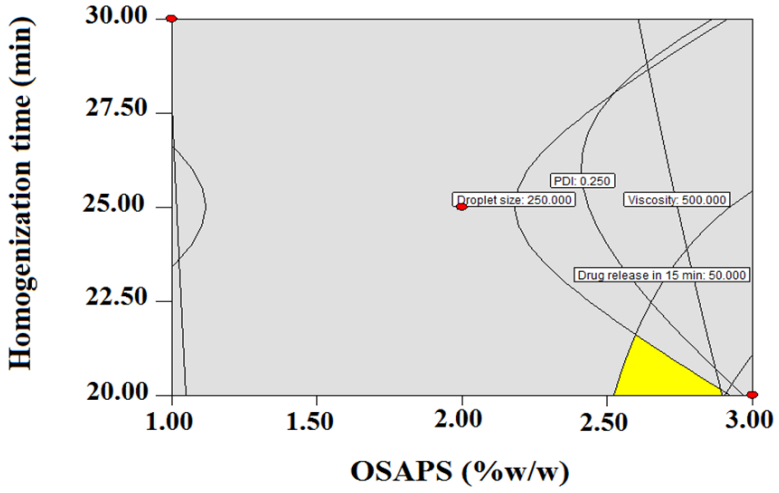

Figure 30 Overlay plots of graphical optimization displaying the area of feasible response values in the factor space for ITZ-loaded nanoemulsion preparation between (a) OSAPS and polysorbate 80 and (b) OSAPS and homogenization time while other two factors kept at center points (Yellow color satisfies the constraints whereas grey color indicates for the area which does not meet the optimum criteria).

Table 17 Analysis of variance (ANOVA) results for the response surface models of ITZ-loaded nanoemulsion preparation

Source	Model	df	Sum square	Mean square	*F-value*	*LOF F-value*	*LOF P-value*	*P-value*	r^2	RMSE
Droplet size-model	Quadratic	6	5725.46	954.24	4.4	1.11	0.4597 (model fit)	0.0291	0.7674	10.7547
Residual		8								
Total		14								
PDI-model	Linear	3	0.071	0.024	18.34	0.51	0.7942	0.0001	0.8334	0.0308
Residual		11								
Total		14								
Viscosity-model	Quadratic	7	211700	30243.41	324.17	0.096	0.9582	<0.0001	0.9969	6.6707
Residual		7								
Total		14								
Drug release within 15 min-model	Quadratic	6	5756.34	959.39	8.23	0.38	0.8166	0.0045	0.8606	7.8827
Residual		8								
Total		14								

LOF: Lack of fit; df: degrees of freedom; r^2: correlation coefficient; RMSE: root-mean-square error.

Table 18 Regression coefficients values of final reduced models made by RSM for ITZ-loaded nanoemulsion preparation

Regression coefficients	Droplet size	Polydispersity index	Viscosity	*In vitro* drug release (%) within 15 min
Intercept	-133.824	1.246	1588.833	1514.667
X_1	52.48	-0.052	-191.5	-107.833
X_2	112.17	-0.037	-224.76	-155.044
X_3	-42.21	-0.006	10.7	5.8
X_1X_2	N/A	N/A	15.4	9.4
X_1X_3	N/A	N/A	2.3	-2.7
X_2X_3	N/A	N/A	-0.6	N/A
X_1^2	-15.91	N/A	N/A	N/A
X_2^2	-3.43	N/A	7.4	3.63556
X_3^2	0.84	N/A	N/A	N/A

X_1: OSAPS (%); X_2: polysorbate 80 (%); X_3: Homogenization time (min); N/A: not available.

Table 19 Experimental and predicted values of external validation four runs and predicted r^2 for verification of each response of ITZ-loaded nanoemulsion preparation.

Runs	Independent variables			Observed responses							
				Droplet size (nm)		PDI		Viscosity (Pa.s)		*In vitro* drug release (%) within 15 min	
	X_1	X_2	X_3	Experimental	Predicted	Experimental	Predicted	Experimental	Predicted	Experimental	Predicted
EV 1	2	20	30	246	273	0.26	0.24	342	387	42	40
EV 2	3	20	25	238	225	0.27	0.22	395	545	46	51
EV3	2.5	17.5	20	295	305	0.39	0.36	201	237	46	37
EV4	1	15	25	299	286	0.48	0.50	3	23	102	118
Predicted r^2		**-**		**0.6188**		**0.8525**		**0.7123**		**0.8642**	

X_1: Octenyl succinic anhydride (OSA) modified pineapple starch concentration (%w/w), X_2: polysorbate 80 concentrtion (%w/w), X_3: Homogenization time (min), EV: External validation

Table 20 Experimental and predicted values of four responses at optimized conditions of ITZ-loaded nanoemulsion preparation.

Droplet size (nm)			PDI			Viscosity (Pa.s)			*In vitro* drug release (%) within 15 mins		
Experimintal	Predicted	%error	Experimintal	Predicted	%error	Experimintal	Predicted	%error	Experimintal	Predicted	%error
246	250	1.60	0.25	0.25	0	517	500	3.28	61	60	1.00

Optimum condition: OSAPS 3%w/w, polysorbate 80 19.8%w/w, Homogenization time 20 min with a desirability value of 0.98

Chapter 5

Conclusion

The stem and rhizome waste of pineapple plant (*Ananas comosus* L. Merr.) is normally disposed of via a burning process, which can lead to pollute the environment. Fortunately, the pineapple starch was extracted from stem and rhizome waste in the recent year. However, starch has some limited properties in the native form. Therefore, the pineapple starch was modified with OSA in order to improve the limited properties of native pineapple starch.

The OSA modification of pineapple starch was successful and FTIR spectroscopy confirmed the substitution of the hydroxyl groups in the pineapple starch molecules with the carbonyl groups of OSA. XRD revealed that there was no change in the A-type crystallinity pattern of pineapple starch after OSA modification. The DS value of OSA-modified pineapple starch increased with increasing OSA concentration. The OSA modification of pineapple starch resulted in an increase in the viscosity; however, the surface tension, gelatinization temperature and enthalpy were found to decrease. The OSA-modification conditions of pineapple starch were successfully optimized using RSM. The proposed model could predict the DS, surface tension, and enthalpy values with a reasonable degree of accuracy. The multiple responses were obtained in factor space. In case of crude emulsion preparation in the absence of surfactant polysorbate 80, the OSA-modified pineapple starch showed better emulsifying property than NPS which showed phase separation of oil and water within short time.

Moreover, the surface and interfacial tension property of OSAPS having different DS (0.001, 0.02 and 0.03) were lower than that of NPS against various concentration of 0.5-5%, where the rheological property of OSAPS were enhanced. OSAPS tended to increase viscosity with increasing DS. Therefore, OSAPS having high DS 0.03 was selected to prepare ITZ-loaded nanoemulsions.

The solubility studies demonstrated that combination of castor oil and oleic acid (1:1) provided high drug solubility. The prepared ITZ-loaded nanoemulsions using CCF design exhibited nanoscale droplet size <500 nm. The results indicated that the concentration of OSAPS and polysorbate 80 affected droplet size and PDI. An increase in OSAPS and polysorbate 80 concentration reduced droplet size and PDI of

ITZ-loaded nanoemulsions. Moreover, the droplet size decreased with increasing homogenization time (p<0.05) whereas PDI was not affected by homogenization time. However, the longer the homogenization time, the smaller the droplet size was formed.

The ITZ-nanoemulsions showed strongly negative zeta potential and 100% drug content. In addition, the viscosity of the nanoemulsions was also affected by all three independent variables. Increasing OSAPS, polysorbate 80 concentration and homogenization time raised the nanoemulsion viscosity. The viscosity of ITZ-nanoemulsions containing OSAPS was higher than that of nanoemulsions containing NPS. The prepared ITZ-loaded nanoemulsions showed shear thinning behavior, followed pseudoplastic flow and fitted the power law model.

Dissolution test of ITZ indicated that dissolution and release of ITZ from nanoemulsions was faster and higher in SGF media than intact ITZ powder. In addition, the release of ITZ nanoemulsion containing OSAPS and surfactant polysorbate 80 concentration was dramatically increased as compared to control nanoemulsion and nanoemulsion containing NPS. However, the drug release from nanoemulsions was found more than 60% after 30 min except Run 10, Run 11 and Run 14. Moreover, all prepared ITZ-loaded nanoemulsions well fitted to Weibull model with high R^2. Non-parametric bootstrap results demonstrated that dissolution profiles of prepared ITZ-nanoemulsions and intact ITZ were considered to be non-similar shown by the result of bootstrap 5% percentiles (below 50).

Accelarated stability test results for ITZ nanoemulsions of Run 15, Run 1 and Run 5 containing OSAPS 1%, 2% and 3%, respectively, control as well as nanoemulsion containing NPS indicated that different storage temperature at 4˚C and 25˚C for 90 days affected droplet size of Run 1 containing 2%w/w OSAPS plus 20%w/w polysorbate 80 and Run 5 containing 3%w/w OSAPS and 20%w/w polysorbate 80 and showed statistically different (p<0.05) between each temperature, whereas no impact on PDI of Run 1 after 90 days (p>0.05). However, 4˚C storage temperature affected PDI value of Run 5 and showed smallest PDI over 90 days. A slight increase in droplet size was more distinct at 25˚C than storage at 4˚C over 90 days. Control and NPS also showed no difference in droplet size and PDI between 4˚C and 25˚C storage after 90 days except PDI of control which showed highest

among five formulations till 30 days at 25˚C storage. Six cycles of temperature cycling test affected PDI of three ITZ-loaded nanoemulsions of control, Run 1 and nanoemulsion containing 2%w/w NPS and showed an increase in PDI after temperature cycling, where PDI of control was higher than Run 1 and NPS before and after temperature cycling. For droplet size, Run 1 of ITZ nanoemulsion exhibited a slight increase while control and NPS had no distinct change in droplet size after temperature cycling. In addition, the ITZ-loaded nanoemulsions of Run1, control and NPS showed stable and no obvious change in zeta potential as well as phase separation or creaming (100% creaming) after accelerated stability test for three months and six cycles of temperature cycling test, suggesting as thermodynamically stable of ITZ-loaded nanoemulsions.

The preparation condition of ITZ-loaded nanoemulsions could be optimized by RSM. The obtained model could exhibit good performance for predicting the values of droplet size, PDI, viscosity and *in vitro* drug release within 15min with a reasonable degree of accuracy of predicted r^2. The optimum conditions were 3%w/w OSAPS, 19.8%w/w polysorbate 80 and 20 min homogenization time, with a predicted droplet size value of 250 nm, PDI of 0.25, viscosity of 500 Pa.s, and *in vitro* drug release (%) within 15 mins of 60%, with desirability value of 0.98. The experimental values of the nanoemulsion containing 3%w/w OSAPS and 20%w/w polysorbate 80 (Run 5) were close to predicted values since the %error was found to be minimal, suggesting that this formulation of 3%w/w and 20%w/w polysorbate 80 meets the optimum criteria.

In summary, this study provides valuable considerations for OSA modification of pineapple starch from stem and rhizome using multiple desired response optimization. The multiple responses were obtained in factor space. The functional properties of native pineapple starch was improved with respect to high DS after modification with OSA. ITZ-loaded nanoemulsion containing OSAPS as was successfully prepared by simple homogenization method. The preparation condition of ITZ-loaded nanoemulsions was successfully optimized for multi-responses. The dissolution and drug release of ITZ from nanoemulsion containing OSAPS and NPS was faster and higher than intact ITZ. OSAPS could be applied as co-emulsifier and stabilizer for ITZ-loaded nanoemulsions. These findings would be useful for

pharmaceutical application and next development at a pilot scale or industrial scale utilizing economical and efficiency optimization technique.

Future direction of research

This study has revealed the physicochemical characteristics and functional properties of OSAPS in order to be applied as emulsifier and stabilizer for ITZ-loaded nanoemulsion using simple homogenization method which improved dissolution and *in vitro* drug release of ITZ by decreasing droplet size to nanoscale. The prepration condition could be optimized using RSM to save the time and cost. The development of freeze-dried reconstituted form should be further investigated. Moreover, *in vivo* bioavailability and pharmacokinetics of freezed dried ITZ-loaded nanoemulsion reconstituted form compared to market sample (Sporanox®) should be more thoroughly investigated.

REFERENCES

Abbas, S., Bashari, M., Akhtar, W., Wei, W., & Zhang, X. (2014). Process optimization of ultrasound-assisted curcumin nanoemulsions stabilized by OSA-modified starch. *Ultrason- Sonochem, 21*, 1265-1274.

Abiddin, Z., N. F., Yusoff, A., & Ahmad, N. (2015). Optimisation of reaction conditions of octenyl succinic anhydride (OSA) modified sago starch using response surface methodology (RSM). *Int Food Res J, 22*, 930-935.

Adebowale, K. O., Henle, T., Schwarzenbolz, U., & Doert, T. (2009). Modification and properties of African yam bean (*Sphenostylis stenocarpa*) Harms starch I: Heat moisture treatments and annealing. *Food Hydrocoll, 23*(7), 1947-1957.

Alcázar-Alay, S. C., & Meireles, M. A. A. (2015). Physicochemical properties, modifications and applications of starches from different botanical sources. *Food Sci Technol, 35*(2), 215-236.

Ali, H. H., & Hussein, A. A. (2017). Oral nanoemulsions of candesartan cilexetil: formulation, characterization and in vitro drug release studies. *AAPS Pharm Sci Tech, 3*(1), 1-16.

Amidon, G. L., Lennernas, H., Shah, V. P., & Crison, J. R. (1995). A theoretical basis for a biopharmaceutic drug classification: The correclation of in vitro drug product dissolution and in vivo bioavailability. *Pharm Res, 12*(3), 413-420.

Arancibia, C., Navarro-Lisboa, R., Zúñiga, R. N., & Matiacevich, S. (2016). Application of CMC as thickener on nanoemulsions based on olive oil: physical properties and stability. *Int J Polym Sci, 4*, 1-10.

Aulton, M. E. (1988). Pharmaceutics: The science of dosage form design (Part One-Chapter 4). New York, Churchill Livingstone; pp 50-53.

Bai, Y., Kaufman, R. C., Wilson, J. D., & Shi, Y. C. (2014). Position of modifying groups on starch chains of octenylsuccinic anhydride-modified waxy maize starch. *Food Chem, 153*, 193-199.

Bai, Y., & Shi, Y.-C. (2011). Structure and preparation of octenyl succinic esters of granular starch, microporous starch and soluble maltodextrin. *Carbohydr Polym, 83*(2), 520-527.

Bai, Y., Shi, Y.-C., Herrera, A., & Prakash, O. (2011). Study of octenyl succinic

anhydride-modified waxy maize starch by nuclear magnetic resonance spectroscopy. *Carbohydr Polym, 83*(2), 407-413.

Bai, Y. & Shi, Y. C. (2013). Reaction of octenylsuccinic anhydride with a mixture of granular starch and soluble maltodextrin. *Carbohydr Polym, 98*(2), 1599-1602.

Bello-Flores, C. A., Nuñez-Santiago, M. C., Martín-Gonzalez, M. F. S., BeMiller, J. N., & Bello-Pérez, L. A. (2014). Preparation and characterization of octenylsuccinylated plantain starch. *Int J Biol Macromol, 70*, 334-339.

Bello-Pérez, L. A., Aparicio-Saguilán, A., Méndez-Montealvo, G., Solorza-Feria, J., & Flores-Huicochea, E. (2005). Isolation and partial characterization of mango (*Magnifera indica* L.) starch: Morphological, physicochemical and functional studies. *Plant Foods Hum Nutr, 60*, 7-12.

BeMiller, J., & Whistler, R. (2009). Starch: chemistry and technology. Third edition, New York, Academic press; pp 194-195.

Berben, P., Mols, R., Brouwers, J., Tack, J., & Augustijns, P. (2017). Gastrointestinal behavior of itraconazole in humans - Part 2: The effect of intraluminal dilution on the performance of a cyclodextrin-based solution. *Int J Pharm, 526*(1-2), 235-243.

Bezerra, M. A., Santelli, R. E., Oliveira, E. P., Villar, L. S., & Escaleira, L. A. (2008). Response surface methodology (RSM) as a tool for optimization in analytical chemistry. *Talanta, 76*(5), 965-977.

Bhattacharjee, A., Verma, S., Verma, P. R. P., Singh, S. K., & Chakraborty, A. (2017). Fabrication of liquid and solid self-double emulsifying drug delivery system of atenolol by response surface methodology. *J Drug Deliv Sci Technol, 41*, 45-57.

Bhosale, R., & Singhal, R. (2006). Process optimization for the synthesis of octenyl succinyl derivative of waxy corn and amaranth starches. *Carbohydr Polym, 66*(4), 521-527.

Burapapadh, K., Kumpugdee-Vollrath, M., Chantasart, D., & Sriamornsak, P. (2010). Fabrication of pectin-based nanoemulsions loaded with itraconazole for pharmaceutical application. *Carbohydr Polym, 82*(2), 384-393.

Caldwell, C. G., Hills, F., Wurzburg, O. B., & Babylon, N. Y. (1953). Polysaccharides derivatives of substituted dicarboxylic acids. United States Patent, US 2,661,349.

Calligaris, S., Plazzotta, S., Bot, F., Grasselli, S., Malchiodi, A., & Anese, M. (2016). Nanoemulsion preparation by combining high pressure homogenization and high power ultrasound at low energy densities. *Food Res Int, 83*, 25-30.

Campechano-Carrera, E., Corona-Cruz, A., Chel-Guerrero, L., & Betancur-Ancona, D. (2007). Effect of pyrodextrinization on available starch content of Lima bean (*Phaseolus lunatus*) and Cowpea (*Vigna unguiculata*) starches. *Food Hydrocoll, 21*(3), 472-479.

Candioti, L. V., Zan, M. M. D., Camara, M. S., & Goicoechea, H. C. (2014). Experimental Design and Multiple Response Optimization. Using the desirability function in analytical methods development. *Talanta, 124*, 123-128.

Casella, G., & Berger, R. L. (2002). Statistical inference. Second edition. United States of America. Duxbury; pp 555-557.

Cerdeira, A. M., Mazzotti, M., & Gander, B. (2013). Formulation and drying of miconazole and itraconazole nanosuspensions. *Int J Pharm, 443*(1-2), 209-220.

Chang, F., He, X., Fu, X., Huang, Q., & Qiu, Y. (2014). Preparation and characterization of modified starch granules with high hydrophobicity and flowability. *Food Chem, 152*, 177-183.

Chen, H., Khemtong, C., Yang, X., Chang, X., & Gao, J. (2011). Nanonization strategies for poorly water-soluble drugs. *Drug Discov Today, 16*(7-8), 354-360.

Chen, Y. M., & Liu, H. (1972). Studies on stem bromelain and Stem starch from pineapple plants. *Tawainia, 17*(3), 266-276.

Chhabra, G., Chuttani, K., Mishra, A. K., & Pathak, K. (2011). Design and development of nanoemulsion drug delivery system of amlodipine besilate for improvement of oral bioavailability. *Drug Dev Ind Pharm, 37*(8), 907-916.

Das, D., Jha, S., & Kumar, K. J. (2015). Effect of carboxymethylation on physicochemical and release characteristics of Indian Palo starch. *Int J Biol Macromol, 77*, 181-187.

Daudt, R. M., Külkamp-Guerreiro, I. C., Cladera-Olivera, F., Thys, R. C. S., & Marczak, L. D. F. (2014). Determination of properties of pinhão starch: Analysis of its applicability as pharmaceutical excipient. *Ind Crop Prod, 52*, 420-429.

De Smet, L., Saerens, L., De Beer, T., Carleer, R., Adriaensens, P., Van Bocxlaer, J., et

al. (2014). Formulation of itraconazole nanococrystals and evaluation of their bioavailability in dogs. *Eur J Pharm Biopharm, 87*(1), 107-113.

Debnath, S., Satayanarayana., & Kumar, G. V. (2011). Nanoemulsion: A method to improve the solubility of lipophilic drugs. A review. *Int J Adv Pharm Sci, 2*(3), 71-83.

Dokić, L., Krstonošić, V., & Nikolić, I. (2012). Physicochemical characteristics and stability of oil-in-water emulsions stabilized by OSA starch. *Food Hydrocoll, 29*(1), 185-192.

Engers, D., Teng, J., Jimenez-Novoa, J., Gent, P., Hossack, S., Campbell, C., et al. (2010). A solid-state approach to enable early development compounds: selection and animal bioavailability studies of an itraconazole amorphous solid dispersion. *J Pharm Sci, 99*(9), 3901-3922.

Fonseca, L. M., Gonçalves, J. R., El Halal, S. L. M., Pinto, V. Z., Dias, A. R. G., Jacques, A. C., & Zavareze, E. d. R. (2015). Oxidation of potato starch with different sodium hypochlorite concentrations and its effect on biodegradable films. *Food Sci Technol, 60*(2), 714-720.

Frost, K., Kaminski, D., Kirwan, G., Lascaris, E., & Shanks, R. (2009). Crystallinity and structure of starch using wide angle X-ray scattering. *Carbohydr Polym, 78*(3), 543-548.

Fu, Q., Li, B., Zhang, D., Fang, M., Shao, J., Guo, M., et al. (2015). Comparative studies of the in vitro dissolution and in vivo pharmacokinetics for different formulation strategies (solid dispersion, micronization, and nanocrystals) for poorly water-soluble drugs: A case study for lacidipine. *Colloids Surf B Biointerfaces, 132*, 171-176.

Gbenga, L. B., Olakunle, O., & Adedayo, A. M. (2014). Influence of pregelatinization on the physicochemical and compressional characteristics of starches obtained from two local varieties of Dioscorea rotundata. *J Pharm, 4*, 2250-3013.

Glasmacher, A., & Prentice, A. (2006). Current experience with itraconazole in neutropenic patients: a concise overview of pharmacological properties and use in prophylactic and empirical antifungal therapy. *J Clin Microbiol Infect, 12*, 84-90.

Gotlieb, & Capelle. (2005). Starch derivatization: Fascinating and unique industrial opportunities. The Netherlands, Wagenin Academic; pp 28-31.

Gregorová, E., Pabst, W., & Bohačenko, I. (2006). Characterization of different starch types for their application in ceramic processing. *J Eur Ceram Soc, 26*(8), 1301-1309.

Gupta, A., Eral, H. B., Hatton, T. A., & Doyle, P. S. (2016). Nanoemulsions: formation, properties and applications. *Soft Matter, 12*(11), 2826-2841.

Gupta, R., Shea, J., Scafe, C., Shurlygina, A., & Rapoport, N. (2015). Polymeric micelles and nanoemulsions as drug carriers: Therapeutic efficacy, toxicity, and drug resistance. *J Control Release, 212*, 70-77.

Gutiérrez, T. J., Morales, N. J., Pérez, E., Tapia, M. S., & Famá, L. (2015). Physico-chemical properties of edible films derived from native and phosphated cush-cush yam and cassava starches. *J Food Pack Shelf Life, 3*, 1-8.

Hanlor, V. V., Pande, V. V., Borawake, D. D., & Nagare, H. S. (2018). Nanoemulsion: A noval platform for drug delivery system. *J Mater Sci Nanotechnol, 6*(1), 1-10.

Harika, K., Debnath, S., & Babu, M. N. (2015). Formulation and evaluation of nanoemulsion of amphotericin B. *Int J Novel Trends Pharm Sci, 5*(4), 114-122.

Hategekimana, J., Masamba, K. G., Ma, J., & Zhong, F. (2015). Encapsulation of vitamin E: Effect of physicochemical properties of wall material on retention and stability. *Carbohydr Polym, 124*, 172-179.

Hernández-Jaimes, C., Bello-Pérez, L. A., Vernon-Carter, E. J., & Alvarez-Ramirez, J. (2013). Plantain starch granules morphology, crystallinity, structure transition, and size evolution upon acid hydrolysis. *Carbohydr Polym, 95*, 207-213.

Hoover, R., Hughes, T., Chung, H. J., & Liu, Q. (2010). Composition, molecular structure, properties, and modification of pulse starches: A review. *Food Res Int, 43*(2), 399-413.

Hui, R., Qi-he, C., Ming-liang, F., Qiong, X., & Guo-qing, H. (2009). Preparation and properties of octenyl succinic anhydride modified potato starch. *Food Chem, 114*(1), 81-86.

Jain, K., Kumar, R. S., Sood, S., & Gowthamarajan, K. (2013). Enhanced oral bioavailability of atorvastatin via oil-in-water nanoemulsion using aqueous

titration method. *J Pharm Sci Res, 5*, 18-25.

Kalepu, S., Manthina, M., & Padavala, V. (2013). Oral lipid-based drug delivery systems-An overview. *Acta Pharm Sin B, 3*(6), 361-372.

Karmakar, R., Ban, D. K., & Ghosh, U. (2014). Comparative study of native and modified starches isolated and conventional and nonconventional sources. *Int Food Res J, 21*, 597-602.

Kaur, B., Ariffin, F., Bhat, R., & Karim, A. A. (2012). Progress in starch modification in the last decade. *Food Hydrocoll, 26*(2), 398-404.

Kaur, M., Singh, N., Sandhu, K. S., & Guraya, H. S. (2004). Physicochemical, morphological, thermal and rheological properties of starches separated from kernels of some Indian mango cultivars (*Mangifera indica* L.). *Food Chem, 85*(1), 131-140.

Khani, S., Keyhanfar, F., & Amani, A. (2016). Design and evaluation of oral nanoemulsion drug delivery system of mebudipine. *Drug Deliv, 23*(6), 2035-2043.

Kittipongpatana, O. S., Sirithunyalug, J., & Laenger, R. (2006). Preparation and physicochemical properties of sodium carboxymethyl mungbean starches. *Carbohydr Polym, 63*(1), 105-112.

Koester, L. S., Ortega, G. G., Mayorga, P., & Bassani, V. L. (2004). Mathematical evaluation of in vitro release profiles of hydroxypropylmethylcellulose matrix tablets containing carbamazepine associated to beta-cyclodextrin. *Eur J Pharm Biopharm, 58*(1), 177-179.

Kotta, S., Khan, A. W., Ansari, S. H., Sharma, R. K., & Ali, J. (2015). Formulation of nanoemulsion: a comparison between phase inversion composition method and high-pressure homogenization method. *Drug Deliv, 22*(4), 455-466.

Kumar, M., Pathak, K., & Misra, A. (2009). Formulation and characterization of nanoemulsion-based drug delivery system of risperidone. *Drug Dev Ind Pharm, 35*(4), 387-395.

Latt, S. S., Boontara, K., Teeraprasatkul, T., Yangngam, W., Patomchaiviwat, V., Sriamornsak, P., & Piriyaprasarth, S. (2016). Preparation and physical properties of itraconazole-loaded nanoemulsions using pineapple starch as co-emulsifier.

Asian J Pharm Sci, 11(1), 110-111.

Latt, S. S., Patomchaiviwat, V., Sriamornsak, P., & Piriyaprasarth, S. (2019). Modification of pineapple starch from stem and rhizome using multiple desired response optimization and its characterization. *Pharm Sci Asia*. doi: 10.29090/psa.2019.04.018.0046.

Lawal, O. S., Lechner, M. D., & Kulicke, W. M. (2008). Single and multi-step carboxymethylation of water yam (Dioscorea alata) starch: synthesis and characterization. *Int J Biol Macromol, 42*(5), 429-435.

Lee, H. L., & Yoo, B. (2011). Effect of hydroxypropylation on physical and rheological properties of sweet potato starch. *Food Sci Technol, 44*(3), 765-770.

Lefnaoui, S., & Moulai-Mostefa, N. (2015). Synthesis and evaluation of the structural and physicochemical properties of carboxymethyl pregelatinized starch as a pharmaceutical excipient. *Saudi Pharm J, 23*(6), 698-711.

Li, Hong, Y., Gu, Z., Cheng, L., Li, Z., & Li, C. (2018). Effect of a dual modification by hydroxypropylation and acid hydrolysis on the structure and rheological properties of potato starch. *Food Hydrocoll, 77*, 825-833.

Li, Wang, L., & Wang, B. (2017). Optimization of encapsulation efficiency and average particle size of *Hohenbuehelia serotina* polysaccharides nanoemulsions using response surface methodology. *Food Chem, 229*, 479-486.

Liang, R., Shoemaker, C. F., Yang, X., Zhong, F., & Huang, Q. (2013). Stability and bioaccessibility of beta-carotene in nanoemulsions stabilized by modified starches. *J Agric Food Chem, 61*(6), 1249-1257.

Liu, J., Wang, B., Lin, L., Zhang, J., Liu, W., Xie, J., & Ding, Y. (2014). Functional, physicochemical properties and structure of cross-linked oxidized maize starch. *Food Hydrocoll, 36*, 45-52.

Lu, Y., & Park, K. (2013). Polymeric micelles and alternative nanonized delivery vehicles for poorly soluble drugs. *Int J Pharm, 453*(1), 198-214.

Masina, N., Choonara, Y. E., Kumar, P., du Toit, L. C., Govender, M., Indermun, S., & Pillay, V. (2017). A review of the chemical modification techniques of starch. *Carbohydr Polym, 157*, 1226-1236.

Mason, T. G., Wilking, J. N., Meleson, K., Chang, C. B., & Graves, S. M. (2006).

Nanoemulsions: formation, structure, and physical properties. *J Physics: Condensed Matter, 18*(41), 635-666.

Massicotte, L. P., Baille, W. E., & Mateescu, M. A. (2008). Carboxylated high amylose starch as pharmaceutical excipients. Structural insights and formulation of pancreatic enzymes. *Int J Pharm, 356*(1-2), 212-223.

Matsugume, L. S., Lacerda, L. G., Schnitzler, E., Filho, M. A. S. C., Franco, C. M. L., & Demiate, I. M. (2009). Characterization of native and oxidized starches of two varieties of Peruvian Carrot (*Arracacia xanthorrhiza*, B.) from two production areas of Paraná State, Brazil. *Braz Arch Biol Technol, 52*(3), 701-713.

McEovy, G. k., Snow, E. K., Miller, J., Kester, L. M. S., Mendham, N. A., & Welsh, O. H., et al. (2016). American Hospital Formulary Service (AHFS). Drug information., pp 498-507.

Mehmood, T., Ahmad, A., Ahmed, A., & Ahmed, Z. (2017). Optimization of olive oil based O/W nanoemulsions prepared through ultrasonic homogenization: A response surface methodology approach. *Food Chem, 229*, 790-796.

Miao, M., Li, R., Jiang, B., Cui, S. W., Zhang, T., & Jin, Z. (2014). Structure and physicochemical properties of octenyl succinic esters of sugary maize soluble starch and waxy maize starch. *Food Chem, 151*, 154-160.

Montgomery, D. C. (1998). Design and analysis of experiments. Seventh edition. New York, Wiley; pp 402-403.

Moorthy, S. N., Sajeev, M. S., & Shanavas, S. (2012). Sweet Potato Starch : Physico-chemical , functional , thermal and rheological characteristics. *Cereal Sci Biotechnol*, 6(1), 124-133.

Myers, R. H., Montgomery, D. C., & Anderso-Cook, C. M. (2009). Response Surface Methodology. In: Balding DJ, Cressie NAC, Fitzmaurice GM, editors. Process and product optimization using designed experiments. New York, Wiley; pp 325-368.

Nagi, A., Iqbal, B., Kumar, S., Sharma, S., Ali, J., & Baboota, S. (2017). Quality by design based silymarin nanoemulsion for enhancement of oral bioavailability. *J Drug Deliv Sci Technol, 40*, 35-44.

Nakthong, N., Wongsagonsup, R., & Amornsakchai, T. (2017). Characteristics and

potential utilizations of starch from pineapple stem waste. *Ind Crop Prod, 105*, 74-82.

Neelam, K., Vijay, S., & Lalit, S. (2012). Various techniques for the modification of starch and the application of its derivatives. *Int Res J Pharm, 3*(5), 25-31.

Nilsson, L., & Bergenståhl, B. (2007). Adsorption of hydrophobically modified anionic starch at oppositely charged oil/water interfaces. *J Colloid Interface Sci, 308*, 508-513.

Nwokocha, L. M., Senan, C., & Williams, P. A. (2011). Structural, physicochemical and rheological characterization of *Tacca involucrata* starch. *Carbohydr Polym, 86*(2), 789-796.

Ocaña, J., Frutos, G., & Sánchez O, P. (2009). Using the similarity factor f2in practice: A critical revision and suggestions for its standard error estimation. *Chemom Intell Lab Syst, 99*, 49-56.

Odeku, O. A., & Akinwande, B. L. (2012). Effect of the mode of incorporation on the disintegrant properties of acid modified water and white yam starches. *Saudi Pharm J, 20*(2), 171-175.

Okunlola, A., & Akingbala, O. (2013). Characterization and evaluation of acid-modified starch of *Dioscorea oppositifolia* (Chinese yam) as a binder in chloroquine phosphate tablets. *Brazilian J Pharm Sci, 49*(4), 699-708.

Pal, J., Singhal, R. S., & Kulkarni, P. R. (2002). Physicochemical properties of hydroxypropyl derivative from corn and amaranth starch. *Carbohydr Polym, 48*, 49-53.

Parmar, K., Patel, J., & Sheth, N. (2015). Self nano-emulsifying drug delivery system for embelin: Design, characterization and in-vitro studies. *Asian J Pharm Sci, 10*(5), 396-404.

Parveen, R., Baboota, S., Ali, J., Ahuja, A., Vasudev, S. S., & Ahmad, S. (2011). Oil based nanocarrier for improved oral delivery of silymarin: *in vitro* and *in vivo* studies. *Int J Pharm, 413*(1-2), 245-253.

Patomchaiviwat, V., Piriyaprasarth, S., Koorattanasiri, P., Kanoknirumdom, S., & Rattanasiha, A. (2011). Evaluation of native and pregelatinized arrowroot (*Maranta Arundinacea*) starches as disintegrant in tablet formulation. *Adv Mater*

Res, 197-198, 127-130.

Patravale, V. B., Date, A. A., & Kulkarni, R. M. (2004). Nanosuspensions: a promising drug delivery strategy. *J Pharm Pharmacol, 56*(7), 827-840.

Pearce, K. N., & Kinsella, J. E. (1978). Emulsifying properties of proteins: evaluation of a turbidimetric technique. *J Agric Food Chem, 26*(3), 716-723.

Peeters, J., Neeskens, P., Tollenaere, J. P., Van Remoortere, P., & Brewster, M. E. (2002). Characterization of the interaction of 2-hydroxypropyl-beta-cyclodextrin with itraconazole at pH 2,4, and 7. *J Pharm Sci, 91,* 1414-1422.

Piao, Z. Z., Choe, J. S., Oh, K. T., Rhee, Y. S., & Lee, B. J. (2014). Formulation and in vivo human bioavailability of dissolving tablets containing a self-nanoemulsifying itraconazole solid dispersion without precipitation in simulated gastrointestinal fluid. *Eur J Pharm Sci, 51,* 67-74.

Piriyaprasarth, S., Patomchaiviwat, V., Sriamornsak, P., Seangpongchawal, N., Ketwongsa, P., Akeuru, P., et al. (2010). Evaluation of Yam (*Dioscorea* sp.) Starch and Arrowroot (*Maranta arundinacea*) Starch as Suspending Agent in Suspension. *Adv Mater Res, 93-94,* 362-365.

Pongsamart, K., Kleinebudde, P., & Puttipipatkhachorn, S. (2016). Preparation of fenofibrate dry emulsion and dry suspension using octenyl succinic anhydride starch as emulsifying agent and solid carrier. *Int J Pharm, 498*(1-2), 347-354.

Rao, J., & McClements, D. J. (2010). Stabilization of phase inversion temperature nanoemulsions by surfactant displacement. *J Agric Food Chem, 58*(11), 7059-7066.

Rengsutthi, K., & Charoenrein, S. (2011). Physico-chemical properties of jackfruit seed starch (*Artocarpus heterophyllus*) and its application as a thickener and stabilizer in chilli sauce. *Food Sci Technol, 44*(5), 1309-1313.

Rodrigues, A., & Emeje, M. (2012). Recent applications of starch derivatives in nanodrug delivery. *Carbohydr Polym, 87*(2), 987-994.

Rolland-Sabaté, A., Sánchez, T., Buléon, A., Colonna, P., Jaillais, B., Ceballos, H., & Dufour, D. (2012). Structural characterization of novel cassava starches with low and high-amylose contents in comparison with other commercial sources. *Food Hydrocoll, 27*(1), 161-174.

Samavati, V. (2013). Polysaccharide extraction from *Abelmoschus esculentus*: optimization by response surface methodology. *Carbohydr Polym, 95*(1), 588-597.

Sandhu, K. S., & Singh, N. (2007). Some properties of corn starches II: Physicochemical, gelatinization, retrogradation, pasting and gel textural properties. *Food Chem, 101*, 1499-1507.

Santana, A. L., Angela, A., & Meireles, M. (2014). New starches are the trend for industry applications: A Review. *Public Health, 4*(5), 229-241.

Santos, L. F., Dias, V. M., Pilla, V., Andrade, A. A., Alves, L. P., Munin, E., et al. (2014). Spectroscopic and photothermal characterization of annatto: Applications in functional foods. *Dyes Pigm, 110*, 72-79.

Scholz, P., & Keck, C. M. (2015). Nanoemulsions produced by rotor-stator high speed stirring. *Int J Pharm, 482*, 110-117.

Segura-Campos, M., Chel-Guerrero, L., & Betancur-Ancona, D. (2008). Synthesis and partial characterization of octenylsuccinic starch from *Phaseolus lunatus*. *Food Hydrocoll, 22*(8), 1467-1474.

Sharif, K. M., Rahman, M. M., Azmir, J., Mohamed, A., Jahurul, M. H. A., Sahena, F., & Zaidul, I. S. M. (2014). Experimental design of supercritical fluid extraction-A review. *J Food Eng, 124*, 105-116.

Sharif, H. R., Williams, P. A., Sharif, M. K., Khan, M. A., Majeed, H., Safdar, W., et al. (2017). Influence of OSA-starch on the physico chemical characteristics of flax seed oil-eugenol nanoemulsions. *Food Hydrocoll, 66*, 365-377.

Shi, S.-S., & He, G.-Q. (2012). Process optimization for cassava starch modified by octenyl succinic anhydride. *Procedia Eng, 37*, 255-259.

Shogren, R., & Biresaw, G. (2007). Surface properties of water soluble maltodextrin, starch acetates and starch acetates/alkenylsuccinates. *Colloids and Surfaces A, 298*(3), 170-176.

Silva, H. D., Cerqueira, M. Â., & Vicente, A. A. (2011). Nanoemulsions for food applications: Development and characterization. *Food Bioprocess Tech, 5*(3), 854-867.

Singh, V. & Ali, S. Z. (2008). Properties of starches modified by different acids. *Int J*

Food Prop, 11(3), 495-507.

Singh, J., Kaur, L., & McCarthy, O. J. (2007). Factors influencing the physico-chemical, morphological, thermal and rheological properties of some chemically modified starches for food applications-A review. *Food Hydrocoll, 21*(1), 1-22.

Song, X., Chen, Q. H., Ruan, H., He, G. Q., & Xu, Q. (2006). Synthesis and paste properties of octenyl succinic anhydride modified early *indica* rice starch. *J Zhejiang Univ Sci B, 7*(10), 800-805.

Song, X., Pei, Y., Zhu, W., Fu, D., & Ren, H. (2014). Particle-stabilizers modified from *indica* rice starches differing in amylose content. *Food Chem, 153*, 74-80.

Sriamornsak, P., & Burapapadh, K. (2015). Characterization of recrystallized itraconazole prepared by cooling and anti-solvent crystallization. *Asian J Pharm Sci, 10*(3), 230-238.

Sui, Z., & BeMiller, J. N. (2013). Relationship of the channels of normal maize starch to the properties of its modified products. *Carbohydr Polym, 92*(1), 894-904.

Sui, Z., Huber, K. C., & Bemiller, J. N. (2013). Effects of the order of addition of reagents and catalyst on modification of maize starches. *Carbohydr Polym, 96*(1), 118-130.

Sweedman, M.C., Hasjim, J., Tizzotti, M. J., Schafer, C., & Gilbert, R. G. (2013). Effect of octenylsuccinic anhydride modification on β-amylolysis of starch. *Carbohydr Polym, 97*(1), 9-17.

Sweedman, M. C., Schafer, C., & Gilbert, R. G. (2014). Aggregate and emulsion properties of enzymatically-modified octenylsuccinylated waxy starches. *Carbohydr Polym, 111,* 918-927.

Sweedman, M. C., Tizzotti, M. J., Schafer, C., & Gilbert, R. G. (2013). Structure and physicochemical properties of octenyl succinic anhydride modified starches: a review. *Carbohydr Polym, 92*(1), 905-920.

Talegaonkar, S., Mustafa, G., Akhter, S., & Iqbal, Z. I. (2010). Design and development of oral oil-in-water nanoemulsion formulation bearing atorvastatin: in vitro assessment. *J Disper Sci Technol, 31*(5), 690-701.

Tan, S. F., Masoumi, H. R., Karjiban, R. A., Stanslas, J., Kirby, B. P., Basri, M., & Basri, H. B. (2016). Ultrasonic emulsification of parenteral valproic acid-loaded

nanoemulsion with response surface methodology and evaluation of its stability. *Ultrason Sonochem, 29*, 299-308.

Thirathumthavorn, D., & Charoenrein, S. (2006). Thermal and pasting properties of native and acid-treated starches derivatized by 1-octenyl succinic anhydride. *Carbohydr Polym, 66*(2), 258-265.

Vanier, N. L., El Halal, S. L. M., Dias, A. R. G., & da Rosa Zavareze, E. (2017). Molecular structure, functionality and applications of oxidized starches: A review. *Food Chem, 221*, 1546-1559.

Wang, X., Li, X., Chen, L., Xie, F., Yu, L., & Li, B. (2011). Preparation and characterisation of octenyl succinate starch as a delivery carrier for bioactive food components. *Food Chem, 126*(3), 1218-1225.

Woggum, T., Sirivongpaisal, P., & Wittaya, T. (2015). Characteristics and properties of hydroxypropylated rice starch based biodegradable films. *Food Hydrocoll, 50*, 54-64.

Woitiski, C. B., Veiga, F., Ribeiro, A., & Neufeld, R. (2009). Design for optimization of nanoparticles integrating biomaterials for orally dosed insulin. *Eur J Pharm Biopharm, 73*(1), 25-33.

Wurzburg, O. B. (1986). Modified starches: Properties and Uses. Boca Raton, Florida, CRC press; pp 244-251.

Xu, J., Zhou, C.-w., Wang, R.-z., Yang, L., Du, S.-s., Wang, F.-p., et al. (2012). Lipase-coupling esterification of starch with octenyl succinic anhydride. *Carbohydr Polym, 87*(3), 2137-2144.

Ye, F., Miao, M., Lu, K., Jiang, B., Li, X., & Cui, S. W. (2017). Structure and physicochemical properties for modified starch-based nanoparticle from different maize varieties. *Food Hydrocoll, 67*, 37-44.

Zhang, Y., Huo, M., Zhou, J., Zou, A., Li, W., Yao, C., & Xie, S. (2010). DDSolver: an add-in program for modeling and comparison of drug dissolution profiles. *AAPS Pharm Sci Tech, 12*(3), 263-271.

Zhang, Y., Wang, X.-L., Zhao, G.-M., & Wang, Y.-Z. (2012). Preparation and properties of oxidized starch with high degree of oxidation. *Carbohydr Polym, 87*(4), 2554-2562.

Zhang, K., Yu, H., Luo, Q., Yang, S., Lin, X., Zhang, Y., et al. (2013). Increased dissolution and oral absorption of itraconazole/Soluplus extrudate compared with itraconazole nanosuspension. *Eur J Pharm Biopharm, 85*(3), 1285-1292.

Zhao, Y., Khalid, N., Shu, G., Neves, M. A., & Kobayashi, I. (2017). Formulation and characterization of O/W emulsions stabilized using octenyl succinic anhydride modified kudzu starch. *Carbohydr Polym, 176*, 91-98.

Zhou, W., Yang, J., Hong, Y., Liu, G., Zheng, J., Gu, Z., & Zhang, P. (2015). Impact of amylose content on starch physicochemical properties in transgenic sweet potato. *Carbohydr Polym, 122*, 417-427.

Zhu. F. (2014). Structure, physicochemical properties, and uses of millet starch. *Food Res Int, 64*, 200-211.

Zhu, J., Li, L., Chen, L., & Li, X. (2013). Nano-structure of octenyl succinic anhydride modified starch micelle. *Food Hydrocoll, 32*(1), 1-8.

Zhu, F. & Wang, Y. J. (2013). Characterization of modified high-amylose maize starch-alpha-naphthol complexes and their influence on rheological properties of wheat starch. *Food Chem, 138*(1), 256-262.

Zorzi, G. K., Carvalho, E. L. S., von Poser, G. L., & Teixeira, H. F. (2015). On the use of nanotechnology-based strategies for association of complex matrices from plant extracts. *Rev Bras Farmacogn, 25*(4), 426-436.

APPENDICES

Appendix 1: Design expert ANOVA for response surface reduced quadratic model DS for OSA synthesis of pineapple starch.

	Sum of		Mean	F	p-value	
Source	Squares	df	Square	Value	Prob > F	
Model	0.00206	10	0.000206	12.45	0.0002	significant
A-OSA	0.000425	1	0.000425	25.68	0.0005	
B-pH	8.01E-05	1	8.01E-05	4.84	0.0525	
C-Temp	5.18E-05	1	5.18E-05	3.13	0.1074	
D-Time	3.03E-06	1	3.03E-06	0.18	0.6778	
AD	3.97E-05	1	3.97E-05	2.4	0.1524	
BC	5.44E-05	1	5.44E-05	3.28	0.1	
BD	3.72E-05	1	3.72E-05	2.25	0.1648	
CD	5.22E-05	1	5.22E-05	3.16	0.106	
A^2	8.64E-05	1	8.64E-05	5.22	0.0454	
B^2	0.000153	1	0.000153	9.24	0.0125	
Residual	0.000166	10	1.66E-05			
Lack of Fit	0.000162	6	0.000027	30.8	0.0026	significant
Pure Error	3.51E-06	4	8.77E-07			
Cor Total	0.002226	20				

Std. Dev.	0.004068	R-Squared	0.9256
Mean	0.017	Adj R-Squared	0.8513
C.V. %	23.29	Pred R-Squared	0.4646
PRESS	0.001192	Adeq Precision	11.625

	Coefficient		Standard	95% CI	95% CI	
Factor	Estimate	df	Error	Low	High	VIF
Intercept	0.023	1	0.001294	0.02	0.026	
A-OSA	0.015	1	0.002877	0.008169	0.021	5
B-pH	-0.00633	1	0.002877	-0.013	8.27E-05	5
C-Temp	0.002275	1	0.001286	-0.00059	0.005142	1
D-Time	0.000551	1	0.001286	-0.00232	0.003417	1
AD	-0.00498	1	0.003216	-0.012	0.002184	5
BC	-0.00261	1	0.001438	-0.00581	0.000598	1
BD	0.00482	1	0.003216	-0.00235	0.012	5
CD	0.002555	1	0.001438	-0.00065	0.00576	1
A^2	-0.00517	1	0.002261	-0.01	-0.00013	1.62
B^2	-0.00688	1	0.002261	-0.012	-0.00184	1.62

Final regression equation of response DS in terms of coded and actual factors:

Final equation in terms of coded factors:

DS=+0.023+0.015*A-0.00633*B+0.002275*C+0.000551*D-0.00498*A*D
-0.00261*B*C0.00482*B*D+0.002555*C*D-0.00517* ^2-0.00688* B^2

Final equation in terms of actual factors:

DS =-0.36294+0.002569*OSA+0.10026*pH+0.001373*Temp-0.0269*Time
-0.00023*OSA*Time-0.00021* pH*Temp+0.003214*pH *Time+0.000136*Temp*
Time-2.5E-05 *OSA^2-0.00688 *pH^2

Appendix 2: Design expert ANOVA for response surface reduced quadratic model surface tension for OSA synthesis of pineapple starch.

	Sum of		Mean	F	p-value	
Source	Squares	df	Square	Value	Prob > F	
Model	487.56	9	54.17	16.87	< 0.0001	significant
A-OSA	328.67	1	328.67	102.34	< 0.0001	
B-pH	5.26	1	5.26	1.64	0.2271	
C-Temp	0.62	1	0.62	0.19	0.6677	
D-Time	11.53	1	11.53	3.59	0.0846	
BC	4.7	1	4.7	1.46	0.2519	
CD	5.66	1	5.66	1.76	0.2112	
A^2	45.94	1	45.94	14.3	0.003	
B^2	14.33	1	14.33	4.46	0.0584	
D^2	4.31	1	4.31	1.34	0.2714	
Residual	35.33	11	3.21			
Lack of Fit	34.23	7	4.89	17.88	0.0072	significant
Pure Error	1.09	4	0.27			
Cor Total	522.89	20				

Std. Dev.	1.79	R-Squared	0.9324
Mean	59.64	Adj R-Squared	0.8772
C.V. %	3	Pred R-Squared	0.8015
PRESS	103.8	Adeq Precision	12.369

	Coefficient		Standard	95% CI	95% CI	
Factor	Estimate	df	Error	Low	High	VIF
Intercept	57.21	1	0.58	55.93	58.49	
A-OSA	-5.73	1	0.57	-6.98	-4.49	1
B-pH	-0.72	1	0.57	-1.97	0.52	1
C-Temp	-0.25	1	0.57	-1.5	1	1
D-Time	1.07	1	0.57	-0.17	2.32	1
BC	0.77	1	0.63	-0.63	2.16	1
CD	-0.84	1	0.63	-2.24	0.55	1
A^2	4.08	1	1.08	1.7	6.45	1.9
B^2	2.28	1	1.08	-0.096	4.65	1.9
D^2	-1.25	1	1.08	-3.62	1.12	1.9

Final regression equation of response surface tension in terms of coded and actual factors:

Final equation in terms of coded factors:

SurfaceTension=+57.2-15.73*A+0.72*B+0.25*C+1.07*D+0.77*B*C+0.84*C*D +4.08*A^2+2.28*B^2-1.25*D^2

Final equation in terms of actual factors:

Surface Tension=+223.4526-0.99646*OSA-39.45107*pH-0.35337*Temp+6.28208 *Time+0.0613*pH*Temp-.044867*Temp*Time+0.01939*OSA^2+2.27671* pH^2-0.5548*Time^2

Appendix 3: Design expert ANOVA for response surface reduced quadratic model enthalpy for OSA synthesis of pineapple starch.

	Sum of		Mean	F	p-value	
Source	Squares	df	Square	Value	Prob > F	
Model	10.5	9	1.17	7.18	0.0017	significant
A-OSA	0.15	1	0.15	0.94	0.3537	
B-pH	0.018	1	0.018	0.11	0.7426	
C-Temp	1.57	1	1.57	9.68	0.0099	
D-Time	1.22	1	1.22	7.48	0.0194	
AB	1.6	1	1.6	9.86	0.0094	
AC	1.76	1	1.76	10.85	0.0071	
AD	0.36	1	0.36	2.19	0.1669	
A^2	0.27	1	0.27	1.64	0.2264	
B^2	1.56	1	1.56	9.62	0.0101	
Residual	1.79	11	0.16			
Lack of Fit	1.27	7	0.18	1.4	0.3918	not significant
Pure Error	0.52	4	0.13			
Cor Total	12.29	20				

Std. Dev.	0.4	R-Squared	0.8545
Mean	2.18	Adj R-Squared	0.7355
C.V. %	18.53	Pred R-Squared	0.6002
PRESS	4.91	Adeq Precision	12.036

	Coefficient		Standard	95% CI	95% CI	
Factor	Estimate	df	Error	Low	High	VIF
Intercept	1.71	1	0.13	1.43	1.99	
A-OSA	0.12	1	0.13	-0.16	0.4	1
B-pH	-0.096	1	0.29	-0.72	0.53	5
C-Temp	0.4	1	0.13	0.12	0.68	1
D-Time	0.78	1	0.29	0.15	1.41	5
AB	1	1	0.32	0.3	1.7	5
AC	0.47	1	0.14	0.16	0.78	1
AD	-0.47	1	0.32	-1.17	0.23	5
A^2	0.29	1	0.22	-0.21	0.78	1.62
B^2	0.7	1	0.22	0.2	1.19	1.62

Final regression equation of response enthalpy in terms of coded and actual factors:
Final equation in terms of coded factors:

Enthalpy=+1.710.12*A-0.096*B0.4*C+0.78*D+1*A*B+0.47*A*C-0.47*A*D
+0.29*A^2+0.7*B^2

Final equation in terms of actual factors:

Enthalpy=+53.044350.60718*OSA12.2893*pH0.00842*Temp+0.85589*Time+0.069
014*OSA*pH0.002591*OSA*Temp-0.02169*OSA*Time0.001366*OSA^2+
0.69522*pH^2

Appendix 4: ANOVA results for % drug release of ITZ-loaded nanoemulsions at each time point.

	% cumulative drug release of ITZ					
Runs	5 min	15 min	30 min	45 min	60 min	120 min
1	24 ± 0.39^{a}	37 ± 3.04^{abc}	55 ± 2.36^{abc}	68 ± 3.58^{abcd}	78 ± 1.11^{abc}	95 ± 8.11^{ab}
2	24 ± 5.69^{a}	36 ± 0.71^{abc}	65 ± 4.27^{bc}	89 ± 10.29^{def}	99 ± 4.08^{d}	96 ±11.42^{ab}
3	34 ± 2.42^{ab}	55 ± 1.25^{de}	76 ± 3.01^{cde}	96 ± 5.21^{ef}	102 ± 3.08^{d}	100 ± 3.93^{ab}
4	104 ± 1.85^{f}	105 ± 2.68^{g}	107 ± 5.67^{f}	106 ± 2.76^{f}	104 ± 3.37^{d}	101 ± 7.30^{ab}
5	44 ± 9.71^{c}	61 ± 6.63^{e}	70 ± 1.52^{bcd}	84 ± 17.06^{cdef}	91 ± 12.28^{bcd}	109 ± 3.82^{b}
6	34 ± 6.24^{ab}	53 ± 11.70^{cde}	73 ± 1.46^{bcde}	87 ± 10.18^{def}	90 ± 3.90^{bcd}	91 ± 2.90^{ab}
7	59 ± 12.92^{cd}	82 ± 8.13^{f}	91 ± 6.57^{def}	93 ± 5.39^{ef}	92 ± 2.20^{cd}	93 ± 7.28^{ab}
8	26 ± 0.81^{a}	44 ± 2.99^{bcd}	62 ± 2.57^{bc}	76 ± 2.23^{bcde}	79 ± 1.43^{abc}	94 ± 4.96^{ab}
9	26 ± 7.56^{a}	42 ± 6.14^{bcd}	63 ± 5.85^{bc}	78 ± 9.30^{bcde}	85 ± 7.84^{bcd}	87 ± 12.01^{ab}
10	27 ± 7.37^{a}	31 ± 10.76^{ab}	40 ± 1.81^{a}	58 ± 6.99^{ab}	60 ± 9.06^{a}	95 ± 13.99^{ab}
11	18 ± 1.98^{a}	28 ± 1.74^{ab}	41 ± 5.16^{a}	62 ± 4.42^{abc}	79 ± 3.82^{abc}	91 ± 3.66^{ab}
12	22 ± 6.06 ^{a}	34 ± 1.80^{ab}	54 ± 7.71^{ab}	76 ± 2.46^{bcde}	88 ± 12.66^{bcd}	84 ± 14.49^{a}
13	18 ± 0.93^{a}	32 ± 6.44^{ab}	55 ± 5.04^{abc}	78 ± 12.08^{bcde}	79 ± 7.93^{abc}	94 ± 8.41^{ab}
14	19 ± 3.93^{a}	24 ± 2.70^{a}	35 ± 1.36^{a}	49 ± 3.77^{a}	72 ± 5.37^{ab}	95 ± 7.30^{ab}
15	29 ± 2.92^{ab}	44 ± 1.83^{bcd}	66 ± 3.79^{bc}	85 ± 2.44^{def}	91 ± 7.44^{bcd}	98 ± 1.19^{ab}
CF	88 ± 2.64 ^{ef}	94 ± 2.00^{fg}	93 ± 3.46^{ef}	94 ± 2.00^{ef}	92 ± 1.34^{cd}	94 ± 0.73^{ab}
NF	71 ± 2.61^{de}	87 ± 1.88^{f}	92 ± 4.12^{ef}	94 ± 0.96^{ef}	101 ± 7.22^{d}	97 ± 2.19^{ab}

All data are presented as mean ± SD, (n=3). $^{a\text{-}g}$Different superscript letters in the same column statistically difference ($p<0.05$) by Tukey HSD. CF: Control formulation; NF: Nanoemulsion formulation containing native pineapple starch.

Appendix 5: Design expert ANOVA for response surface reduced quadratic model droplet size for ITZ-loaded nanoemulsion preparation.

	Sum of		Mean	F	p-value	
Source	Squares	df	Square	Value	Prob > F	
Model	5725.46	6	954.24	4.4	0.0291	significant
A-OSAPS	748.17	1	748.17	3.45	0.1003	
B-Polysorbate 80	2242.67	1	2242.67	10.34	0.0123	
C-Homogenization time	0.17	1	0.17	0.0007685	0.9786	
A^2	662.17	1	662.17	3.05	0.1187	
B^2	1199.06	1	1199.06	5.53	0.0466	
C^2	1163.1	1	1163.1	5.36	0.0492	
Residual	1734.94	8	216.87			
Lack of Fit	914.14	4	228.54	1.11	0.4597	not significant
Pure Error	820.8	4	205.2			
Cor Total	7460.4	14				

Std. Dev.	14.73	R-Squared	0.7674
Mean	286.8	Adj R-Squared	0.593
C.V. %	5.13	Pred R-Squared	0.1038
PRESS	6685.71	Adeq Precision	6.742

	Coefficient		Standard	95% CI	95% CI	
Factor	Estimate	df	Error	Low	High	VIF
Intercept	293.29	1	5.46	280.71	305.88	
A-OSAPS	-11.17	1	6.01	-25.03	2.7	1
B- Polysorbate 80	-19.33	1	6.01	-33.2	-5.47	1
C- Homogenization time	-0.17	1	6.01	-14.03	13.7	1
A^2	-15.91	1	9.11	-36.91	5.09	1.38
B^2	-21.41	1	9.11	-42.41	-0.41	1.38
C^2	21.09	1	9.11	0.09	42.09	1.38

Final regression equation of response droplet size in terms of coded and actual factors:

Final equation in terms of coded factors:

Droplet size =+293.29-11.17 *A-19.33*B-0.17*C-15.91*A^2-21.41* B^2+21.09 *C^2

Final equation in terms of actual factors:

Droplet size = -133.82353+52.48039*OSAPS+112.17255 *polysorbate 80-42.2098* Homogenization time-15.91176*OSAPS^2-3.42588* polysorbate 80^2+0.84353* Homogenization time^2

Appendix 6: Design expert ANOVA for response surface linear model PDI for ITZ-loaded nanoemulsion preparation.

	Sum of		Mean	F	p-value	
Source	Squares	df	Square	Value	Prob > F	
Model	0.071	3	0.024	18.34	0.0001	significant
A-OSAPS	0.016	1	0.016	12.37	0.0048	
B-Polysorbate 80	0.05	1	0.05	38.94	< 0.0001	
C-Homogenization time	4.82E-03	1	4.82E-03	3.72	0.08	
Residual	0.014	11	1.30E-03			
Lack of Fit	6.72E-03	7	9.61E-04	0.51	0.7942	not significant
Pure Error	7.52E-03	4	1.88E-03			
Cor Total	0.085	14				

Std. Dev.	0.036	R-Squared	0.8334
Mean	0.36	Adj R-Squared	0.788
C.V. %	10.01	Pred R-Squared	0.7336
PRESS	0.023	Adeq Precision	15.427

	Coefficient		Standard	95% CI	95% CI	
Factor	Estimate	df	Error	Low	High	VIF
Intercept	0.36	1	9.29E-03	0.34	0.38	
A-OSAPS	-0.052	1	0.015	-0.084	-0.019	1
B-Polysorbate 80	-0.092	1	0.015	-0.12	-0.059	1
C-Homogenization time	-0.028	1	0.015	-0.061	4.00E-03	1

Final regression equation of response PDI in terms of coded and actual factors:

Final equation in terms of coded factors:

PDI = +0.36-0.052*A-0.092*B-0.028*C

Final equation in terms of actual factors:

PDI =+1.246-0.051667*OSAPS-0.036667*polysorbate 80-0.00567*
Homogenization time

Appendix 7: Design expert ANOVA for response surface quadratic model viscosity for ITZ-loaded nanoemulsion preparation.

	Sum of		Mean	F	p-value	
Source	Squares	df	Square	Value	Prob > F	
Model	211700	7	30243.41	324.17	< 0.0001	significant
A-OSAPS	36720.5	1	36720.5	393.6	< 0.0001	
B-T80	31500.5	1	31500.5	337.65	< 0.0001	
C-Homogenization time	1152	1	1152	12.35	0.0098	
AB	1976.33	1	1976.33	21.18	0.0025	
AC	176.33	1	176.33	1.89	0.2116	
BC	75	1	75	0.8	0.3997	
B^2	7709.88	1	7709.88	82.64	< 0.0001	
Residual	653.06	7	93.29			
Lack of Fit	43.86	3	14.62	0.096	0.9582	not significant
Pure Error	609.2	4	152.3			
Cor Total	212400	14				

Std. Dev.	9.66	R-Squared	0.9969
Mean	217.73	Adj R-Squared	0.9938
C.V. %	4.44	Pred R-Squared	0.995
PRESS	1057.19	Adeq Precision	72.868

	Coefficient		Standard	95% CI	95% CI	
Factor	Estimate	df	Error	Low	High	VIF
Intercept	199.22	1	3.22	191.61	206.84	
A-OSAPS	135.5	1	6.83	119.35	151.65	3
B-Polysorbate 80	125.5	1	6.83	109.35	141.65	3
C-Homogenization time	24	1	6.83	7.85	40.15	3
AB	38.5	1	8.36	18.72	58.28	3
AC	11.5	1	8.36	-8.28	31.28	3
BC	-7.5	1	8.36	-27.28	12.28	3
B^2	46.28	1	5.09	34.24	58.32	1

Final regression equation of response viscosity in terms of coded and actual factors:
Final equation in terms of coded factors:

Viscosity = +199.22+ 135.5*A+125.5*B+24*C+38.5*A*B+11.5*A*C-7.5*B*C +46.28 * B^2

Final equation in terms of actual factors:

Viscosity = +1588.83333-191.5*OSAPS-224.75556*Polysorbate 80+10.7 * Homogenization time+15.4*OSAPS*polysorbate 80+2.3*OSAPS* Homogenization time-0.6*polysorbate 80*Homogenization time+7.40444 * polysorbate 80^2

Appendix 8: Design expert ANOVA for response surface quadratic model *in vitro* drug release within 15 mins for ITZ-loaded nanoemulsion preparation.

	Sum of		Mean	F	p-value	
Source	Squares	df	Square	Value	Prob > F	
Model	5756.34	6	959.39	8.23	0.0045	significant
A-OSAPS	704.17	1	704.17	6.04	0.0394	
B-Polysorbate 80	1012.5	1	1012.5	8.69	0.0185	
C-Homogenization time	8	1	8	0.069	0.7999	
AB	736.33	1	736.33	6.32	0.0361	
AC	243	1	243	2.09	0.1867	
B^2	1858.68	1	1858.66	15.95	0.004	
Residual	932.06	8	116.51			
Lack of Fit	254.86	4	63.71	0.38	0.8166	not significant
Pure Error	677.2	4	169.3			
Cor Total	6688.4	14				

Std. Dev.	10.79	R-Squared	0.8606
Mean	47.2	Adj R-Squared	0.7561
C.V. %	22.87	Pred R-Squared	0.6039
PRESS	2649.58	Adeq Precision	10.156

	Coefficient		Standard	95% CI	95% CI	
Factor	Estimate	df	Error	Low	High	VIF
Intercept	38.11	1	3.6	29.81	46.41	
A-OSAPS	-10.83	1	4.41	-20.99	-0.67	1
B-Polysorbate 80	-22.5	1	7.63	-40.1	-4.9	3
C-Homogenization time	2	1	7.63	-15.6	19.6	3
AB	23.5	1	9.35	1.94	45.06	3
AC	-13.5	1	9.35	-35.06	8.06	3
B^2	22.72	1	5.69	9.6	35.84	1

Final regression equation of response *in vitro* drug release (%) within 15 mins in terms of coded and actual factors:

Final equation in terms of coded factors:

In vitro drug release (%) within 15 mins = +38.11-10.83*A-22.5*B+2*C+23.5*A*B-13.5*A*C+22.72*B^2

Final equation in terms of actual factors:

In vitro drug release (%) within 15 mins = +1514.667-107.833*OSAPS-155.044*polysorbate 80+5.8*Homogenization time+9.4*OSAPS*polysorbate 80-2.7*OSAPS*Homogenization time+3.63556*polysorbate 80^2

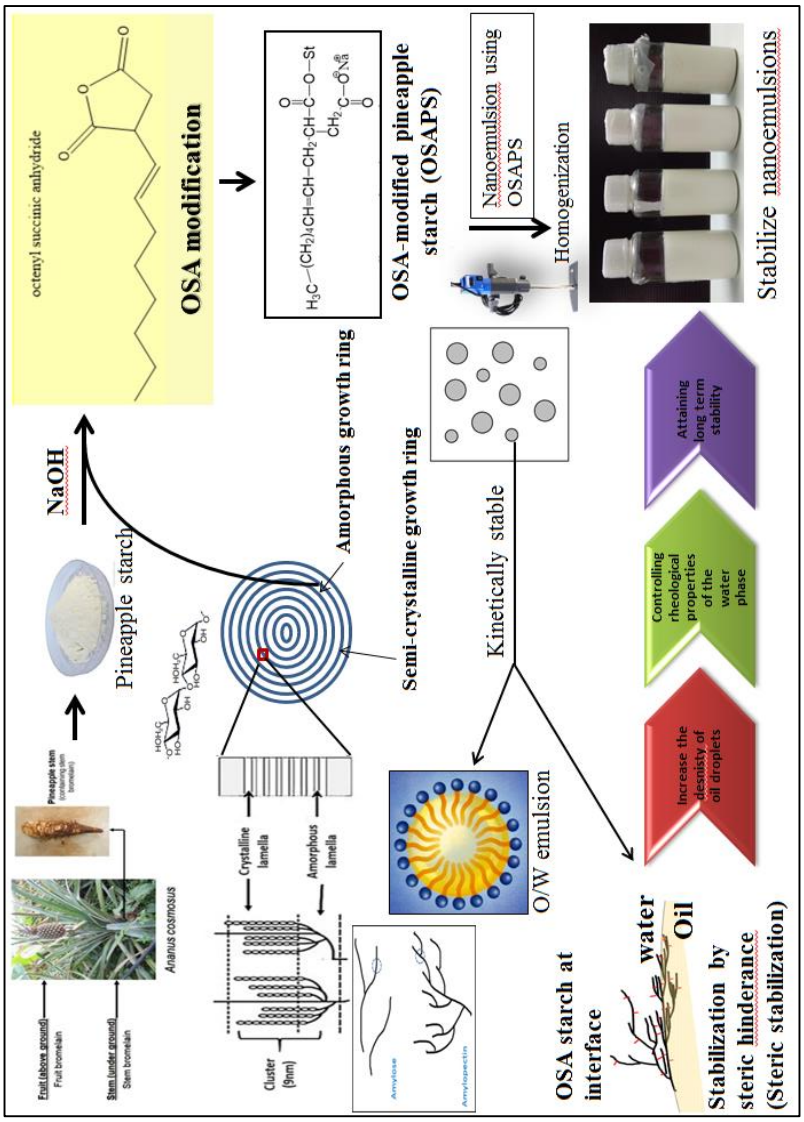

Appendix 9: Schematic diagram showing steric stabilization mechanism of OSAPS.

VITA

NAME	Miss Su Su Latt
DATE OF BIRTH	20 November 1979
PLACE OF BIRTH	Myeik-Hti-Lar
INSTITUTIONS ATTENDED	University of Pharmacy (Mandalay), Myanmar University of Pharmacy (Yangon), Myanmar Falculty of Pharmacy, Silpakorn University, Thailand
HOME ADDRESS	No. 31, 5 quarter B6, Chan-Mya-Tharsi twonship, Myothit, between 68x69 street, Mandalay
PUBLICATION	Latt, S. S., Boontara, K., Teeraprasatkul, T., Yangngam, W., Patomchaiviwat, V., Sriamornsak, P., & Piriyaprasarth, S. (2016). Preparation and physical properties of itraconazole-loaded nanoemulsions using pineapple starch as co-emulsifier. Asian J Pharm Sci, 11(1), 110-111. Latt, S. S., Patomchaiviwat, V., Sriamornsak, P., & Piriyaprasarth, S. (2019). Modification of pineapple starch from stem and rhizome using multiple desired response optimization and its characterization. Pharm Sci Asia. doi:10.29090/psa.2019.04.018.0046.
AWARD RECEIVED	AFPS Nagai Best Paper Award 2015 “Bronze Medal” for poster presentation.